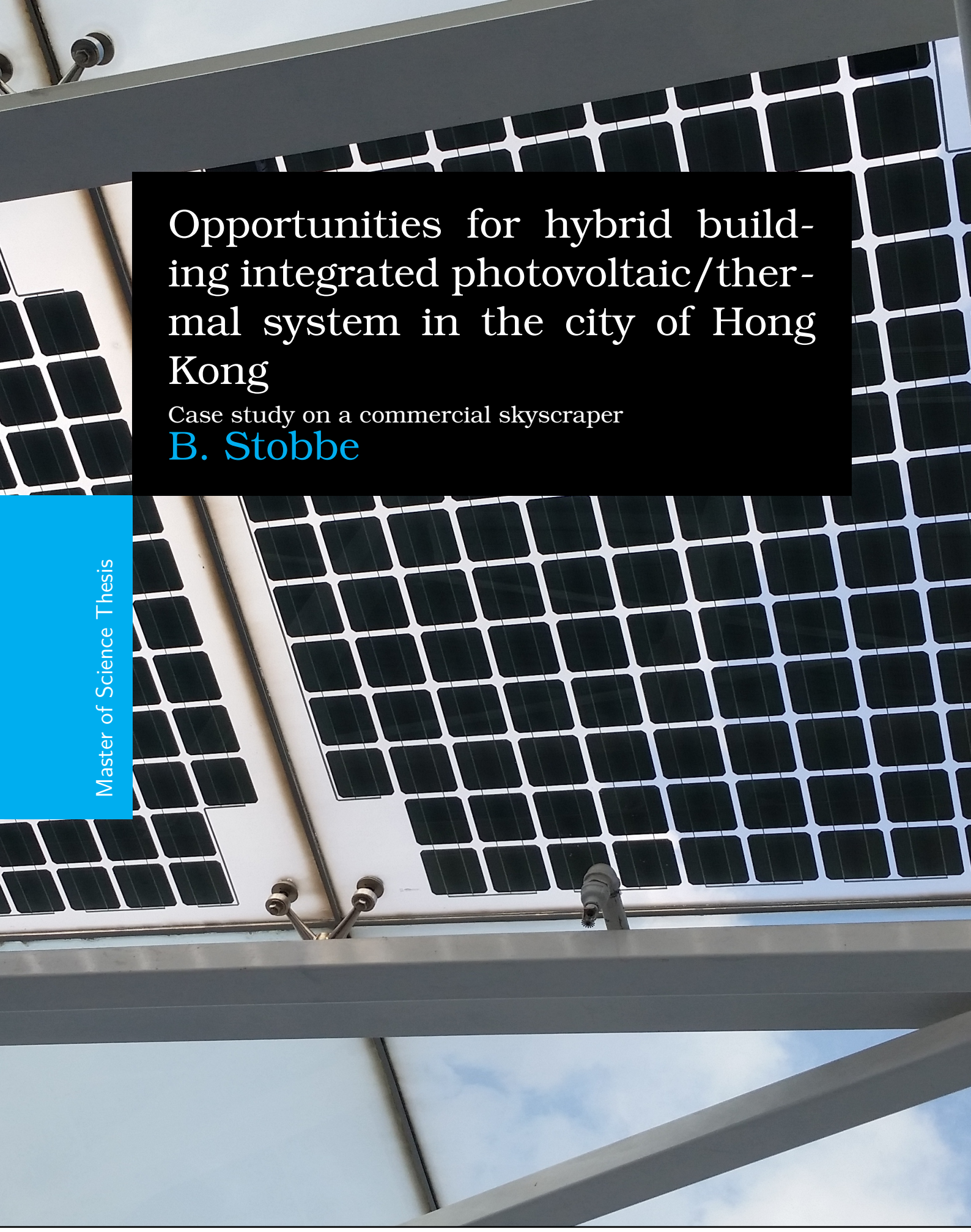

Opportunities for hybrid building integrated photovoltaic/thermal system in the city of Hong Kong

Case study on a commercial skyscraper

B. Stobbe

Master of Science Thesis

TU Delft Delft University of Technology

Photovoltaic Materials and Devices

Opportunities for hybrid building integrated photovoltaic/thermal system in the city of Hong Kong

Case study on a commercial skyscraper

Master of Science Thesis

For the degree of Master of Science in Electrical Power Engineering (Electrical Sustainable Energy) at Delft University of Technology

B. Stobbe

October 3, 2016

Faculty of Electrical Engineering, Mathematics and Computer Science (EEMCS) · Delft University of Technology

The work in this thesis was supported by the Hong Kong University of Science and Technology. Their cooperation is hereby gratefully acknowledged.

Delft University of Technology
Department of
Photovoltaic Materials and Devices (pmd)

The undersigned hereby certify that they have read and recommend to the Faculty of Electrical Engineering, Mathematics and Computer Science (EEMCS) for acceptance a thesis entitled

Opportunities for hybrid building integrated photovoltaic/thermal system in the city of Hong Kong

by

B. Stobbe

in partial fulfillment of the requirements for the degree of

Master of Science of Electrical Power Engineering (Electrical Sustainable Energy)

Dated: October 3, 2016

Supervisor(s):

Dr.ir. O. Isabella

Dr.ir. L.F. NG Moses

Reader(s):

prof.dr.ir. M. Zeman

Dr.ir. O. Isabella

Dr.ir. M. Ghaffarian Niasar

Dr. R. Santbergen

Abstract

The modern world is facing challenges like the depletion of fossil fuels and the rising demand of energy while decreasing CO_2 emission to counteract climate change. As the vast majority of mankind populates (mega-)cities, one option of tackling these challenges could be the installation of photovoltaic/thermal(PV/T) hybrid-solar systems on the facades of skyscrapers. This thesis investigates this option using Hong Kong as the study site due to the fact that it is one of the most densely populated cities in the world packed with high-rise buildings. The PV/T hybrid solar panel technology encompasses both a solar collector and solar cells. The heat produced by the solar cells can be used to heat up water and such heat can be transferred away from the solar cells, which increases the electrical performance. Our envisioned system will be installed on a commercial skyscraper the International Commerce Centre(ICC) and includes PV/T hybrid-solar panels, micro-inverters, pumps and heat storage.

The main question of this thesis is: What are the opportunities for hybrid building integrated photovoltaic/thermal solar systems in the city of Hong Kong? The primary objective is to model such a system for a skyscraper in Hong Kong and investigate the thermal and electrical performance. The secondary objective is to assess the likely economic and environmental costs.

The building is modeled in SketchUp. It will allow solar irradiance and shadowing effects to be taken into account following Sun's path. The exact position of the building with its facades orientation relative to the position of the sun and meteorological data from Meteonorm, are the inputs of the irradiance model running in Matlab and of the thermal model running in TrnSys. We have deployed the Perez model and taken into account the albedo component for modeling the diffused irradiance. The results of the irradiance and the thermal model are inputs for the total hybrid-solar system model, which outputs the electric and thermal yield and the water temperature as function of altitude on the building's facade.

The simulated efficiencies in our hybrid-solar system are 53.1% for the thermal part and 16.5% for the electrical part. We have found that the temperature of panels does not exceed 40°C, which benefits the overall electrical efficiency. On the ICC 19,808 panels can be installed without covering any windows. According to our study, which does not take into account hydraulic losses when scaling up the hybrid-solar system to the whole building, the annual electrical and thermal energy yield are 3.39 GWh and 12.5 GWh, respectively. The thermal yield could be used in (pre-)heating water while the electrical yield could be fed back to the grid or also used internally.

Acknowledgements

First of all, I would like to express my gratitude towards all the people that helped and supported me during the year I spent working on my thesis project, starting with supervisors from the universities: Dr. ir Olindo Isabella and Dr.Ir. L.F. NG Moses who gave me the inputs I needed and were there when I needed help or had questions. Especially Olindo for being patient with me, my thesis took longer than I expected, but Olindo was there all the time. I want to thank the university of Delft, to make it able to do research in Hong Kong. Furthermore I want to thank Rudi Santbergen for his help during my thesis project and my thesis writing, he gave good feedback.

I would like also to thank Mart Huijbregts a friend with who I had many discussions about my results and my work and who helped me improve my final results. Next to Mart I would like to thank some of my new colleagues from Ricardo for their input and suggestions on my work and my draft presentation.

Finally I would like to thank my family for their unconditional love, always supporting me and keeping me motivated to finish my thesis. They also helped with reviewing my thesis on academic level and English, especially Tim Beaver, Ir. Arie Stobbe and my Father, Mr. Jan Stobbe.

Benjamin Stobbe

Delft, October 3, 2016

Table of Contents

List of Figures

List of Tables

Chapter 1

Introduction

1.1 The facing challenges by human kind

Mankind all over the world is undertaking more development of its cities and infrastructure. With such development comes an increased demand for energy. The last years and coming years a stable energy usage is projected in the Organisation for Economic Co-operation and Development (OECD) countries, well developed parts of the world like Europe, North America and Japan. On the other hand in the non-OECD countries the energy consumption is growing significant and projected to grow further, see Figure 1.1b. OECD countries are highlighted in blue see Figure 1.1a. What can be seen as well is that a China, India and whole of Africa are not colored. China, India and countries in Africa are also countries which are now upcoming economies. So a higher energy demand can be expected which is also illustrated in the second Figure 1.1b. Another indication of an upcoming raise in demand could be the energy usage per capita. For example China's energy usage per capita is three times lower than for a OECD country like the Netherlands [2]. According to the United Nations [10] is the world population still rising, this means also a rise in energy demand because all humans use energy. Can this demand of energy be responsibly answered by a production of more sustainable renewable energy?

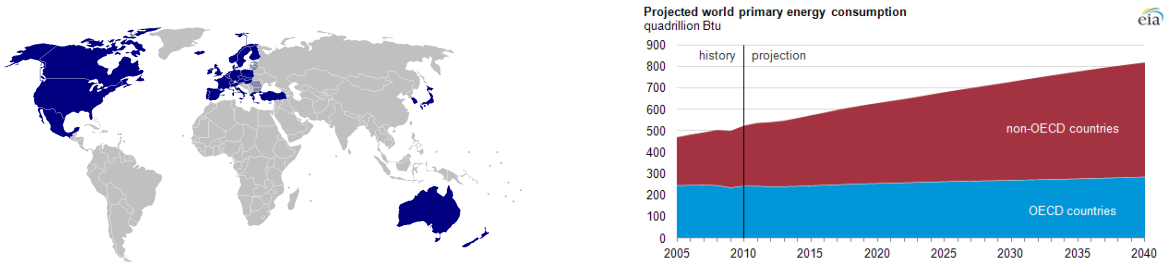

(a) (b)

Figure 1.1: a) Overview of the locations of the OECD countries highlighted in blue [1] and b) The projected world primary energy consumption (quadrillion Btu) divided in OECD countries (lightblue) and non-OECD countries (red) [2].

It is widely acknowledged, that there is ongoing depletion of fossil fuels stores in the earth, which are still the main contributor to the energy production. According to data from the United States Energy Information Administration (*EIA*) [2] and the world fact-book from the Central Intelligent Agency [11] there remains approximately 50 years of oil and natural gas and approximately 110 years of coal, but this are calculations done with the production levels of 2014. If China or India decides they need more this production will rise and even less reserves will result. In the Table 1.1 below is an overview of the reserves, with their production and amount of time left until depletion. Will there be some reserves left for the next generation?

Table 1.1: Fossil fuels, their reserves, production and time to depletion (Mtoe = Million ton of oil equivalent)

Fossil Fuel	Reserves(Mtoe)	production level(Mtoe annual)	time to depletion(years)
Coal	$6.22 \cdot 10^5$	$5.52 \cdot 10^3$	112.8
Natural gas	$2.42 \cdot 10^5$	$4.97 \cdot 10^3$	48.7
Oil	$1.81 \cdot 10^5$	$3.83 \cdot 10^3$	47.3

The last challenge for now is the demanded CO_2 emission reductions. The climate is changing and according to some scientists one of the reasons is CO_2 emissions which are polluting the atmosphere. World leaders have met each other in different climate change conferences and came to the decision that a worldwide decrease in CO_2 emissions are needed. In recent years only an increase in CO_2 emissions have been measured, see Figure 1.2. In the graph on the right side is the role of the OECD countries in comparison with the non OECD countries. What can be concluded from the graphs is that a significant rise of emissions from non-OECD countries against a small rise for OECD counties for the last twenty-four years. How will the world tackle CO_2 emissions if they are the byproduct of the production and use of fossil fuels? Which is the main energy source widely used in the world.

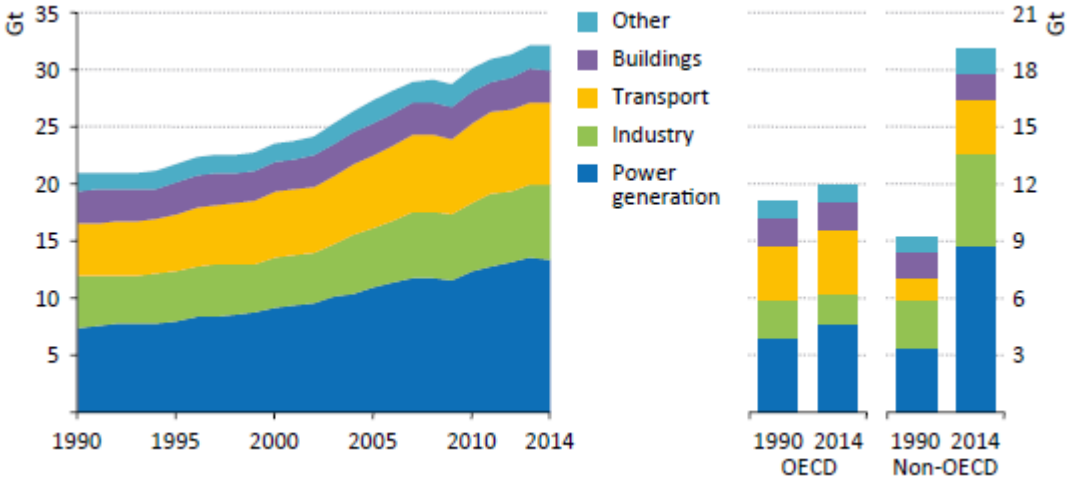

Figure 1.2: The Global energy-related CO_2 emission by sector and region in Gigatonne [3]. The left side shows the difference between OECD and Non-OECD countries

1.2 Motivation of this thesis

The Delft University of Technology is one of the top universities in the world and with this position it should also help solve challenges like those described in the introduction. These challenges cannot be met in one day and with only one idea and by one student or university. It needs solutions and ideas from all over the world.

In recent years there has been developments in solar energy technology with new innovation resulting in increased efficiences. For example right here in the Netherlands more and more buildings are having solar panels on their roof. During summer Germany produces so much electricity by solar power that it had to pay the consumers to use electricity [12, 13]. Large-scale solar plants are installed all over the world [14]. Think of the Millenium bridge in London, the train-station in the bridge is partly powered by solar panels on top of the bridge. Can solar energy not help solve the facing challenges?

One innovation is the use of hybrid solar panels, which is a combination of two solar technologies. The bottom of the panel consists of the tubes of a solar collector and the top of the panel of a photovoltaic module, in this way thermal energy and electricity is produced simultaneously.

The main motivation of this thesis are the challenges described in the introduction and the responsibility as an Electrical Engineer to help solve these challenges with solutions that are not obvious. This thesis will not provide a specific solution but will give a part of the solution that can be a motivation and example for new, other projects. It includes one case of harvesting solar energy in Hong Kong. This will be done with not the conventional solar panels and not on a horizontal surface but with solar panels which produce electrical and thermal power and are part of a buildings facades.

The motivation for Hong Kong comes from the fact that China now is becoming one of the main contributors to the global energy demand, to the increase in CO_2 emissions if the projections are true this will only increase. Hong Kong, as one of the most densely populated cities of the world and with no space to harvest sustainable energy in a traditional way, makes it the perfect place for the envisioned system. The vast majority of mankind populates (mega-)cities. If it is possible in a city such as Hong Kong to accomplish a reduced demand of conventional energy it should be possible in other cities around the world that have less pressure in terms of populace and available space.

1.3 Hybrid building-integrated photovoltaic

PV, BIPV, BAPV and PV/T, are all abbreviations well-known in the photovoltaic sector, but what do they mean? This section will give a basic explanation of every aspect of *hybrid building-integrated photovoltaic*. To begin at the very basic level photovoltaic PV and ending with a hybrid building-integrated photovoltaic or BIPV/T.

Photovoltaic effect

Our economy is getting infiltrated more and more by photovoltaic technology, but what is photovoltaic exactly and how does it work? In short a photovoltaic device (i.e. a solar cell) converts solar energy into electricity. Light can be seen as photons carrying energy. Solar cells use semiconductor materials to capture this energy of the photons. Semiconductor materials are materials which lies between insulators, which can not carry electricity like glass or rubber and conductors which are electricity carriers like copper.

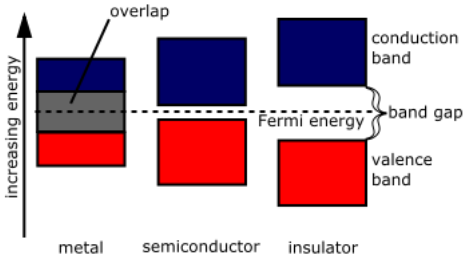

Figure 1.3: A sketch illustrates the difference between a metal(conductor) on the right, semiconductor an insulator on the left via energy band diagrams [4]

In Figure 1.3 the difference between the materials is shown in an energy diagram. Every picture has two bands a conduction band and a valence band, these are energy levels. For electrical current to flow the electrons have to jump from the valence band to the conduction band. In conductors like metals the bands are overlapping and this is why electrical current easily flows in a metal. By a "perfect" insulator a big gap between the two bands can be noticed which results in a charge not being able to move freely and make a closed path which is needed for electricity. A perfect insulator does not exist when applying high voltages to insulators even they will conduct.

By semiconductor materials there is also a gap but this gap can be crossed if the energy received by the electrons in the valence band is big enough to let them cross this gap and leave a hole behind. A hole can be seen as a positive elementary charge. This is what happens when these photons from light get absorbed by the semiconductor. These photons excite the electrons and generate an electron-hole pair. The electron crosses the gap allowing charge carriers to move which is the definition of electrical current. Because they can move from the valence band to the conductor band, normally the electrons fall back to their original energy level and find a hole to combine with. For electricity the free electrons and holes have to be captured and this occurs when membranes are formed on both sides to capture the holes and

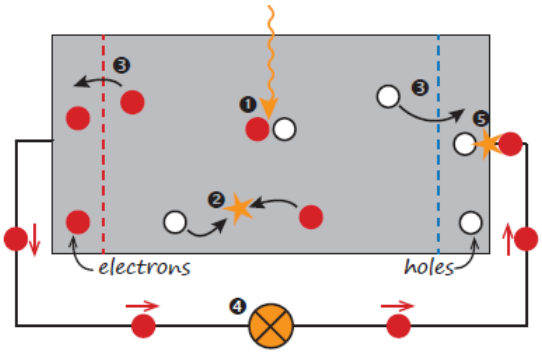

Figure 1.4: This sketch illustrates a simple model of solar cell [5]. The red circles are representing (negative) electrons and the white dots (positive) holes. First light comes in(1) creating a hole electron pair(2). The electron and holes get separated by the field(3). Finally the electrons move via an extern circuit back to the holes(4).

the electrons and in this way let them recombine through a circuit, see a simple model in Figure 1.4.

Nowadays there are different kind of solar panels, popular commercial technologies are: monocrystalline, polycrystalline, thin film technologies and hetero-junction technologies. In the Table 1.2 below a comparison of the solar panel technology is shown.

Table 1.2: Comparison of the different solar panel technologies

Technology	cost	weight	efficiency	influence of temperature	building-integrated
monocrystalline	-	+/-	+	-	-
polycrystalline	+/-	+/-	+/-	-	-
thin film	++	++	-	+	+
hetero-junction	–	+/-	++	+	-

As can be seen, the hetero-junction technology and thin film technology are having a lot of pluses. Monocrystalline is a well established technology in the industry because the efficiency is good, but the hetero-junction technologies performs better on efficiency although it is more expensive. If a lighter panel is feasible, for example for building integrated system, a thin film solar panel is the best choice.

The influence of temperature is positive if the efficiency of the solar panel drops less in comparison with the other technologies. Thin film and hetero-junction have less influence of temperature then monocrystalline and polycrystalline. The difference between polycrystalline and monocrystalline is that polycrystalline is cheaper but the efficiency is lower.

Building-integrated photovoltaic

Building-integrated photovoltaic or short BIPV are solar panels used in the structure of the building, for example replacing a part of the wall, glass facade or roof. In this way there is a

saving in the cost of the material otherwise used to cover the part of the building. It combines the function of the wall with producing electricity for the building or the national grid. BIPV is nowadays the fastest growing market segment in the field of photovoltaic. [15].

More reasons to choose BIPV or PV on buildings are: (i) The facades covered with BIPV system gain less heat, because a part of the solar energy is converted to electricity, this decreases the demand of air conditioning units. (ii) The producer and consumer are close to each other, so the losses in transportation can be neglected. These two reasons also decrease the demand and level out the peaks on the grid during day hours.

Solar collector

Solar collector is a technology widely used to convert the solar energy into thermal energy. A solar collector is a dark glass plate with below tubes with water or air flowing through which is heated up by the temperature increase of the plate due to solar radiance.

Hybrid building-integrated photovoltiac

The last step is the hybrid building-integrated photovoltiac. On the market there are three types of solar panels:

1. The solar panels consisting of solar cells, converting solar power to electricity
2. The solar collectors, use the solar power to heat water or air
3. A combination of both and this is a hybrid solar panel or PV/T

The hybrid building-integrated photovoltiac technology encompasses both solar cells and a solar collector integrated in the building, so the heat produced by the solar cells can be used to heat up water or air and such heat can be transferred away from the solar cells, thus keeping (mostly) unaltered their electrical performance. An example of a hybrid solar panel is shown in Figure 1.5.

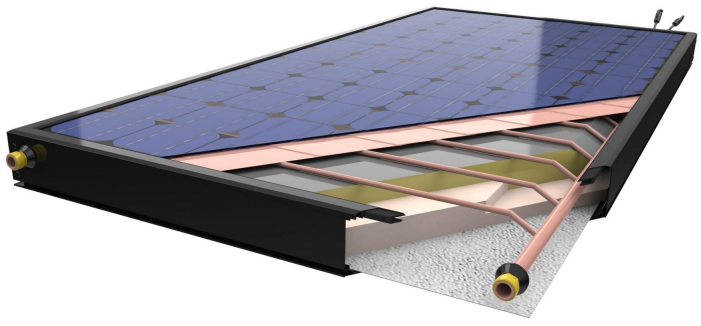

Figure 1.5: A picture of a hybrid solar panel, provided by [6] showing the stacking of photovoltaic cells on tubes.

By combining the two types into one solar panel, space is saved. Half the space is required by positioning the solar cells on top of the solar collector and the hybrid panel will produce electricity and thermal energy in water or air, that can be used for (pre)heating of water or heating up a space.

Photovoltaic cells combined with collectors is still a novel concept, but different papers have already investigated combining the two concepts. There are three methods of combining the two techniques:

- air PV/T collector
- liquid PV/T collector
- PV/T concentrator

The combination of air with solar panels is a technique that has the advantage of lower construction and operating costs compared with the systems with liquid, but the systems with water are more effective in removing heat from the solar panels. [16] Another beneficial property of water is that it absorbs mainly light from the infrared region and is thus compatible with solar cells. [17]. A disadvantage of liquid collectors is that the liquid can become frozen and damage the solar panel, but in case of Hong Kong this is not a concern due to the warm climate. In the case of the subtropical climate of Hong Kong warm water is preferable above hot air, because warm water can be reused and there is not a demand for hot air. PV/T concentrators are not chosen for this system, because of the high solar path in combination with the tilt of the solar panel, these panels are less widely available on the market and a complex implementation on a facade.

BIPV has already proven its advantages in different projects in Hong Kong. [18] These BIPV systems are implemented on government buildings, commercial buildings, schools and institutional buildings. The motivation behind the BIPV instead of PV was the price, by using BIPV as part of the building envelop, costs can be saved. Which decreases the biggest disadvantage of solar panels, the initial costs.

1.4 Work already being done

In this field of work a lot of research is already done and this thesis will not develop a new model, rather it will combine different models together into one framework to calculate the electrical and thermal yield of a building integrated hybrid solar system. This system is built on the facade of the building. The thermal model is built in TrnSys which has a good reputation in modeling, handling and simulating energy thermal models. Matlab is used for the electrical part, this is because of the powerful calculation capability and easy modeling properties and finally SketchUp in combination with Meteonorm is used to acquire the specific 3D model and determine the irradiance data on the facade including height and shadow. The combination of these tools has not been undertaken before. The modeling in my thesis will be further elaborated in Chapter 3.

There are different ways to model a hybrid solar panel system. Some studies based their modeling on the control-volume finite difference approach, this is a developed dynamic model. The model divides the component into different nodes and by doing so allowing a better analysis of the transient behavior of different parts inside of collector. [19, 20] The model was verified with measurement data and it showed a good alignment. One study [21] compared a dynamic model with three different steady state models, with different degradations in which information is included. All the four models are well in range with the experimental data. The steady state models which are easier to implement and less time consuming, perform in the same range as the dynamic model. A conclusion which was drawn is the error made by neglecting the dynamic effects is very small. Although the one-dimensional steady state model performs as well as the two and the three dimensional, are the 2D and the 3D in favour because they are more flexible in case of more complex hybrid panels. Nevertheless in case the collector temperature at the starting point differs from the one at the end of the measurement the time-dependent model is needed for an accurate prediction of the thermal yield. Another way to model a hybrid panel is via the energy balance equations of the different components in the solar panel, the model assumes the system to be quasi steady state. The model also shows good alignment with experimental data. [22]

Hybrid building integrated photovoltaic in Hong Kong are modeled and simulated before [23–25], conclusions which were found are a reduction in space cooling energy consumption. In summer the space heat gain reduced with an average of 50-56%. The combination of the two technologies has a greater effectiveness in reducing than just the BIPV, because the heat from the photovoltaic cell is transported away. A 10-25% increase in electricity production was found in a simulation comparing BIPV with a hybrid BIPV for the climate of Athene. [26]

Some papers looked into the effect of flowrate on the performance of the solar panel [7]. The simulations performed showed that there is an optimum flow rate, where the benefits of PV cooling comes together with a good thermal performance. One of the research questions in this paper will look into the flow rate and the effects on both the electrical and thermal yield. Three other studies looked into a thermosyphon water heating system [19, 27, 28], this is making use of natural circulation of the water, because of gravity and heating up of water. Results showed that a high water temperature can be achieved after one day of solar exposure. The advantage of the system is the elimination of the cost for pumping. Both studies showed that an application with photovoltaic combined with thermal can bring down the payback period. It combines the two solar systems on one surface.

A topic in building integrated hybrid solar panels nowadays is how to improve the efficiency of the hybrid panel. Key parameters are the fin efficiency, the thermal conductivity between the cells and the supporting structure and the lamination method. [29] Another aspect found in this paper, which will also be investigated in this thesis, is the difference in cost when integrating solar panels in the building instead of mounting the solar panels on the building. There are also some studies regarding the cover of the solar panel. Normally by solar collectors, covers are used to capture more heat, but for solar cells it degrades the performance,due to the extra layer which has some reflection. A relative new concept is to combine the production of hot water, hot air and electricity. In this study they made use of a two-dimensional steady state model. They found that the mass flow rate of the fluid has little effect on the behavior

of the solar air collector part. For a given collector length and mass flow rate they acquired a thermal efficiency of 80% and the cooling of the photovoltaic cells is satisfactory. [30]

These studies did not investigate the potential of making use of the complete facade and they did not include the shadow coefficient into their calculations. This are improvements to the research which will be investigated in this thesis. The different components used in the system is also part of the scope, like the solar panels, converters, pumps and the tank.

Scope of the thesis

For this thesis, focus was on a existing building in Hong Kong financial area, that is the commercial skyscraper International Commerce Centre.

For this case an integrated solar-thermal-energy study and a cost analysis will be made. Futhermore a solar system is designed including the balance of system, by means of simulations carried out with commercial packages (Matlab, SketchUp and TrnSys). The hybrid solar panel used in the system is chosen from available commercial solar panels.

Not included in the scope of this thesis is the cooling influence of the hybrid solar panels on the temperature of the building. The measurement data used in this thesis is done by government parties or universities.

Research questions

In the process of facing the upcoming challenges a framework of questions is formed. The main research question is: What are the opportunities for hybrid building integrated photovoltaic/thermal system in a world city as Hong Kong?

- How much solar energy can be harvested in a city as Hong Kong?
- How does the solar path of Hong Kong influence the orientation of the panels in the system?
- What is the influence of the flowrate on the yield of the solar panels?
- How much electrical/thermal power can be generated by a hybrid photovoltaic systems on a skyscraper?
- How is the yield of the system compared with installed power and with the total electrity demand?
- How does a hybrid photovoltaic system compare with respect to a photovoltaic system from both energetic and economic stand point?
- How long is the economic payback time of the system?

1.5 Thesis outline

The thesis is divided into five chapters.

Chapter 1 - The introduction

Chapter 2 - PV potential in Hong Kong consist of a location survey, a solar study and an energy study of the city of Hong Kong.

Chapter 3 - Modeling framework explains and shows the models used during the project and gives the basic formulas. It will inlcude a description of the irradiance model; direct and diffuse,thermal model made in Trnsys and the total model.

Chapter 4 - Case study: International Commerce Centre begins with a description of the case and the location. Secondly a description the results of a solar study, thermal study and an energy study are described. Furtermore a cost analysis with the design of the hybrid BIPV system.

Chapter 5 - Recommendations and conclusions includes topics which are out of the scope of the thesis and recommendations for future work. The second part of this chapter will be the overall conclusion of the research, in which the answers on the research questions will be covered.

Chapter 2

PV potential in Hong Kong

At the end of 2014 Hong Kong was a city with around 7.2 million inhabitants and the population is still growing. [31] With 6 690 persons per square kilometer Hong Kong is one of the most densely populated areas in the world. This chapter will first elaborate more on the location of Hong Kong and will be followed up by information about the energy usage of the city and the amount of energy the Sun delivers to Hong Kong.

2.1 Location survey

Hong Kong is a city located in the South East of China on a latitude of 22°15 Northern Hemispheres and longitude of 114°10 Eastern Hemispheres. It is a coastal city facing the South China Sea. Hong Kong has a total area of $2,755\,km^2$ of which $1,105\,km^2$ is land and $1,649\,km^2$ is sea. [32] The terrain is dominated by hills and mountains and this is why only 34.5% of the total land area is utilized. [33]

According to the Hong Kong observatory [34], the climate of Hong Kong is sub-tropical, with high humidity and much rainfall in spring, hot and humid summers with sporadic showers and thunderstorms, warm autumns with plenty of Sun but also with a good chance of tropical cyclones and soft winters which are more cloudy. The average temperature is between the 16°C in winter until 29°C in summer. The mean rainfall ranges from about 1400 millimeters to more than 3000 millimeters annually. The most of this rain around 80% falls between May and September. The average relative humidity is all year high, around 78.0%.

2.2 Solar potential

Hong Kong has 1835.6 Sun hours a year and a mean global solar radiation of 1302.8 kWh/m^2. Every hour during the daytime the area of Hong Kong receives 500 GW of solar power, this is more than 100 times the power usages of the whole city of Hong Kong. The mean of 1302.8 kWh/m^2 has been calculated over 29 years by the Hong Kong Observatory, from 1981 to 2010. The last three years this global insolation was higher than the average which can be seen in table 2.1. Due to the average amount of cloud cover of 68% Hong Kong has a significant part of diffuse radiation in the global solar radiation.

Table 2.1: The global solar radiation measured over 29 years, 2013, 2014 and 2015 for the city of Hong Kong. [9]

	mean	2013	2014	2015
Global solar radiation (kWh/m^2)	1302.8	1352.8	1412.3	1395.1

Hong Kong is a world city and well known because of having the most skyscrapers in the world, it is a high density and high rise city. This makes it difficult to find a suitable location to harvest this solar potential. Around the world rooftops are getting used for installing solar panel installations, but in Hong Kong this is not that easy because of the high rise buildings the solar panels on the roof can never support the high electricity or hot water demand for all the building floor levels. That is why in this thesis facades will be investigated as possible locations for solar systems.

Solar path

To find out the potential of the Sun a closer look to the solar path is required. The position of the Sun through the year is also needed to calculate the irradiance on the solar panel. Due to the low latitude of Hong Kong a high solar height is expected. An overview of the position of the Sun in the sky seen from fixed point like the earth at the same time of the day throughout a year is given in a solar analemma. Two angles are of importance to make the solar analemma: The altitude of the Sun and the azimuth of the Sun. The method to calculate the altitude and the azimuth is presented by a course "PV Systems" given at the Delft University of Technology [35]. In this section the most important formulas will be presented with an explanation of different angles for a more throughout derivation the manual can be consulted.

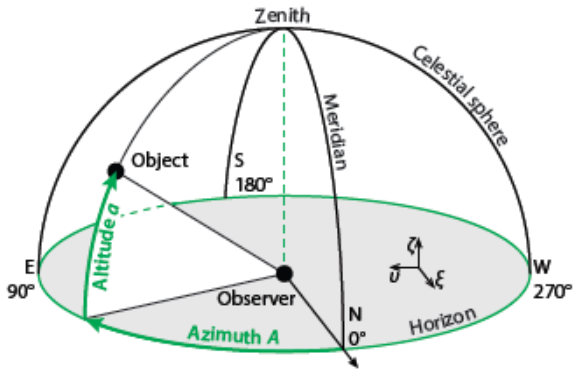

Figure 2.1: Sketch taken from [5] illustrating the altitude and azimuth

Altitude of the Sun

First of all the altitude of the Sun a_s or the elevation angle of the Sun is the angular height of the Sun in the sky measured from the horizontal, with an angular range $a_s \in [-90°, 90°]$. The maximum is at solar noon or zenith and it is 0° at sunset and sunrise. For an explaining illustration of this angle Figure 2.1 can be advised.

$$a_S = \arcsin(\cos\phi_0 \cos\theta_L \cos\lambda_S - (\cos\phi_0 \sin\theta_L \cos\varepsilon) \sin\lambda_S) \tag{2.1}$$

where
ϕ_0 = Latitude angle
θ_L = local mean sidereal time in degree
λ_S = ecliptic longitude of the Sun
ε = axial tilt of the earth

The latitude angle depends on the location on earth you are, it is positive for the Northern Hemisphere and negative for the Southern Hemisphere. The local mean sidereal time measures the rotation of the earth relative to the stars on a specific location and can be calculated with the next formula:

$$\theta_L = GMST \cdot 15°/hour + \lambda_0 \tag{2.2}$$

where
GMST = Greenwich mean Sidereal Time
λ_0 = Longitude

The Greenwich mean sidereal time is the sidereal time calculated on the Greenwich line. The longitude is also location dependent and positive for the Eastern Hemisphere and negative for the Western Hemisphere.

The ecliptic longitude of the Sun is the longitude of the Sun in the ecliptic coordinate system. This system takes into account that the Sun is not exactly moving over the equator but that the earth is slightly tilted. This axial tilt is defined by ε. Both variables are a function of the

time elapsed since Greenwich noon, Terrestrial Time, on 1 January 2000 in days. A better understanding of these two variables can be found in Figure 2.2.

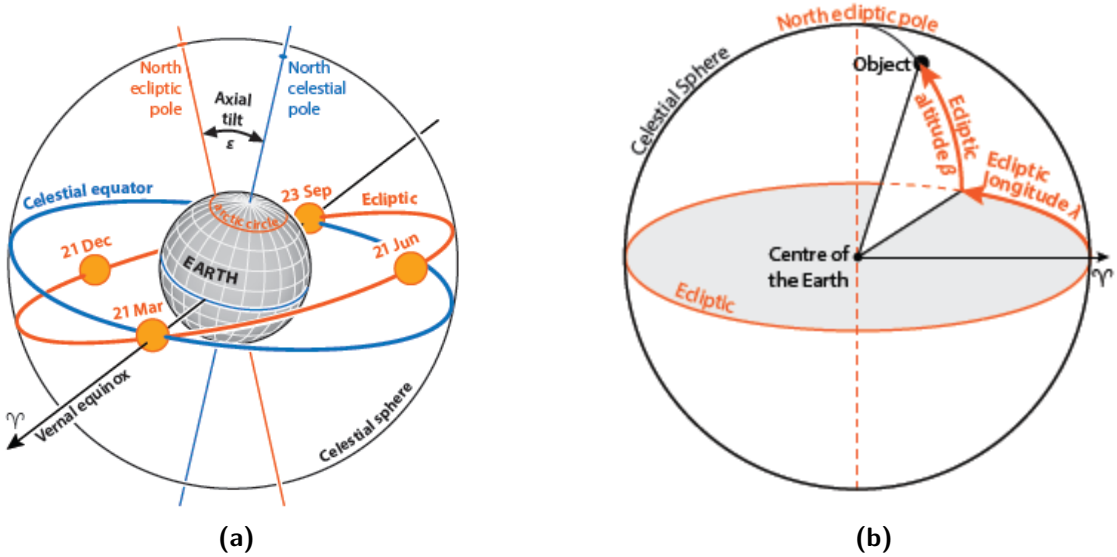

Figure 2.2: Two sketches taken [5] to explain the ecliptic coordinate system. a) The ecliptic coordinate system, with the definition of the axial tilt ε and the movement of the Sun through the year. b) The definition of the ecliptic longitude and altitude with respect to the centre of the Earth

Azimuth of the Sun

The azimuth angle A_S of the Sun is defined as the compass direction the sunlight is coming from. It is defined as 0° for the North direction, 90° for the East direction, 180° for South and 270° for the West direction. This can also be found in Figure 2.1.

$$A_S = \arctan \frac{-\sin\theta_L \cos\lambda_S + \cos\theta_L \cos\varepsilon \sin\lambda_S}{-\sin\phi_0 \cos\theta_L \cos\lambda_S - (\sin\phi_0 \sin\theta_L \cos\varepsilon - \cos\phi_0 \sin\varepsilon)\sin\lambda_S} \tag{2.3}$$

where
ϕ_0 = Latitude angle
θ_L = local mean sidereal time in degree
λ_S = ecliptic longitude of the Sun
ε = axial tilt of the Earth

An explanation of the different angles can be found in the last section. In the following Figure 2.3 the altitude and the azimuth as function of time through the year can be seen. In Figure 2.3a you can see that in the summer months the altitude of the Sun is the highest and almost reaches 90° this means that the Sun is exactly above your head so there are almost no shadows. In the winter it can be seen that the altitude is much lower this is because the days and solar path are shorter. In December the biggest shadow is expected. The azimuth

shows the same pattern, it is wider in the summer and during the winter the days are shorter so the azimuth range is also smaller.

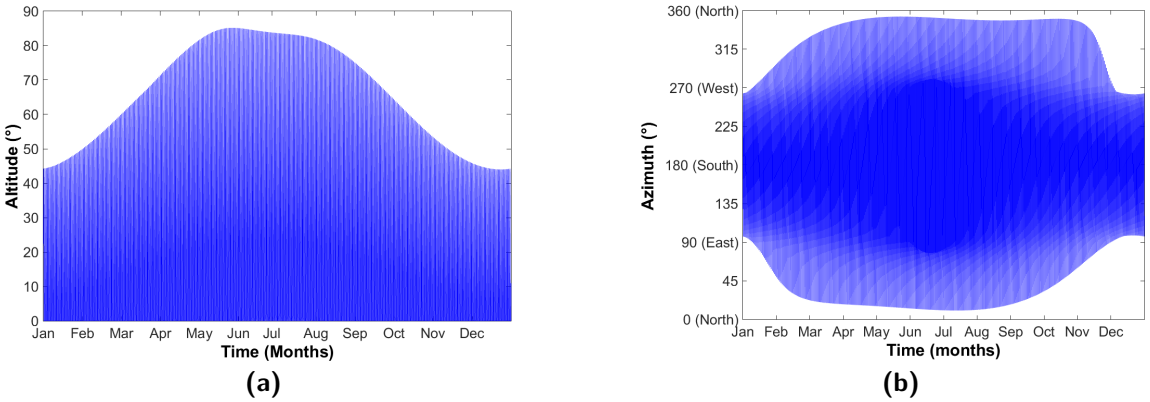

Figure 2.3: a) The altitude and b) the azimuth of the Sun given through the year for the location of the ICC in Hong Kong

With both the altitude and the azimuth as function of time, the solar path can be determined by plotting the altitude as function of the azimuth for different times in the year. This is shown in Figure 2.4. The thick lines shows the Sun on the same time every day of the year. The thinner lines show the different solstice and equinox. The December (winter) solstice is the lowest one and has a altitude range from 0° to 45° and the June (summer) solstice has the biggest range from 0° to almost 90°. The March and September equinox are almost the same as this is also according to the definition of the equinox [36]: *"An equinox is a day when the Sun is in its zenith over the Equator, and the Earth experiences days and nights of generally equal length."* With the solar path the shadow coefficient can be determined on a building surface. With the shadow coefficient the estimation of the radiation on the surface through the year is closer to reality.

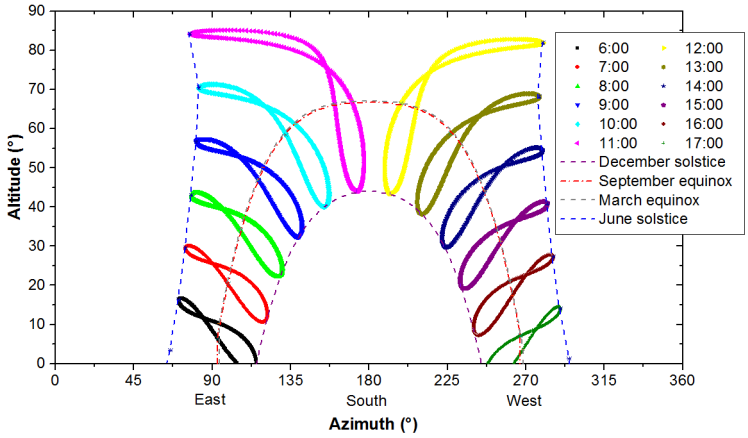

Figure 2.4: The Sun analemma of Hong Kong

2.3 Energy analysis

According to the annual energy report of 2015 [37] published by the Census and Statistics Department the annual total energy consumption is 88.5 TWh, from which 34.9 TWh is electricity consumption. With a population of 7.155 million people this leads to a consumption of 4.8 MWh per capita. Of this 34.9 TWh, 11.7 TWh is imported this is equivalent to 33.5%. Only 0.57% of the energy is renewable and from this 0.57% only 1.5% is solar energy.

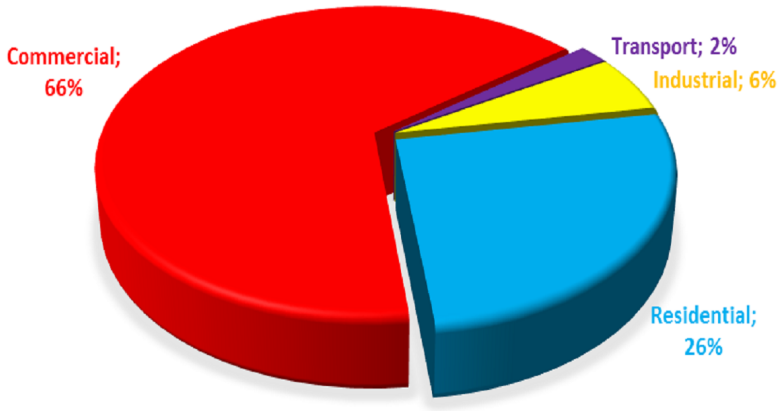

Figure 2.5: The electricity consumption of Hong Kong divided over the different sectors

Hong Kong does not have much available land and because of that not much industry. Figure 2.5 shows the electricity consumption by the different sectors. The biggest sector is the commercial sector, this is also the sector that the economy of Hong Kong is based on. The

second biggest is the residential. The commercial sector will be further investigated in this paper.

The next step is to take a closer look on the end-uses of the electricity. The following Figure 2.6 shows on the left the total electricity end-uses and Figure 2.6b and Figure 2.6c show respectively the end-uses of the residential and the commercial sector. The space conditioning is a big part of this electricity end-use. Next to space conditioning, lighting has also a significant part more in the commercial then in the residential sector. Hybrid solar panels can reduce the demand of space-conditioning, lighting and hot water.

Air-conditioning is the biggest consumer of electricity in Hong Kong with 30 % this is not that strange with an average of 23.3 °C. This consumption can be reduced by solar panels on the facade, because the solar panels will reduce the incoming solar power and reduce in the same time the heating of the building. Secondly lighting can be reduced if transparent solar panels are used which reduces the direct light in the room. Why not use the Sun as a lighting source? Finally, by using thermal solar collectors the energy of the Sun can be converted into thermal energy in water and by doing so reducing the energy needed to heat up water.

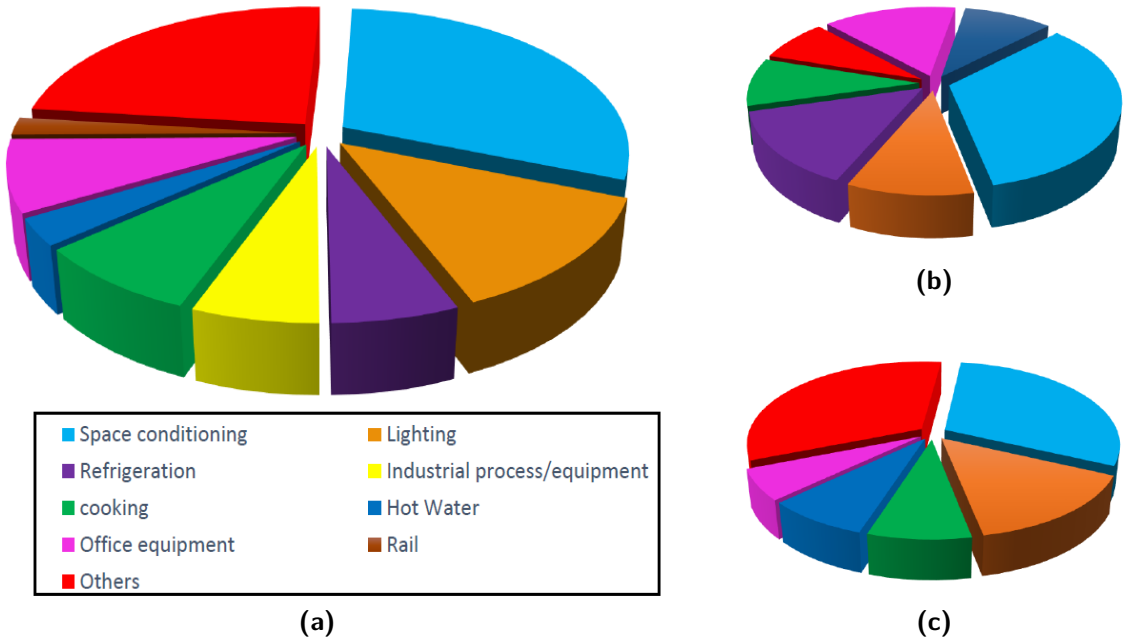

Figure 2.6: Pie charts depicting (a) the electricity end-uses in Hong Kong, (b) the residential electricity end-uses and (c) the commercial electricity end-uses.

2.4 Summary

Hong Kong is a city located in the South East of China on a latitude of 22°15 Northern Hemispheres and longitude of 114°10 Eastern Hemispheres. Hong Kong has 1835.6 Sun hours a year and a mean global solar radiation of 1302 kWh/m^2. Every hour during the day the area of Hong Kong receives 500 GW of solar power. As expected the altitude of the Sun becomes high during the summer according to the Sun anelemma of Hong Kong, see Figure 2.4. During the winter the Sun altitude reaches around 40°, in summer it almost reaches 85°.

The energy consumption of Hong Kong is 88.5 TWh, from which 34.9 TWh is electricity . The commercial sector is with 66% the biggest consumer of electricity. One of the biggest loads are the air-conditioning units in Hong Kong with 30%. One of the by-products of this thesis project is the decreasing of air-conditioning units.

Chapter 3

Modeling framework

Models are needed to be able to do calculations on systems which do not exist yet and to make an analysis before drawing conclusions. In this chapter the different models used will be described, an irradiance model, a thermal model and the final model which is the hybrid solar system. Different software tools are used to make these models. Next to the three different models, there is a section about the metrics used in the life cycle assessment.

3.1 The irradiance model

The irradiance model used is made in MATLAB [38] a powerful computing software. The model exists of different parts. The goal of the model was to calculate, with given data from the weather station, the direct, diffuse and total irradiance on the panel as function of the altitude interval of the building (i) and the orientation of the facade on hourly basis. The model for the direct irradiance is based on the framework described by the European Solar radiation Atlas [39]. To include the altitude of the building in the model the building is divided in altitude intervals(i).

$$G_m^{tot}(t,o,p) = G_m^{dir}(t,o,p) + G_m^{dif}(t,o,p) \tag{3.1}$$

Where:
G_m^{tot} = Total irradiance on facade in W/m^2
G_m^{dir} = Direct irradiance on facade in W/m^2
G_m^{dif} = Diffuse irradiance on facade in W/m^2
t = time in hours
o = orientation in °
i = building interval

The input of the irradiance model is data from the weather station, this data is acquired with meteonorm [40] this software is often used by the industry, think of parties like Siemens, Sharp, Universities or ABB. The tool collects the weather data from different weather station around the world and stores it. For the irradiance model the diffuse horizontal irradiance,

global horizontal irradiance and the direct normal irradiance for Hong Kong is used as input. The location, the orientation, the tilt of the module and the location of the sun calculated in subsection 2.2 are inputs of the system.

Direct irradiance on the solar panel

Direct irradiance is sometimes also called the beam irradiance and this is the part of solar light what has a straight line from the sun to the earth and in this case module. The first step is calculating the direct irradiance on the solar panel. Which is given by:

$$G_m^{dir} = DNI \cdot \cos(AOI) \tag{3.2}$$

Where:
G_m^{dir} =direct irradiance on solar module
DNI = Direct normal irradiance
AOI = Angle of incidence

The angle of incidence is the angle between the normal from the solar panel and the incident direction of the sunlight. The complete derivation can be found in the book written by the photovoltaic group of the Delft University [41], the resulting formula is:

$$\cos(AOI) = \cos(a_M)\cos(a_s)\cos(A_M - A_s) + \sin(a_M)\sin(a_s) \tag{3.3}$$

Where:
a_M = altitude of the module, which is also $90 - \theta$.
θ = tilt of the module.
a_S = the solar altitude(2.1).
A_M = the module azimuth.
A_S = the solar azimuth(2.3).

In the case of the system which is built on facades the tilt is 90°and the formula for the angle of incidence can be simplified to:

$$\cos(AOI) = \cos(a_s)\cos(A_M - A_s) \tag{3.4}$$

The direct normal irradiance can be used from the meteonorm data or can be calculated with the next formula:

$$DNI = I_a \cdot \exp[-0.8662 T_L(AM2) m \delta_R(m)] \tag{3.5}$$

Where:
I_a = extraterestrial irradiance
$T_L(AM2)$ = The Linke turbidity factor for an air mass equal to 2
m = relative optical air mass
$\delta_R(m)$ = integral Rayleigh optical thickness

The extraterrestrial irradiance is the intensity of the sun at the top of the Earth atmosphere. It fluctuates with 6.9 during the year from 1.415 kW/m^2 in January to 1.321 kW/m^2 in July.

The average is 1.367 kW/m^2 and is called the solar constant. The function to described this fluctuates is:

$$I_a = I_0 \times (1.00011 + 0.034221\cos(b) + 0.00128\sin(b) + 0.000719\cos(2b) + 0.000077\sin(2b)) \quad (3.6)$$

Where:
I_0 = is the solar constant $1.367 kW/m^2$
$b = 2\pi \cdot DOY/65$
DOY = Day of the year

The linke turbidity factor is: *"an indicator of the number of clean dry atmospheres that would be necessary to produce the same attenuation of the extra-terrestrial solar radiation that is produced by the real atmosphere."* [42]. As input for the model the Linke turbidity factor on monthly based is used from a nine year study done by the City University of Hong Kong. [42].

The relative optical air mass is the ratio between the optical path length of the sunlight through the atmosphere and the shortest path, which is the optical path through a standard atmosphere at sea level with the Sun at zenith. The relative optical air mass has no unit and is a function of the solar altitude [43]

$$m(a_s) = \frac{\exp(-z/z_h)}{\sin(a_s) + 0.50572(a_s + 6.07995)^{-1.6364}} \quad (3.7)$$

Where:
a_s = the solar altitude
z = the elevation of the solar module
z_h = The scale height of the Rayleigh atmosphere near the earth surface, given 8.345 m.

Finally the Rayleigh optical thickness is the optical thickness of a Rayleigh scattering atmosphere, along a defined path length as function of the relative air mass.

$$\delta_R(m) = 6.62960 + 1.75130m - 0.12020m^2 + 0.00650m^3 - 0.00013m^4 \quad (3.8)$$

Diffuse irradiance

The next component is the diffuse irradiance on the solar module. For the diffuse irradiance model different models are known. The following calculations is based on the model of Perez et al. [44]. This choice for the model of Perez et al. [44] is based on two studies done by the City University of Hong Kong on building facades in Hong Kong [45, 46] and an evaluation done in Bangkok with 12 models, where the model of Perez et al. [44] shows the best agreement with the measured tilted data. [47].

The diffuse irradiance exist of two parts a sky diffuse part and a ground diffuse part:

$$G_m^{dif} = G_m^{sky} + G_m^{ground} \quad (3.9)$$

Where:
G_m^{sky} = Diffuse irradiance in kW/m^2 coming from the sky
G_m^{ground} = Diffuse irradiance in kW/m^2 coming from the ground (albedo component).

The sky diffuse irradiation describes the sunlight that has been scattered in the atmosphere, but that still made it down to the earth and in this case to the solar module. In case of diffuse irradiance, the highest yield is expected from a horizontal module. It is given by the formula:

$$G_m^{sky} = DHI[(1 - F_1)\frac{(1 + \cos(\theta))}{2} + F_1(a/b) + F_2 \sin(\theta)] \tag{3.10}$$

Where:
DHI = Diffuse horizontal irradiance
F_1 and F_2 are the Perez coefficients, which describe circumsolar and horizon brightness.
θ = the tilt angle of the module.
a and b are functions.

The next step is defining the Perez coefficients and the functions a en b

$$F_1 = \max[0, (f_{11} + f_{12}\Delta + \frac{\pi\theta_Z}{180^\circ} f_{13})] \tag{3.11}$$

$$F_2 = f_{21} + f_{22}\Delta + \frac{\pi\theta_Z}{180^\circ} f_{13} \tag{3.12}$$

Where:
$f_{11}, f_{12}, f_{13}, f_{21}, f_{22}, f_{23}$ are Perez coefficient which can be found in the tables of Perez [44]
$\Delta = DHI \times m/I_a$
$\theta_Z = 90^\circ - a_S$

Finally function a and b are defined as:

$$a = \max[0, \cos(AOI)] \tag{3.13}$$

$$b = \max[\cos(\theta_Z), \cos(85)] \tag{3.14}$$

This model is made in Matlab with the help of one of the toolboxes in Matlab: *PV_LIB toolbox* made by the Sandia National Laboratories. [48]

The second part of the diffuse irradiance is the ground diffuse irradiance. This is the light reflecting back from the ground to the solar module. It is defined as:

$$G_m^{ground} = GHI \cdot \alpha \cdot (1 - SVF) \tag{3.15}$$

Where:
GHI = Global horizontal irradiance
α = albedo or reflection coefficient of the ground.
SVF = sky view factor

The albedo or reflection coefficient of the ground defines how much the ground reflects the sunlight and in the model a constant is used, found in literature. The sky view factor tells how much of the sky is visible from a point of view. For a building facade this is always less than 50% and in the case of buildings in close surroundings, blocking the sky, it drops more. The sky view factor can be calculated by a formula, but in that case the tilt of the module is only taken into account. To include also data from the surroundings this factor is calculated with SketchUp, which also includes the surrounding buildings. This is done with the plugin from LSS Chronolux. [49]

3.2 Thermal model

This section will describe what the thermal model looks like and what the inputs and the outputs are. It will begin with an overview of the total model and then zoom in on the smaller parts of the model. The thermal model is made in TRNSYS [50] a software tool made by the University of Wisconsin with the focus on thermal and electrical energy systems. TRNSYS is well known and well used software tool in the market and under scientists. The input of the thermal model is the data from the weather station and the outputs are: the temperature of the hybrid solar panel, the thermal yield of the panel, the thermal efficiency and the increase in water temperature.

TRNSYS is a simulation tool with a library full of different models. Next to the software a description of all the models is also provided by the university. It is possible to change the models yourself, but this is not done during this research. It is a simple model and does not include yet data from the building's air conditioning savings, this is possible but was not in the scope of this research. The aim was to get thermal data of a hybrid solar panel system.

The final model of the system is a model for the whole system on one building, it is a function of which building, because the weather data is dependent on the orientation of the solar system. In Appendix A the model can be found. The thermal model build is a scale version of the reality, this is because it is not ideal to make a simulation in TRNSYS with 19000 hybrid solar panels. Figure 3.1 give a small overview of the different components in the model.

To begin with examining the main part the water system. A tank is located on top of every residential building in Hong Kong, this is the start of our system. This tank is filled by the government, this is not included in the model. The first assumption is the tank will always be full. The first line coming in the tank is from the left bottom corner this is the load demand of the building and can be scaled down if needed with the calculator symbol. The load for the Riveria Garden is based on four people in a family, 200 apartments in the building and a 25 storey building. A daily hot water consumption of 160 liter for one family is taken. [51] The color of this line is blue, this means a cold water connection. The blue lines are also between the tanks and the pumps, the pumps distribute the water to a series of parallel panels. From the panels back to the tank are red lines which shows the water is heated up. From the tank to the pipes is a purple line because the water is already cooled down a bit because of the colder water in the tanks.

In the total model every facade has a pump and the pump is connected to four panels, the amount of connected panels to the pump does not have to be four, it merely illustrates more panels can work on one pump. Every facade has also his own controller which compares the input and output temperature from the solar panel on the facade and monitors the temperature to the load. When the temperature at the output of the solar panel is higher than the input the pump should be on and when this is not the case the controller assures that the pump is off. To save pumping energy.

Next to the water network there is the weather inputs from Meteonorm on the left side of the schematics. Information from these files goes to the solar panels, tanks, pipes but also to the

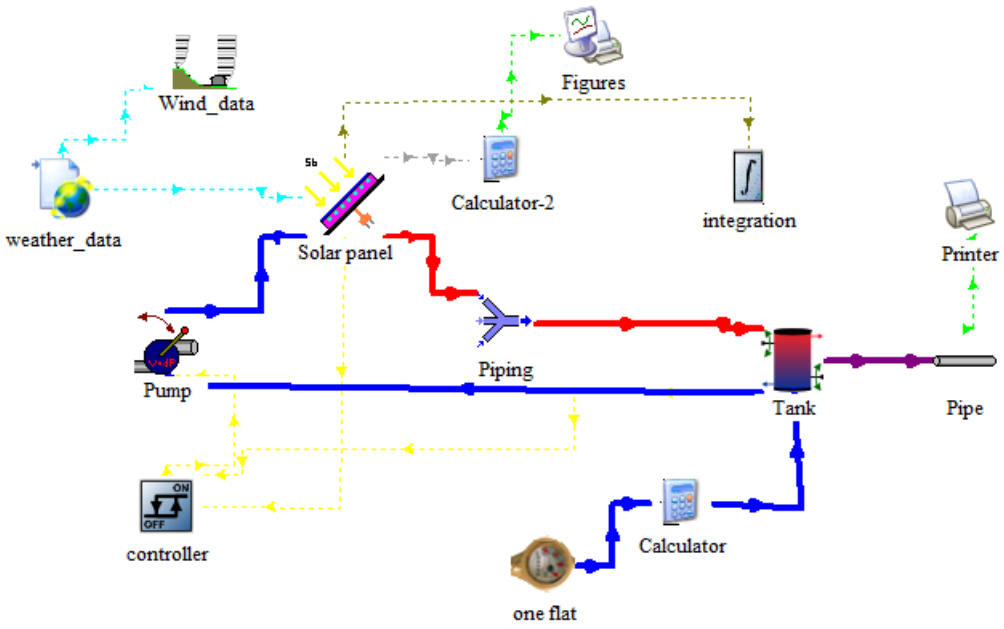

Figure 3.1: A simple overview of the different parts of the thermal model in TrnSys. Below the pictures is a small explanation of what the function of that part is. The lines connect to the different parts with each other.

output as reference and as input for calculators. Hourly data which is used in the program is:

- Dry bulb temperature or ambient temperature
- Effective sky temperature
- Total and diffuse horizontal radiation
- Total tilted surface radiation
- Angle of incidence for surface
- Slope of the surface
- Ground reflectance

The last part of the schematics are the data lines, calculators, integration units and the outputs. There are graphs which show temperatures, power outputs and flow rates and some integration units to calculate total power output on yearly basis. The model works using an hourly basis. All the data lines are dotted and have different colors which signifies their function. The lines for calculators are grey, the lines to/from the controller are yellow, lines for the integration units are light brown and the lines to the data and figure outputs are green. Light blue dotted lines are used for weather data.

In the thermal model wind speed and ambient temperatures at different height is calculated and taken into account. The wind speed and the height is getting into the model of the solar panel via the top loss coefficient and the ambient temperature. The ambient temperature at a certain height is given by [52]

$$T_a^{height} = T_a^{weather} - (height \cdot 0.0065) \tag{3.16}$$

Where:
$T_a^{weather}$ = Ambient temperature at the weather station level.
$height$ = Mounting height of the hybrid solar panel

The top convection loss coefficient (h_{cl}) is a coefficient which exists of two parts: i) a natural convection loss and ii) a forced part. The top convection loss coefficient is given by [53]:

$$\begin{aligned} h_{cl} &= \sqrt[3]{h_{nat}^3 + h_{forc}^3} \\ &\begin{cases} h_{nat} = k(sin(\theta)(T_m - T_a))^{1/3} \\ h_{forc} = av^p \end{cases} \end{aligned} \tag{3.17}$$

Where:
T_a = ambient temperature (°C)
T_m = module temperature (°C)
h_{nat} = natural convection losses
h_{forc} = forced convection losses

θ = tilted angle of the solar panel (90°)
v = wind speed
The parameters $\{k, a, p\}$ are given by literature [53] and were obtained by performing experiments and measurement with different values and searching a minimum value of the root mean square error. The wind speed at different heights is calculated by a model from TrnSys libraries. This is partly done in the wind data tool see Figure 3.1 and partly by a calculator. The wind speed at the height of the weather station is an input for this model and is given by the meteorological data.

Pump

The pump assures that the water from the tank goes to the solar panels and back from the solar panel to the tank. The flow rate, fluid density and fluid specific heat are parameters which can be set in the pump. As input the pump works on a control signal from the controller, it gets a flow rate and fluid temperature from the tank and the efficiency can be inputted. The flow rate from the tank does not do anything in the model, it exists just for balance checking. Another important input is the pressure drop this one is set and changes when more panels are connected to the pump. A pump with power dependence on flow rate, pressure drop and efficiency is chosen, because not one but more panels are connected to one pump. This is to save on pumps in the system and also saves space for these pumps. The flow rate used is found from a range specified in the data sheet from the hybrid solar panels and is decided after a simulation to see which flow rate gives the best efficiency for the whole system.

In this system each facade has their own pump and all the outputs are connected to each other and flowing into the same tank. By taking a high flow rate, the water will transport the heat from the panel faster away which decreases the solar panel temperature and increase the electrical efficiency. Alternatively, by increasing the flow rate the power consumption by the pumps will also increase and the water temperature will increase less compared with a lower flow rate. Another factor in this system is the influence of the four facades on each other because the water which is flowing to the system is coming all out of one tank and goes back to the same tank.

The flow rate which flows through the pump is a function of the rated flow rate and the control signal:

$$\dot{m} = \gamma \cdot \dot{m}_{rated} \tag{3.18}$$

Where:
$\dot{m}$ = average mass flow rate (kg/h)
γ = control signal (input coming from controller)
$\dot{m}_{rated}$ = rated flow rate (kg/h) (parameter)

Another important output is the power consumption of the pump and which percentage this is of the total yield. The power consumption is given by:

$$P_{pump} = \frac{\Delta p \dot{m}}{1000 \rho_{fluid}} \tag{3.19}$$

Where:
P_{pump} = power consumption (kj/h)
Δp = pressure difference (kPa)
$\dot{m}$ = average flow rate (kg/h)
ρ_{fluid} = fluid density (kg/m^3)

Hybrid solar panels

The model used for the hybrid solar panel is made by the Thermal Energy System Specialists (TESS), this is an engineering consulting company specializing in the modeling and analysis of innovative energy systems and buildings. It is a combined PV/T solar collector. It models an un-glazed solar collector which produces electrical power and thermal power from photovoltaic cells. These cells are embedded on top of a absorber plate on which tubes are bonded which leads the heat via a fluid stream out of the solar panel.

The electricity model is a linear model which relates the electrical efficiency to the cell temperature and the solar radiation received by the panel. In this research the electrical part of the model is done in Matlab, so this will not get elaborated in this part. In TRNSYS the focus will be on the thermal model. The thermal model is based on Chapter 6 of the "Solar Engineering of Thermal Processes" textbook by Duffie and Beckman. [54] In the book they make use of an one dimensional steady state thermal model actually designed for a flat plate thermal collector, but with some small adjustment also applicable for the thermal part of a hybrid solar panel. In this thesis the basic formulas are presented, for more complete derivations the following papers can be consulted [7, 29] or the derivation by the company TESS. [55]

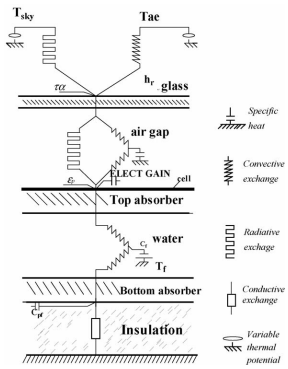

Figure 3.2: The heat flow network [7] divided in different interfaces

The hybrid solar panel can be divided in different interfaces with different heat flows and losses see Figure 3.2. On top the ambient and the sky layer, followed by the glass layer. Then the air gap, cell layer and the top absorber. Next are the water layers(the tubes), the bottom layer and finally the insulation. The overall heat loss coefficient can be expressed into three parts.

$$U_L = U_{top} + U_{frame} + U_{bottom} \tag{3.20}$$

The top loss coefficient describes the interface from collector plate to the front glazing and is a function of the ambient temperature, the mean plate temperature, the wind velocity, the different emittances and the tilt angle.

The frame loss coefficient or the edge loss coefficient is a function of the dimensions of the collector, the thermal conductivity and the thickness of the insulation material at the edge. The bottom loss coefficient is a function of the back surface temperature, the absorber plate temperature and the resistance to heat transfer provided by the insulation material, which is high. This last coefficient is usually small and can be neglected.

Another important output is the useful heat gain that can be calculated with:

$$Q = F_R A_{coll}[G_m^{tot}\tau\alpha_{abs}(1-\xi) + G_m^{tot}\tau\alpha_{cell}\xi - G_m^{tot}\tau\xi\eta_{cell} - U_L(T_{in} - T_a)] \tag{3.21}$$

Where:
F_R = heat removal factor
A_{coll} = The collector area (m^2)
G_m^{tot} = incoming solar radiation on solar panel(W/m^2)
τ = transmittance of glass cover
α_{abs}, α_{cell} = absorptance of absorber plate and photovoltaic cell respectively
ξ = packing factor
η_{cell} = photovoltaic cell efficiency
U_L = Overall heat coefficient (W/m^2K)
T_{in} = Temperature at the inlet temperature (K)
T_a = ambient temperature (K)

The heat removal factor describes the amount of heat which can be guided away and takes into account the mass flow rate and the specific heat of the cooling medium, water in this case. The values of the transmittance and the absorptance are found in the literature [7, 29] and these describe material properties. The packing factor describes the ratio between the collector plate area and the solar panel area on top of it.

The average temperature of the photovoltaic module is a function of the temperatures and the heat transfer coefficients on the top layer and is calculated with the following formula :

$$T_m = \frac{S + h_{outer}T_a + h_{rad}T_{sky} + \frac{T_{abs}}{R_T}}{h_{outer} + h_{rad} + 1/R_T} \tag{3.22}$$

Where:
S = The netto absorbed solar radiation (total absorbed - PV power) (kJ/hr)
h_{outer} = The heat transfer coefficient from the top of the PV surface to the ambient air (kJ/hm^2K).
h_{rad} = The radiative heat transfer coefficient from the top of the PV surface to the sky (kJ/hm^2K).
T_{sky} = effective sky temperature ($°C$).
T_a = ambient temperature ($°C$).

T_{abs} = temperature of the absorber ($°C$).
R_T = The resistance to heat transfer from the the PV cells to the absorber (hm^2K/kJ).

The parameters used in the model of the hybrid solar panels are partly from the datasheet of the used hybrid solar panel see Appendix C, partly from the defaults of TESS and partly from literature [7,29]. The inputs of the PV/T panel model are provided by the weather data from the Hong Kong Observation and from the tank via the pump.

Tank

The tank used in the model is from the standard library of TrnSys and is modeled as a tank with variable inlets and uniform losses. The tank is divided in different parts and is subject to thermal stratification. Both the heating elements in the tank are turned off, because in the case of Hong Kong the boilers are located inside of the houses and not included in the tank. The tank is divided into six layers. The cold water enters the tank in the bottom layers this is the closest to the temperature of the input water and goes out on the bottom part. The water coming back from the panels is entering the higher layers where again the temperature is the closest to the input temperature. The water going to the apartments is also coming from the top layers. In the case of six nodes and the setting that the water is entering the layer with the smallest temperature difference, a maximum degree of stratification can be accomplished. For the tank loss coefficient the standard of TrnSys is used.

3.3 Hybrid solar system

The last part of the model is made in Matlab and is called the hybrid solar system it is the integrator of the thermal model and the irradiance model. The input consists of the results of the irradiance and the thermal model. The output is the electric and thermal yield of the total system and the increase in water temperature. The yield of the system takes all the system losses into account. The total model includes the efficiencies of the solar panels and the balance of system(BOS). The efficiencies and yield in this model are calculated on hourly and yearly basis, this is to show how the performance changes through the season of the year. To describe the performance of the solar panel as a function of the irradiance on the panel and the hybrid solar panel temperature a framework of formulas is used which is described in the **Solar energy book** by the Delft University of Technology [41]. An overview of the total model is shown in Figure 3.3. The rectangular shapes are the three different model and the circular shapes are inputs.

Next to the efficiencies the yields are also outputs of the system. The thermal yield per four panels per facade on different altitudes is coming directly from the thermal model and only has to be multiplied by the number of panels. In this model the losses because of piping are not taken into account. The scope stops at the tank. Next to the thermal yield the water temperature is also coming from the thermal model.

The thermal yield comes directly out of the thermal model, likewise the water temperature, it is the useful energy gain and is used to derive the thermal efficiency of the system. The

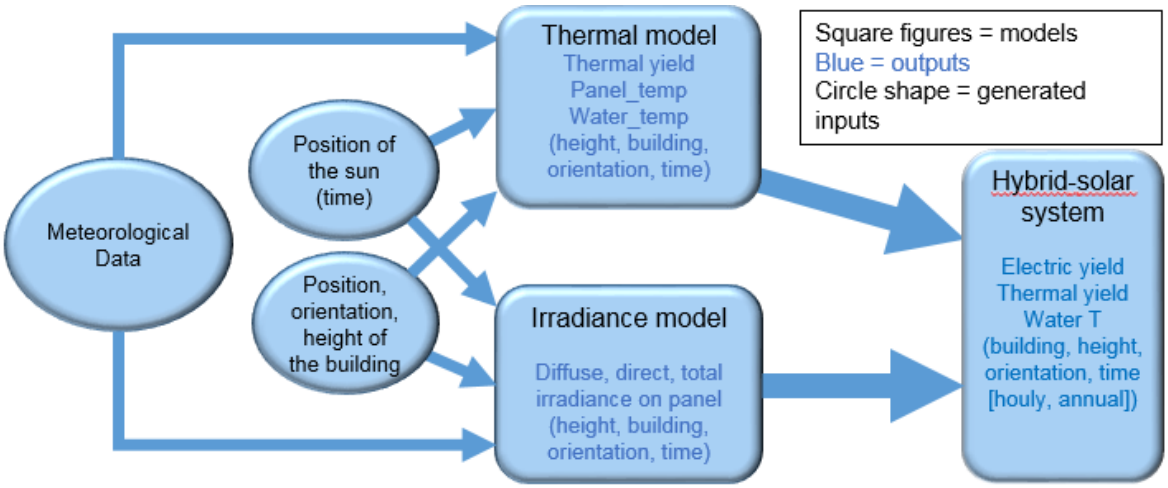

Figure 3.3: An overview of the developed model

thermal yield is calculated per four panels per facade on different altitudes. When multiplied by the total number of solar panels the total thermal yield can be obtained. In this model the losses because of piping is not taken into account. The thermal efficiency is given by:

$$\eta_{ther} = \frac{Thermal_{yield} \cdot A_{tot}}{G_m^{tot} \cdot A_{tot}} \cdot 100 \tag{3.23}$$

Where:
$Thermal_{yield}$ = Thermal yield in (W/m^2)
A_{tot} = Total area of all the panels in the system (m^2)
G_m^{tot} = The total irradiance on the panels (W/m^2)

The electric performance is a function of the temperature of the panel and the irradiance on the panel. The influence of the temperature is given by:

$$\eta(T_m, G_{STC}) = \frac{P_{mpp}(T_m, G_{STC})}{G_{STC} A_{mod}} \tag{3.24}$$

$$P_{mpp}(T_m, G_{STC}) = P_{mpp} + \frac{\partial P_{mpp}}{\partial t}(STC)(T_m - T_{STC}) \tag{3.25}$$

Where:
T_m = The temperature of the module $(°C)$
G_{STC} = The standard test condition irradiance: $1000 W/m^2$
A_{mod} = The area of the module (m^2)
P_{mpp} = Power at maximum power point (W)
$\frac{\partial P_{mpp}}{\partial t}(STC)$ = Temperature coefficient of the power given in the datasheet (-0,43%/°C)
T_{STC} = the temperature at standard test condition (25 °C)

The formula which gives the influence of the irradiance on the efficiency is:

$$\eta(25°C, G_m^{tot}) = \frac{P_{mpp}(25°C, G_m^{pv})}{G_m^{tot} A_{mod}} \tag{3.26}$$

Where:
G_m^{tot} = The total irradiance on the solar module
A_{mod} = The area of the module (m^2)
The power at maximum power point as function of G_m and at a temperature of $25°C$

$$P_{mpp}(25°C, G_m^{tot}) = FF \times V_{oc}(25°C, G_m) I_{sc}(25°C, G_m) \tag{3.27}$$

Where:
FF = is the fill factor of the photovoltaic cells given by $P_{mpp}/(I_{sc} * V_{oc})$
The open circuit voltage as function of the irradiance at a temperature of $25°C$ is given:

$$V_{oc}(25°C, G_m) = V_{oc}(STC) + \frac{nk_BT}{q} \ln \frac{G_m}{G_{STC}} \tag{3.28}$$

Where:
$V_{oc}(STC)$ = is the open circuit voltage at standard test conditions given in the datasheet.
n = the ideality factor of the solar cell has the value of 1.3.
k_B = Boltzmann constant: $1.38 \cdot 10^{-23} J/K$
T = Ambient temperature (K)

The ideality factor is a measure of the quality of the junction and the type of recombination in the photovoltaic cell and has a value between 1 and 2. Finally the short circuit current as function of the irradiance at a temperature of $25°C$:

$$I_{sc}(25°C, G_m) = I_{sc}(STC) \frac{G_m}{G_{STC}} \tag{3.29}$$

Where:
$I_{sc}(STC)$ = The short circuit current at standard test condition given in the datasheet.

To include the temperature variable also in the electrical efficiency the following formula is used:

$$\eta(T_m, G_m^{tot}) = \eta(25°C, G_m^{tot})[1 + \kappa \cdot (T_m - T_{STC})] \tag{3.30}$$

Where:
κ = the same as $\frac{\partial P_{mpp}}{\partial t}(STC) = -0.0043\%$

Combining and integrating the efficiency with the irradiance on the solar panel the electrical DC yield can be acquired.

$$DC_{yield} = \int_{year} \eta(T_m, G_m^{tot}) G_m^{tot} A_{tot} \mathrm{d}t \tag{3.31}$$

Finally the AC yield includes the efficiencies of the balance of system; micro inverter, cable losses and the maximum power point tracker inside of the micro inverter. These efficiencies are all given in the inverter data sheet and the cable losses are assumed.

$$AC_{yield} = DC_{yield} \eta_{inv} \eta_{mpp} \eta_{Others} \tag{3.32}$$

3.4 Environmental and economical life cycle assessment

In the Environmental life cycle assessment two environmental cost-benefit parameters are calculated and in the economical analysis one parameter is used. This section elaborates further on how to calculate these three parameters. The life cycle assessment is a technique to asses various aspects of a product and the potential impact throughout a product's life. [56] With this assessment the BIPVT technology can be compared with already known competing technologies. The evaluations can be done on cost investment, energy uses and Greenhouse Gas(GHG) emissions throughout its entire production and service life.

The first parameter is the cost payback time (CPBT) this is the total investment of all the different components of the system and also the labor including installation and engineering. Next to the initial investment there are annual costs of maintaining, repairing and keeping the system operational (M&O costs). During the product's life time the product generates a cash flow. The CPBT is the time it takes the system to generate the initial investment plus annual costs back.

$$CPBT = \frac{initial\ cost}{cashflow_{in} - annual\ M\&O\ costs} \tag{3.33}$$

The second and third parameters are the energy payback time(EPBT) and the greenhouse gas payback time(GPBT). These two parameters are used to evaluate the time it takes for the environmental benefits to start. [57]

$$EPBT = \frac{E_{emb}^{pvt} + E_{emb}^{bos} + E_{emb}^{mtl}}{E_{out}^{pv} + E_{out}^{ther} - E_{oper}} \tag{3.34}$$

Where:
E_{emb}^{pvt}, E_{emb}^{bos} and E_{emb}^{mtl} are, respectively the embodied energies of the hybrid solar panels, the balance of system(BOS) and the building materials (kWh).
E_{out}^{pv} and E_{out}^{ther} are the useful electricity and thermal output generated by the system in (kWh).
E_{oper} = the energy the system is annually consuming in pumping in (kWh).

$$GPBT = \frac{\Omega_{pvt} + \Omega_{bos} + \Omega_{mtl}}{Z_{pv} + Z_{ther}} \tag{3.35}$$

Where:
Ω_{pvt}, Ω_{bos} and Ω_{mtl} are, respectively the embodied GHG of the hybrid solar panels, the balance of system(BOS) and the building materials in $(kgCO_2 - eq.)$.
Z_{pv} = the reduction in GHG by the local power plant due to the electricity generated by the PV cells in $(kgCO_2 - eq.)$.
Z_{ther} the reduction in GHG by not using town gas due to the thermal output in $(kgCO_2 - eq.)$.

Both equations have a material component in the numerator. In case the hybrid solar panels were installed during the building phase of the building it can be neglected. In the case of the ICC, in this thesis, it is included because the building needs to be adopted for the installation.

3.5 Summary

During this project different models have been built to calculate the performance of a hybrid solar system on the ICC. The framework consists of exists of three sub-models: (i) the irradiance model (built in Matlab) (ii) the thermal model (built in TrnSys) and the integrator model (iii) (built in Matlab). In the modeling of the total system different software tools are used, like SketchUp, Meteonorm, Matlab and TrnSys, in this way the strength of each tool is combined. The final outputs of the model are the thermal yield, electrical yield and the water temperature. The last section includes the formulae used to calculate the parameters for the life cycle assessment. While the theoretical framework presented in this chapter is available in literature as independent sub-models, the innovation of this thesis is to combine all of them using specialized software for accurate calculation

Chapter 4

The International Commerce Centre

ICC is an abbreviation for International Commerce Centre and is located in West-Kowloon. The ICC is right now the biggest skyscraper in Hong Kong, it has 118 floors and is 490 meters high. The ICC is divided into three parts: The upper part a Hotel, the middle and biggest part offices and the lower part the commercial center. Below in Figure 4.1 a picture of the ICC can be found. With around $91200\,m^2$ of facade area there is a lot of space available for solar harvesting, this is comparable with the area of eleven soccer fields. The facades do not have the optimal orientation, but the advantage is that there is no need for transporting the energy far away and there is more space on the sides then on the roof. There are also some further reasons for selecting the ICC:

- The highest skyscraper in Hong Kong, so more area and less shadows
- Only on the northern facades are there buildings which gives shadows
- The use of ICC building represents the three main economic aspects of the city of Hong Kong (hotels, offices and shops).
- It has already a good 3D model in SketchUp plus the surrounding which saves time on the modeling part.

This chapter is about the case study on the ICC, which includes a detailed solar, thermal, energy and cost study and a design of the total system. The chapter includes more small summaries to keep the overview.

4.1 The model

To get a feeling of the surroundings and to do measurements on the building the program SketchUp is used, which can load in models and can perform different calculations on the 3D model. Sketchup is a 3D modelling software package which is commonly used in architectual design. SketchUp is used to calculate the Sunhours through the year and the shadow coefficient on hourly base. The plugins which are used for these operations are SunHours [58],

(a) (b)

Figure 4.1: The International Commerce Center; a) viewed from the harbor (South-West side) and b) from below between the building on the North-East side. Pictures provided by `http://www.chinesearchitecture.cn/` and `http://www.archdaily.com/`

LSS Chronolux [49] and SHADING Tools Plugin v1.0 [59]. The picture below in Figure 4.2a is a screen shot from the SketchUp model, the models of the different buildings are made by Hafidh Ihromi, Bethuko Koti and Sebastian S. The models are placed as they are placed on Google Maps and Geo-located at their location in Hong Kong. The second picture is a view from above and in here the orientation of the model can be found. The ICC is located on the water side that is why there are no buildings on the West side of the model. In the figure the ICC is encircled in white. The ideal facades are expected to be on the South-West and North-West facade. To analyze the ICC model, the building is divided into ten equal intervals plus a bottom interval which has a small angle compared with the rest of the facade.

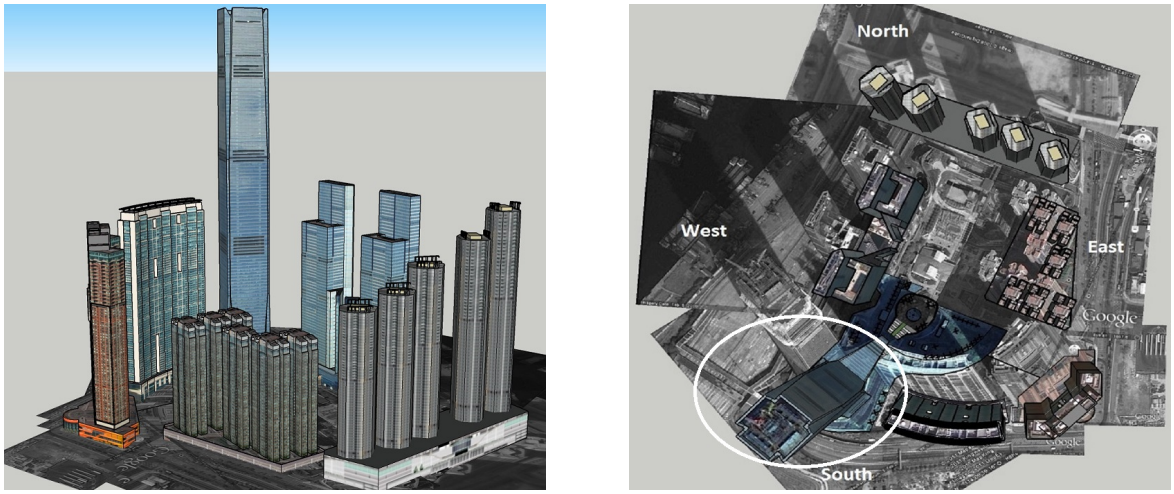

(a) (b)

Figure 4.2: The ICC as model in SketchUp. a) shown from the East and b) from above with the ICC encircled in white and orientations. North is the top of the picture.

4.2 Shadow analysis

In Chapter 2 the location of the Sun was analyzed and the solar path illustrated for the whole year. With the location of the Sun and the location of the building the shadow coefficient can be determined, which is needed for calculating the amount of radiation on the surface. The shadow coefficient is calculated by the plugin Shading Tools [59] in SketchUp. The definition of shadow coefficient by the software is: *"The ratio of solar radiation that enters through a fenestration system relative to that of a standard reference glazing composed of a single plane."* In other words it is the ratio of direct solar radiation received on the surface. The shadow coefficient is calculated for every facade of the ICC and for the whole ICC on hourly basis. Below in Table 4.1 the seasonal and annual shadow coefficients are presented for the facades and the total building.

Table 4.1: Shadow coefficient in percentages for different periods and orientations

	Period	Orientation				Whole
		NW	NE	SW	SE	
Spring	6 Feb - 7 May	40.09	32.89	62.92	55.16	48.74
Summer	8 May - 7 Aug	49.69	48.86	50.67	46.98	48.39
Autumn	8 Aug - 6 Nov	40.61	31.59	64.51	54.88	47.64
Winter	7 Nov - 5 Feb	27.64	14.17	79.09	71.13	47.77
All year	1 Jan - 31 Dec	40.29	32.73	63.93	55.70	48.17

The periods of the seasons are chosen around the equinoxes and solstices, because no weather data is included so these periods make more sense. The shadow coefficients of the spring and the autumn period are similar what can be expected because the solar path is the same, which is also visible in Figure 2.4. The next expected conclusion is that the southern facades

are performing better than the northern ones, this is because Hong Kong is on the Northern Hemisphere. The low shadow coefficient in the summer and high coefficient in the winter on the South facades can be explained because the Sun reaches in the summer almost the zenith and this is why less direct irradiance can reach the facade. By the northern facades winter is the worst season this is because the Sun is low and on the North side there are more obstacles which cause shadow. Overall the different seasons perform in the same range almost 50% and over the whole year the whole building has a shadow coefficient of almost 50%.

The graphs in Figure 4.3 show the shadow coefficient over time on the South-East facade divided over the different parts of the building on a day in June (21st) and respectively December 21st. The different parts of the building are shown with different colors. The biggest part of the facade is divided in ten intervals of each equal size and there is a extra lower interval which has a slight angle, this part is separated from the 100%.

For the example of June 21st all the lines above the eighth 10% are 100% from 6 am until 12 pm. The lower parts have first a rise in shadow coefficient, then a drop and finally a rise and a drop to zero again. This is due to the shadow moving from the left middle to lower right part. For December 21st the shadow coefficient is for the whole building between 8 am and 2 pm 100%, this means no shadow. Then it moves back to the zero line, the lowest parts of the building have the longest time a shadow coefficient above zero.

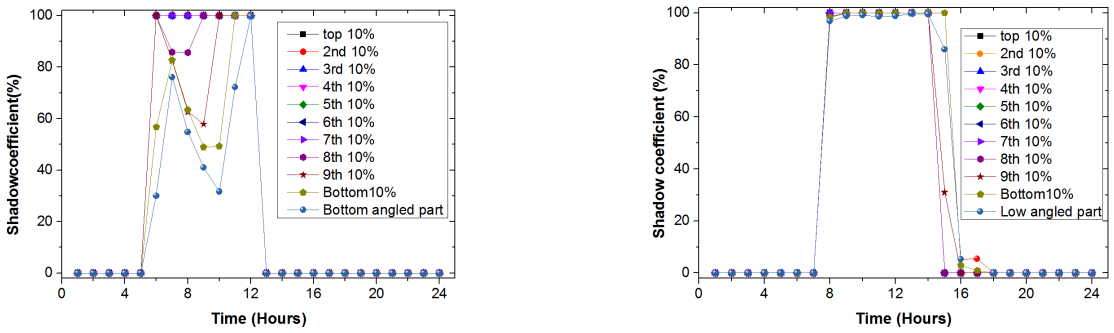

Figure 4.3: Shadow coefficient on the South-East facade as function of time a) on June 21 and b) on December 21

If the Shadow coefficient as function of time on June 21st will be compared to the one of December 21st a clear observation is that the one from June 21 is earlier in the day high and the winter one is shifted to the right. The shadow development is also more constant in the winter than in the summer.

The maximum shading on a surface occurs when the Sun has the lowest altitude angle. This is in the winter, the shadow falls mostly on the East facades, in the next two figures the shadow on the East facades on December 21st and June 21st are illustrated. This does not necessarily mean it has also the most shadow during the day, because on a winter day the facades receive more hours Sun than during summer. Which is due to the solar path, the solar path during

summer is higher than in the winter. The pictures of the summer are included to give a clear comparison. The lines show the insolation duration. This will be further elaborated in the next section. For the calculations the LCC Chronlux plugin is used. The shadow or insulation is measured in a timespan from sunrise until sunset [60] every minute. The timespan for the two different seasons is adopted for that season with sunrise and sunset times.

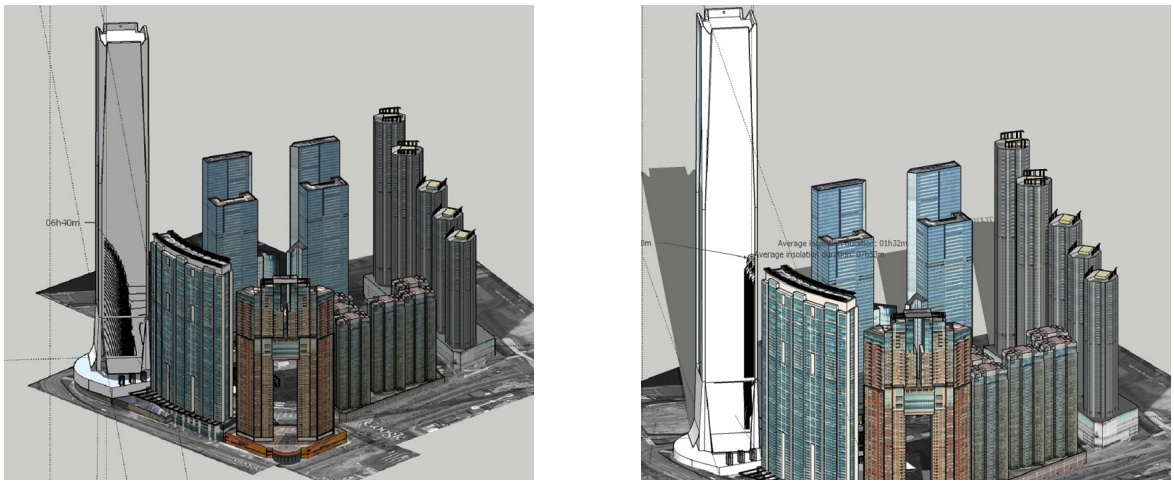

(a) (b)

Figure 4.4: Shadow development on the South-East facade a) on June 21 and b) on December 21

The first two figures in Figure 4.4 show the development of the shadow on the South-East facade. The highest shadow is as expected in the winter, but because of the solar path the solar duration is longer in December, seven hours and fifty minutes in comparison with six hours and forty minutes. In the winter all the shadow is on the right side of the facade and covers around the half of the height of the building. In the summer the shadow shifts from the right side to the left side of the facade this is again due to the solar path, but on June 21st the shadow is thirty meters lower. The reason behind the shadow is the building which is standing next to the South-East facade.

For the North-East facade, the shadow has a different shape, the shadow is now due to the surrounding buildings and it covers the whole width of the building. The winter is again a higher shadow than summer, but this time the duration is also lower, this can be explained by the orientation of the building which is more North facing. Generally, the northern facade is on the Northern Hemisphere the worst facade. In the summer this is not the case, this is because the Sun stands higher in the summer than in the winter.

So to conclude there is almost no shadow on the West facing facades, the only shadow occurs on the East facing facades. The highest shadow is in the winter. On the South-East facade the winter shadow takes one fifth of the width and a half of the height of the building. On the North-East facade the winter shadow is at around the same height as the South-East facade and it takes the whole width of the facade. An overview of the height of the shadows on both facades can be found in the Table 4.2 below. The summer shadow patterns are lower for both

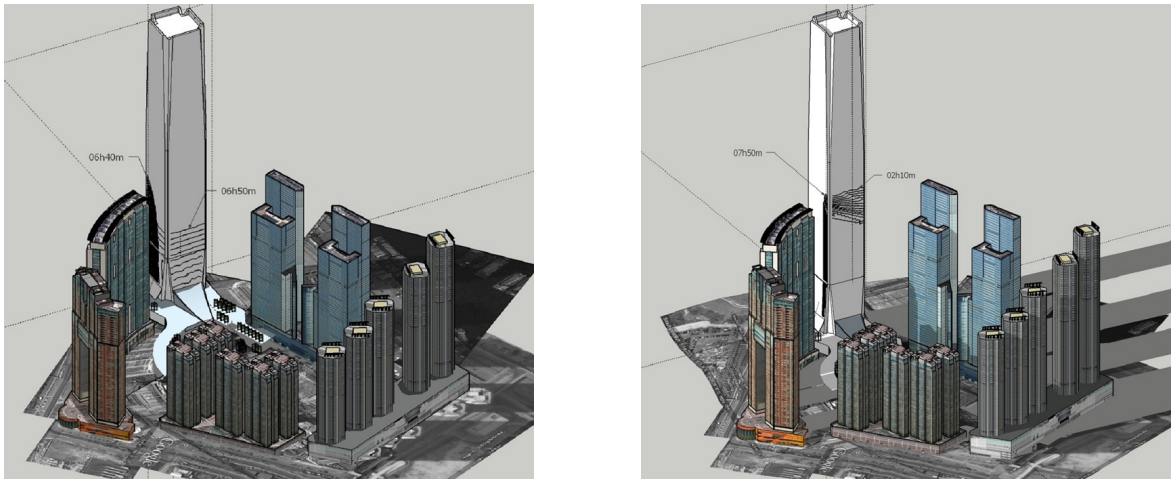

(a) (b)

Figure 4.5: Shadow development on the North-East facade a) on June 21 and b) on December 21

the facades. On the South-East facade the shadow changes from the right side of the facade to the left side.

Table 4.2: Height of the shadow on the two facades with shadow

Facade	Height of the shadow (m)
South-East	216
North-East	220
Total height	462

Summary

The shadow coefficient which is needed to calculate the amount of radiation on a given surface is calculated in SketchUp. The average shadow coefficient of the whole building is around 50%. The most shadows are found on the North-East facade. This is due to the buildings around the ICC. The best performance is measured on the southern facades during the winter months, this can be explained by the tilt of the hybrid solar panels, which is 90° and the solar altitude which is high in the summer. A decrease in altitude on the building gives an increase in shadow, which is due to the surrounding buildings. The shadows are much more uniform on the North-East facade and covering the whole width of the building.

4.3 Sun analysis

This section will discuss the Sun hours on the building and how the solar irradiation looks on the different facades of the building. This data is used to decided which part of the building will be used and how much yield can be expected.

Sun hours

The amount of Sun hours is calculated in SketchUp with the tool SunHours. It calculates the approximate amount of time that the selected point is in the Sun. The time stamp was one hour and the period from sunrise to sunset. First a grid was made on every facade from 8 by 8 meter to make the calculations less heavy. In the simulations five timespans are investigated; the month October (autumn), the month July (summer), the month April (spring) and the month January (winter). The last timespan was the whole year. A summary of the results of the simulations can be found in the Table 4.3. SketchUp makes next to the calculations a plot on the building with the grid and colors which shows the intensity of the Sun hours, an example on the East facades is shown in Figure 4.6. Here a clear difference is visible between the South-East (left) and the North-East (right) facade.

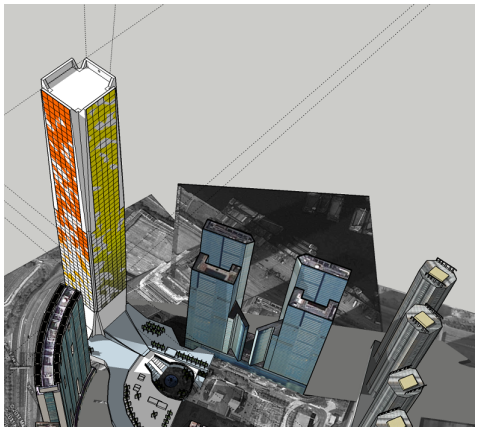

Figure 4.6: The result of the sunhour simulation performed in SketchUp. The color scale is from red(high intensity) to blue (low intensity) The simulation is done for the whole year on the East facades

Table 4.3: The percentage of sunhours on the four different facades in 5 different timespans

Period	Total sunhours	Orientation			
		NW	NE	SW	SE
Januari	305.72	18.9%	30.4%	69.6%	81.1%
April	326.13	32.5%	53.4%	46.6%	67.5%
Juli	344.95	37.1%	62.9%	37.1%	62.9%
October	328.74	24.6%	38.6%	61.4%	75.4%
All year	3876.82	28.4%	46.1%	53.9%	71.6%

	Amount of Sunhours
NW	1101.82
NE	1789.0
SW	2087.82
SE	2775.0

The first column after the timespan is the amount of sunhours in total. The cells on the right side of the table are showing the percentages of total sunhours for the given orientations. As expected are the South facing sides performing better. In the summer the East facing facades are performing better than the West facing and the amount of sunhours decreases for the South facing facades. A reason for this is the path of Sun and that the Sun in the summer almost hits the zenith around noon. Next to the table also a graph is included with the same results see Figure 4.6. The North-West facade is performing the worst through the whole year and the South-East is giving the most constant amount of sunhours. The trends of the North-East and South-West are each other opposites. Overall the summer is performing the worst, which is due to the 90° solar panels tilt and the Sun reaching almost the zenith. The maximum amount of sunhours is on the South-East facade and is 2775 hours a year, which is 71.6% of the total amount of sunhours in Hong Kong.

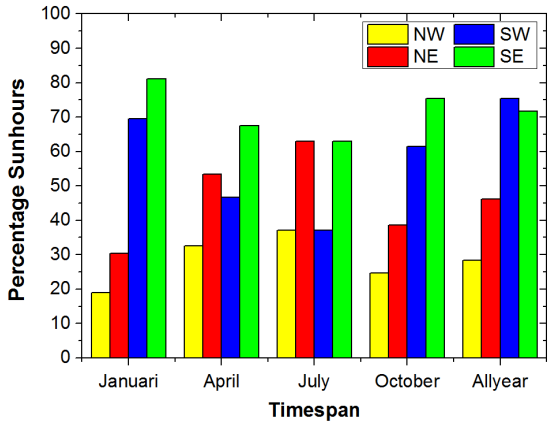

Figure 4.7: Sunhours ICC

Irradiance

The facade of the ICC can be divided in three parts. The lower bended part which will not be taken into consideration because of significant shadow from trees and surroundings. The part which has a slight angle compared with the 90° from the rest of the facade and the biggest part of the facade which has the 90° compared with the earth surface. The big part of the facade is divided into ten equal sections to include into the calculations: the shadows from the surrounding building, the wind and temperature at different altitudes. The lower slightly angled part is calculated separately because easier for the simulation, it is bigger and has a slight angle. In Figure 4.8 the part of the building which is used for the solar system is highlighted in red for the South-West facade.

The amount of irradiance is calculated by the model in Matlab. In the model the irradiance is divided into a diffuse component and a direct component. The diffuse part exists of a ground (albedo) part and sky part. The albedo constant for the ICC which is needed for the ground diffuse irradiance are based on research work done on a similar location in Hong Kong [61]. In the diffuse irradiance calculations the sky view factor is taken into account.

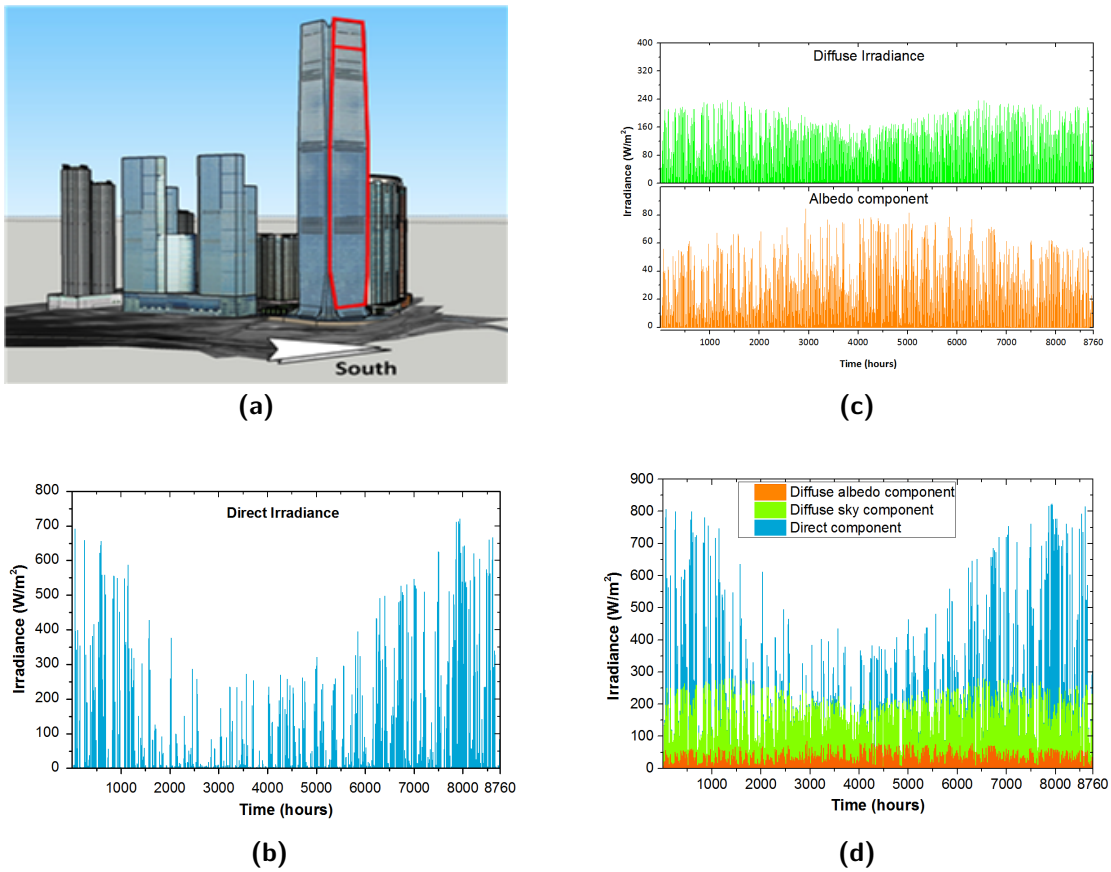

Figure 4.8: (a) The South-West facade of the ICC in Hong Kong (highlighted in red); the extra small red rectangle is the portion of facade for which calculated irradiance components are here reported. (b) Direct component of irradiance; (c) Diffuse component (top panel) and albedo component (bottom panel) of the irradiance; (d) The sum of the different components, the total irradiance; all components of irradiance are calculated per square meter as function of the time in the year.

In the direct irradiance the time-dependent shadow coefficient is taken into account, which Figure 4.8 reports the result of the irradiance model for the top interval of the South-West facade. Through the year the diffuse irradiance is stable as is the albedo component the direct and the total irradiance have a decrease in their characteristics during the summer, because of to the position of the sun which is close to the solar zenith and the orientation of the facades. This was already visible in the Sunhours and the shadow coefficient simulations.

The shadow coefficient and the sky view factor are calculated as function of time and for all the altitude intervals of the facade, eleven for every side, so 44 intervals in total this is done in SketchUp and exported to Matlab. Together with the models is for every interval the different irradiances through the year computed and the results are used as input for the hybrid-solar system model. Only the total irradiance is used as input to calculate the yield from the system. The effect of the shadow and the sky view factor is illustrated in Figure 4.9. The southern facades are performing the best this is probably due to the surrounding which is less at the South side of the building. The influence of the sky view factor and the shadow

on the yearly irradiance is the smallest on the North-West facade this because it is facing the harbor and the total irradiance is also lower on this orientation. All the irradiances are decreasing when the altitude decreases. For the northern facing facades the decrease start earlier. The South-West facing facade is decreasing the fastest

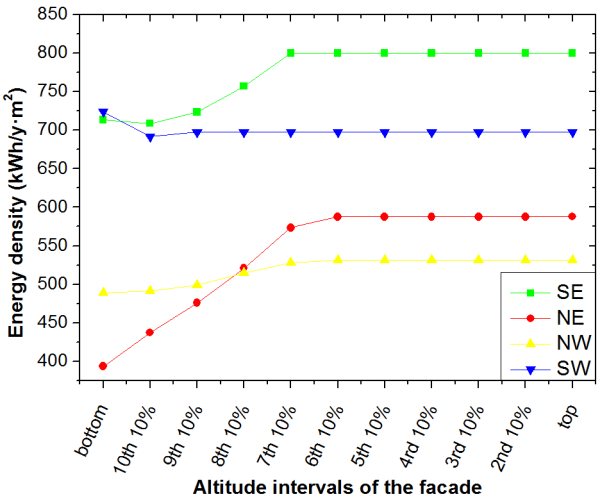

Figure 4.9: The influence of the sky view factor and the shadow on the yearly irradiance at different altitude of the facade; East facades are facing surrounding building, the West facades facing the harbor.

Generally, are the southern facing facades not performing the best in Hong Kong, but the South-West or East facades. An explanation is the role of the tilt of the panel on the irradiance. The tilt of the panel is 90°, which is not optimal for Hong Kong. The optimal tilt is around 22°. The highest direct irradiance is calculated in the winter months, but also in the summer month but for the West and East facing facades. An overview of the direct irradiance calculated for all the facade orientations through the year is shown in Figure 4.10

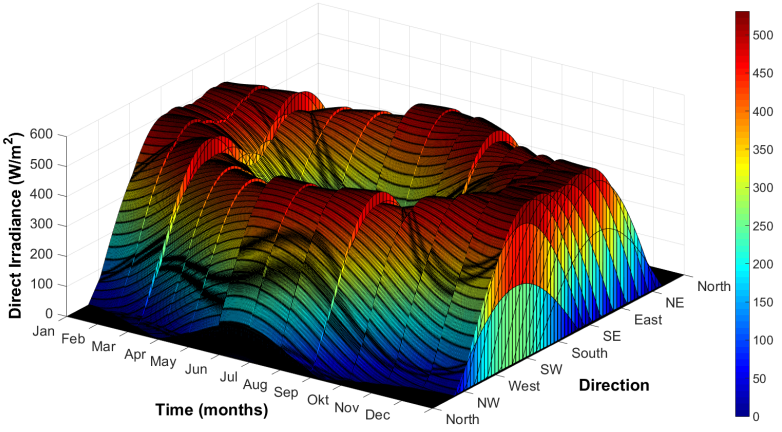

Figure 4.10: The direct irradiance on the facade as function of direction of the facade through the year.

Thermal results

A part of the irradiance is converted into electricity but the same irradiance is also partly converted in heat this section will include some of the results coming out of the thermal model made in TRNSYS. The input for the thermal model is the meteorological data from meteonorm which is the same as for the irradiance model. The output is the temperature of the solar panel to calculate the real efficiency, the water temperature and the thermal yield from the hybrid solar panel. The thermal yield calculated is the yield produced by the hybrid module and is used to heat up water. This yield can be used to heat up water in the tank. By heating up the water, the energy the boiler needs to heat up this water, decreases.

The thermal output is a function of different variables which have to get a value. Some of these values are found in literature and some are chosen. Two of these parameters are the size of the water tank and the demand from the water tank to the apartments. For the ICC there is no literature available with information about the size of the tank or the demand. For the simulation the same size is used as for the living estate which is known out of literature. To see the influence of the size of the water tank and the demand of the load simulations are done with a high demand, low demand and a big tank and a relative small size. The sizes are chosen based on literature from the Hong Kong government. [8]. The size of the big tank is 55000 liters and the size of the small tank is 500 liters, which is common used in thermal systems. The high demand is the demand for a whole estate [51] and the lower demand is based on one family's demand. The amount of the solar panels is less than the amount which will be mounted in the total system. The results of this simulations can be found in the graph in Figure 4.11 and Table 4.4.

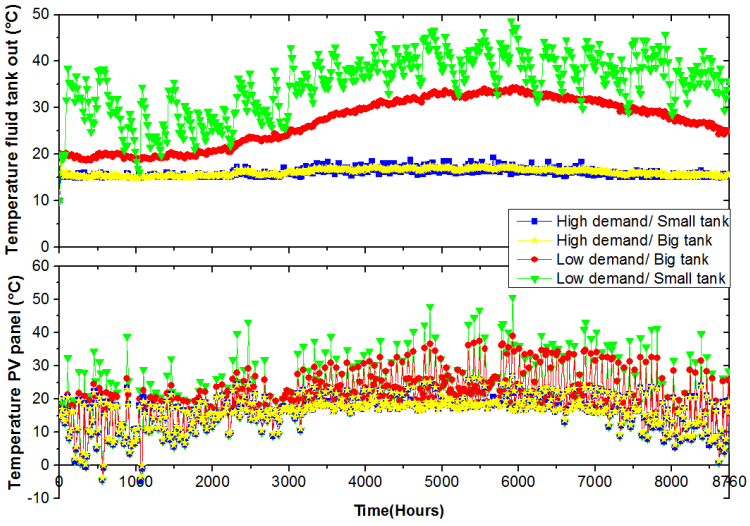

Figure 4.11: The influence of tank size and water demand on: top) the output temperature of the system (tank output) and bottom) the solar panel temperature

The choice for a smaller demand assures a higher output temperature but also a higher hybrid solar panel temperature which decreases the yield which can be seen in the results. A higher

demand assures more cool water in tank which can be pumped to the panels. The size of the tank has an influence, because a bigger tanks means more cold water.

Table 4.4: The influence of tank size and water demand on the thermal and electrical yield on the South-West top interval of the facade. The yield is specified as the annual energy on one m^2

Yield $(kWh/y \cdot m^2)$	high demand		low demand	
	small tank	big tank	small tank	big tank
Electrical	60.0	60.0	58.4	57.7
Thermal	418	409	101.77	49.45

In the case of a high demand the graphs look similar for both the output temperature of the system and the average temperature of the hybrid solar panel. When a high demand is possible the size of the tank is not of importance anymore. In case of a lower demand the temperature rises. The worst scenario is a low demand and a small tank. In this case the temperature of the solar panels increases the most and will the electrical yield decrease, because a decrease in electrical efficiency, which can also be found in the Table 4.4. In the table the thermal yield is also shown for the four different cases which shows the same relation. High demand gives a higher thermal and electrical yield and low demand leads to lower yields. The electrical yield shown, is the one coming out of the thermal model and is not the same as the one from total model. The downside of a higher demand is higher energy usage for the pump. This is a trade-off which has to be taken into account. For the model the high demand together with the big tank was chosen, because these have the highest electrical and thermal yield. The downside of this choice is the small temperature rise in the water. Which is probably because of high demand, the low amount of solar panels in the simulated system and the big size of the tank.

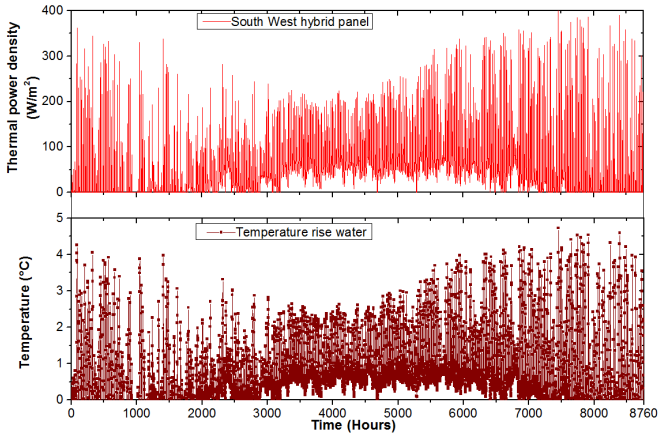

Figure 4.12: The difference in temperature of the in- and output tubes by a hybrid panel on the South-West facade at the top interval of the building. The upper graph shows the thermal power density at the same hybrid panel

In Figure 4.12 a closer look is taken to the real rise in water temperature on the solar panel level, this case on the South-West top interval. In the top graph the useful thermal energy

output is plotted. According to the model the water temperature rises in the summer with around 2 a 3 $°C$ and in winter an even higher rise of 4 a 5 $°C$. In this figure the rise in thermal output is directly visible in a rise in temperature. A part of this temperature increase will get lost in transport and mixing with the other panels and mixing in the tank.

Two parameters which were varied in the model to include the altitude in the solar panel temperature and the thermal output are wind speed and ambient temperature. In Figure 4.13 below the influence of altitude on the yield, the wind speed and the ambient and solar panel temperature is illustrated.

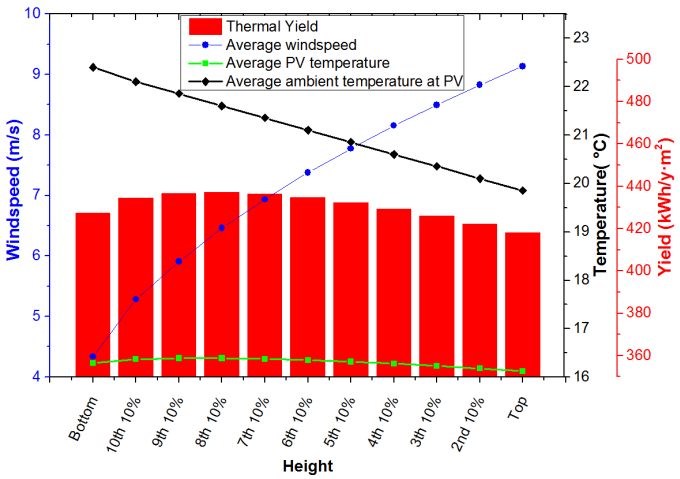

Figure 4.13: The influence of height on the wind speed, ambient and solar panel temperature and on the thermal yield. The simulation is performed on the South-West facade

When there is a decrease in height of the solar panel, the ambient temperature rises. The wind speed is also lower on lower altitudes. With the higher temperatures the yield increases which is expected, but the thermal yield decreases again at the lowest intervals. On the lower two intervals of the building the yield decreases again, this is not what expected. Further investigation shows a probably reason: the influence of the top losses. A bigger temperature difference is found between the ambient temperature and the module temperature on the lower intervals of the building, which increases the convective top losses. The difference between the highest and lowest yield is a small difference of only 19 kWh/m^2 per year, which is 4% of the total yield.

$$Q_{top}^{conv} = A_m \cdot h_{cl} * (T_m - T_a) \tag{4.1}$$

Where:
A_m = Area of the module in (m^2).
h_{cl} = Top convection loss coefficient.
T_m = Temperature of the module $(°C)$.
T_a = Ambient temperature $(°C)$.

Another important parameter is the flow rate of the system. There are two flow rates in the system, one is mentioned above as the demand, this is the flow rate out of the tank to the

consumer. A high flow rate out of the tank increases the thermal output significant. The other flow rate in the system is the one between the panels and the tank. The data sheet of the hybrid solar panel suggests a flow rate between 90 and 150 l/h. The system exists of panels and pumps on four facades. The simulation varied the flow rate between 8 l/h to 200 l/h and the thermal and electrical output were measured. With an increase in flow rate an increase in thermal and electrical output is found, until a certain point, then a decrease is measured. The four different facades are also influencing each other due to the mixing of the water after the hybrid solar panels. On individual facade level an increase in flow rate leads to an increase in yields, this is for all four facades the case. An increase in output is also expected because the panels are getting cooled more and there is more heat exchange possible when there is more water flowing at the back of the panels. The maxima for both electrical and thermal output per facade are found at a flow rate of 200 l/h, but combined the maximum for electrical are with a flow rate of 160, 200, 200 and 200 l/h for the NE, SE, NW and SW pumps. The highest thermal output is found at a uniform 120 l/h which is also in the range of the panel data sheet. The difference between the electrical output on the ideal case and the one with 120 l/h is less than 0.1% and it makes the system less complex. 120 l/h is the flow-rate chosen for the system.

The thermal yield for the top interval of the South-West facade through the year is visualized in Figure 4.14a. It is plotted against the total irradiance received on the same part of the building. The thermal output through the year seems stable and around 200 W/m^2. In the summer the efficiency is the best because of the drop in irradiance but the stable thermal output. The figure shows all day a thermal output around the summer, this is visualized by the blue below the red. It can also be seen in Figure 4.14b showing the yield for different orientations. In the right figure the solarpath in summer from South-East to North-West is clearly visible. Reasons can be the high amount of Sun hours and the ambient temperature which stays in summer easily above 20 degrees also during the night. Which keeps the solar panels warm and still be able to have heat exchange at the back of the panels.

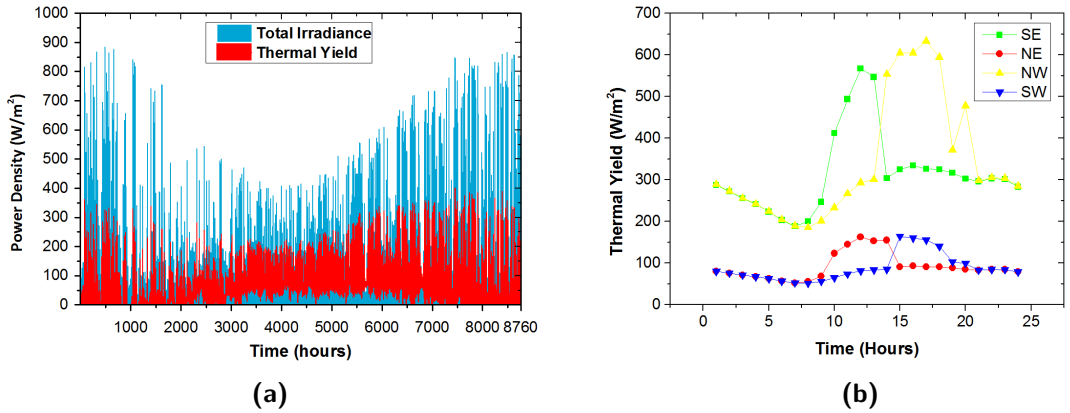

Figure 4.14: a) The thermal yield on the South-West facade as function of time and plotted with in the back the total irradiance and b) the thermal yield for all four facades for a typical summer day as function of time.

The Table 4.5 shows the thermal yield for one solar panel at different heights and different

orientations. As expected are the southern facades having the highest yield, but the solar panels at the northern facades perform better. Overall are the solar panels performing with a thermal efficiency of 53.12%.

Table 4.5: The thermal yields and efficiencies of one solar panel located on the different altitude intervals and facades of the ICC.

Interval	SE		NE		NW		SW	
	Thermal (kWh/year)	efficiency (%)	Thermal (kWh/year)	efficiency (%)	Thermal (kWh/year)	efficiency (%)	Thermal (kWh/year)	efficiency (%)
Top	676	48.96	533	55.45	555	54.54	687	49.72
2nd 10%	683	49.46	538	56.00	560	55.07	694	50.20
3rd 10%	689	49.93	543	56.52	565	55.57	700	50.66
4rd 10%	695	50.35	547	56.95	569	56.00	706	51.07
5th 10%	700	50.71	550	57.31	573	56.35	711	51.43
6th 10%	704	51.01	553	57.56	576	56.61	714	51.71
7th 10%	707	51.22	554	57.69	577	56.74	717	51.91
8th 10%	708	51.32	554	57.64	577	56.72	719	52.00
9th 10%	707	51.26	541	57.36	574	56.48	718	51.94
10th 10%	704	50.97	545	56.75	569	55.93	714	51.66
Bottom	692	50.12	530	55.23	555	54.55	702	50.82

Summary

The southern facades have almost double the sunhours compared to the northern facades. The most sunhours are for the southern facade during the January month and for the North facing facade during April and July. The irradiance is higher in the winter period than in the summer period. The diffuse irradiance is more constant through the year. The decrease in direct irradiance in the summer is expected due to the high altitude of the Sun in combination with the 90° tilt of the facades. The sky view factor is included in the calculations which results in a decrease in effect of the sky view factor on the East facade is higher than on the West facades.

The thermal model is built in TrnSys, in this program the thermal model is simulated and different parameters varied. The focus on modeling is a high electrical yield even if this leads to a lower thermal yield. When decreasing the demand and the size of the tank the water temperature coming out of the hybrid solar panels rises, which is expected because the water temperature in the tank rises which results in a higher panel inlet temperature. The water temperature characteristics follows closely to the thermal power density characteristics. In the model the influence of height on the wind speed, panel temperature and ambient temperature is included. The flow rate is varied in the system and the best flow-rate for the system is chosen to be 120 l/h. On individual facade level 200 l/h was the best option, but combined 120 l/h is. In the range given by the hybrid solar panel data sheet, is an increasing flow rate resulting in an increasing thermal yield. The average thermal efficiency is 53.12%, with the highest efficiencies on the northern facades.

4.4 Total system

The total irradiance as function of altitude, orientation and time is the output of the irradiance model. The outputs of the thermal model are: i) solar panel temperature, ii) thermal yield done by the panel and iii) the water temperature. In this section the results of the total hybrid model, which will combine the outputs of the thermal and irradiance model, are presented and discussed. After the results a small description of the different vital components is included: the hybrid solar panel, the inverter, the pump and the tank.

In this part of the model, the irradiance is converted in an electrical yield. This electrical yield includes the losses in the hybrid solar panel, inverter and cables. Figure 4.15 illustrates the Ac yield as portion of the DC yield and the DC yield as portion of the total irradiance. The DC yield is the received irradiance by the solar panel converted into electrical energy and the AC yield is the yield after the balance of system. The color bars give the irradiance per panel for every facade and the bottom grey part shows the DC part of this irradiance. The black part shows which part is the AC component. There is not much different between the DC and AC component, because the losses are small in the inverter and cables.

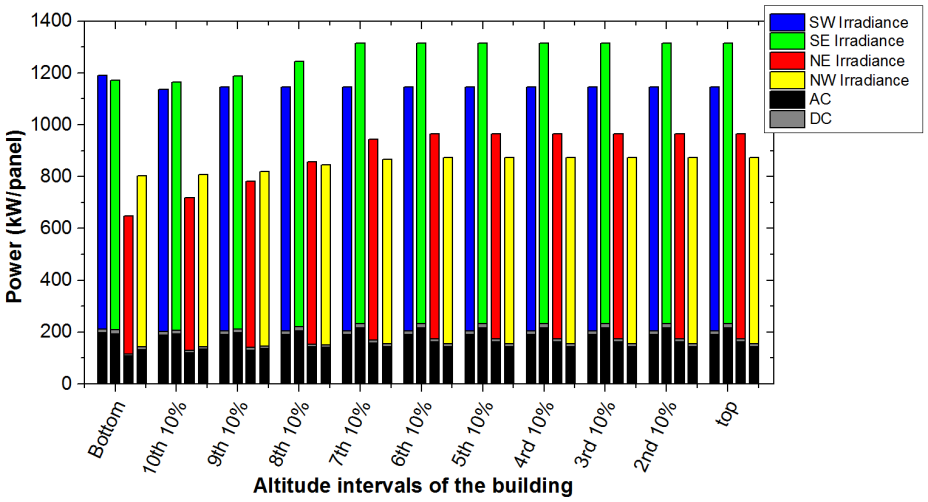

Figure 4.15: The DC yield and AC yield as portion of the irradiance for one panel as function of altitude and orientation

In Table 4.6 some average numbers for every facade are given. The table shows that the highest electrical yield can be expected from the southern facades, which was foreseen because of the results out of the Sun analysis. The results are values based on the surface of one solar panel. The last row shows the efficiencies which is also visualized in the Figure 4.15. The northern facades are performing better if you only look to the efficiency, but because of the lower irradiance the yield on the southern panels is higher.

By cooling the photovoltaic cells with the water flowing on the back of the panel the efficiency stays on a higher level and closer to the specifications than without cooling. Figure 4.16 shows the efficiency in blue through the year, lightblue in case of no cooling and darker blue with cooling. The reason the efficiency stays more constant is because the open circuit voltage is more constant than without cooling, shown in the graph in green. The fluctuations in the

Table 4.6: The annual irradiance received by the solar panel for different facades and the resulting DC and AC yield all in kWh per year per panel.

Orientation	South-West	South-East	North-East	North-West
Irradiance	1148.92	1270.01	885.50	853.45
DC Yield	203.59	225.27	157.94	152.17
AC Yield	189.43	209.59	146.96	141.58
Efficiency	16.49%	16.50%	16.59%	16.59%

open voltage are with cooling around 2, 3 volt and without cooling a drop of around 4 to 5 volt is measured. The difference in average efficiency is more than 1%, it seems small but on a system with a annual output in the Gigawatt hour range it is a big difference.

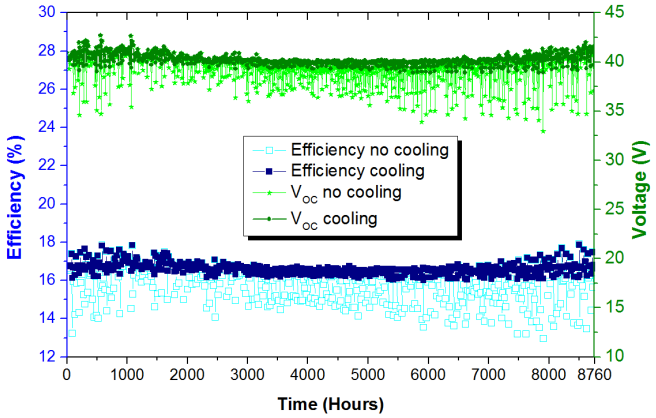

Figure 4.16: The effect of cooling on the open circuit voltage(in green) and on the electrical efficiency of the system(in blue). The darker colors for the one with cooling, the lighter colors for without.

The next graphs in Figure 4.17 shows the AC yields for different orientations on a typical summer day (4.17a) and winter day (4.17b) with in the background the average load pattern in percentage during the day for a typical office building in Hong Kong [62]. In the summer there is a high yield during the morning hours on the East side which can be expected because the Sun comes up in the East. Around noon in the summer the yield falls back this is due to the high Sun position in the summer. In the afternoon the yield does not increase much compared to the winter due to the solar path which moves more to the North-West facade. The West direction can be explained by the Sun going under in the West and the North because the high solar altitude during the summer. If it is compared with the consumption, the grid plays a vital part of providing enough electricity during the day. The winter has a AC yield profile much more fitting to the electricity consumption, this is mainly due to the lower Sun location. Another reason is the Sun moves more over the southern facades during winter. Figure 4.18 provides a overview of the ICC seen from the point of view of the Sun, during three moments of the day, 10:00, noon and 16:00 on a typical day in the summer and winter. These pictures provide an explanation of the AC yield characteristics given in Figure 4.17. The pictures in Figure 4.18 are made in Sketchup in combination with a shadow extension,

which positions the camera at the Sun's location.

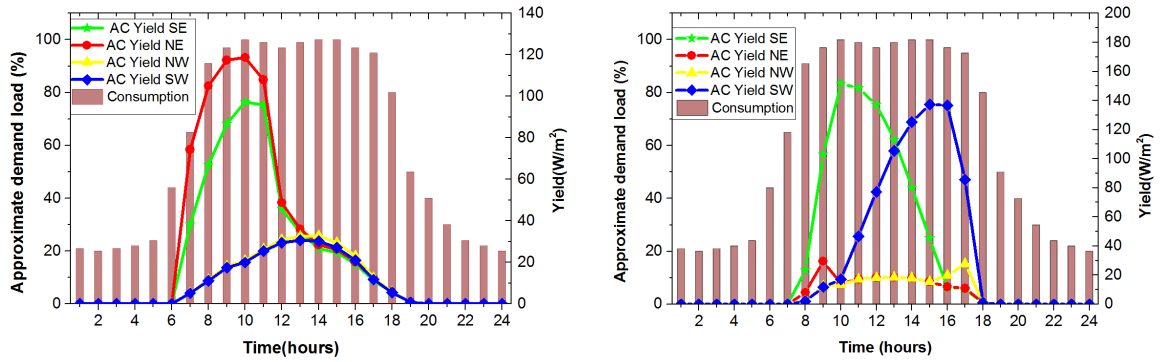

(a) (b)

Figure 4.17: The AC yield in (W/m^2) of the different orientations with in the background the electricity consumption pattern in percentages for a) a typical summer day and b) typical winter day.

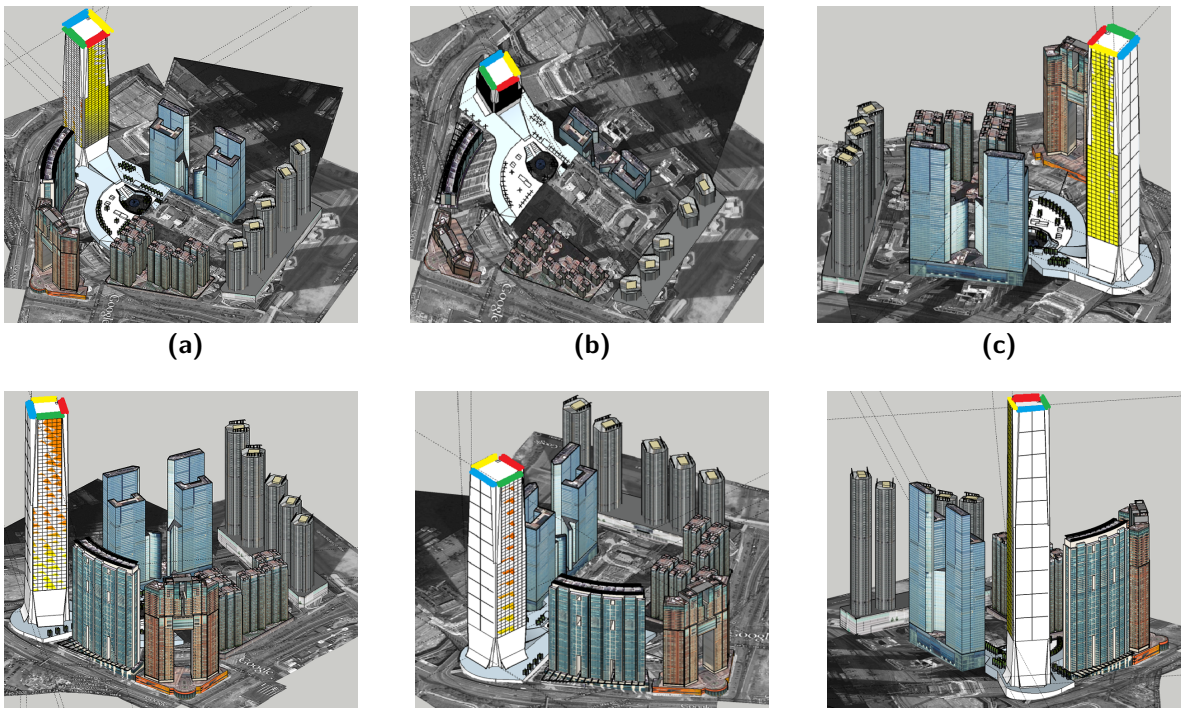

(a) (b) (c)

(d) (e) (f)

Figure 4.18: A overview from the view at the ICC seen from the Sun at a typical summer at a) 10:00, b) 12:00 and c) 16:00 and winter day at d) 10:00, e) 12:00 and f) 16:00. The colors at the top of the facade show the orientation (yellow NW, red NE, blue SW, green SE)

Sizing of the system

The next step is sizing the system. For this step more information about the ICC is needed to find out how many panels can be installed on the different altitude intervals of the facade. The division of the facade into ten equal intervals and an extra bottom interval is used. The ICC has 108 floors above ground and a total height of 484 meter. The equal intervals of the facade are all 38.6 meter high and the bottom interval is 57 meter high. The lower rest of the building is not used for solar panels, because of shadows and constructions. Every interval has a different width, see Table 4.7. All the values are found in the model used in SketchUp.

The facades are existing of two different types of panels;" *3 meter wide fixed spandrel units and 1.5 meter unitzed vision "infill" panels slotted between spandrels above and below."* [63] Spandrel glass is designed to be opaque in order to help hide features between the floors of a building. [64] Every floor has 4.5 meter of wall, from which 3.15 meter is from floor to ceiling. [65] The first column of Table 4.7 shows the eleven intervals of the building, the two following columns are showing the dimension of the intervals. Column four shows how many bands of 3 meter fixed spandrel are available. Finally, the fifth column gives the amount of solar panels installed on the given altitude interval. There is chosen to attach the solar panels on their vertical side to save pipes in connecting the solar panels with each other. The solar panels are chosen to be 1 meter wide instead of the 0.990 meter out of the data sheet, to include some construction materials and one extra meter is subtracted from the total width as simple assumption for construction. The calculation is done for one facade, because of the similarity between the four facades. The North-East is not similar to the other facades but the assumption is that the amount of solar panels is approximately same. The width of the building is increasing with a decreasing altitude resulting in more space for solar panels on a lower level.

Table 4.7: Data about sizing of the system on the ICC

Intervals	Height (m)	Width (m)	Spandrel bands #	solar panels #
Top	38.6	43.4	8	378
2nd 10%	38.6	46.0	9	360
3rd 10%	38.6	48.7	8	432
4th 10%	38.6	51.3	9	400
5th 10%	38.6	53.9	8	477
6th 10%	38.6	55.4	9	432
7th 10%	38.6	55.4	8	486
8th 10%	38.6	55.4	9	432
9th 10%	38.6	55.4	8	486
10th 10%	38.6	55.4	9	432
Bottom	57.0	50.0	13	637
Total	443	55.4	98	4952

Every facade has space for 4952 hybrid solar panels, multiplied by four leads to 19,808 hybrid solar panels good for 5.6 GWp. The final step is to calculate the amount of thermal yield

and electrical yield these hybrid solar panels can produce. In Table 4.8 below the results are shown of sizing up the system. The thermal yield does not include the losses because of scaling up, it is the thermal yield produces at the hybrid solar panel level. The thermal yield can be used to preheat water, the electrical yield is directly available and can be used in the building or fed back to the national grid. The first column shows which orientation of the building is calculated, the next 3 columns present the density and the two yields. The electrical yield is around one fourth of the thermal yield. The electrical yield is equivalent to electricity and the thermal yield is in the form of a rise in water temperature. The next three columns show the total energies for the system with 19,808 panels: The total energy received, thermal energy produced and the AC electric energy produced by the hybrid solar panels after the inverters. A total of 3.39 GWh electric energy and 12.5 GWh of thermal energy can be produced by the total system in one year. The annual energy consumption of the ICC is 46.1 GWh. [66] The electric energy is covering 7.4% of this consumption. The energy consumption exists not only of electric consumption but also of thermal energy. The thermal energy is good for covering 27.1% of the total energy consumption, but this is neglecting the transport, storage and conversion losses if needed.

Table 4.8: A summary of the annual energy density input in MWh/m^2, the annual yields in MWh/m^2, the annual total energy input in GWh and the annual energy outputs in GWh for the total system calculated for the four different orientations and the total building.

Orientation	Energy Density input ($MWh/y \cdot m^2$)	Thermal Yield ($MWh/y \cdot m^2$)	AC electric Yield ($MWh/y \cdot m^2$)	Total Energy (input) (GWh/y)	Thermal energy (GWh/y)	AC electric energy (GWh/y)	Combined energy (GWh/y)
SE	0.77	0.42	0.13	6.26	3.45	1.03	4.49
NE	0.54	0.33	0.09	4.32	2.70	0.72	3.42
SW	0.70	0.43	0.12	4.21	3.51	0.94	4.44
NW	0.52	0.35	0.09	5.70	2.81	0.70	3.51
Total	-	-	-	20.5	12.5	3.39	15.9

The amount of inverters is half the amount of the panels, because every micro-inverter can work with two solar panels simultaneous. With 19,808 hybrid solar panels it leads to 9,904 inverters. The amount of tanks is not included in the thesis, because one of assumptions is: The amount of tank capacity on the ICC is enough for the system. Future work should include this, but it was difficult to find data about the tank capacity on the ICC.

The total amount of pumps used in the system is calculated via the maximum pressure and the maximum flow rate of the pump and the pressure loss and flow rate in the hybrid solar panels. The pressure loss in the panel is $711.5\,mm\,H_2O$ which is equivalent to 0.07 bar per panel. The maximum pressure is 6 bar. When only the pressure loss in the panels is taking into account, the limit of the amount of solar panels per pump can be calculated by: $6/0.07 \approx 85$ panels. The other limitation is the flow rate the pump can produce. The maximum flowrate is $3,300\,l/h$, the flowrate which is used in the system is $120\,l/h$ per panel. If one pump wants to pump water to different hybrid solar panels parallel, which is the case, every flow to the solar panels needs the $120\,l/h$. One pump can pump water to: $3,300/120 \approx 27$ panels. The amount of pumps needed for the system is $19,808/27 \approx 734$. The amount of controllers is the same as the pumps.

In Figure 4.19 both the yields are plotted together with the energy density through the year.

The efficiencies of the system are calculated and are for the thermal part 53.13%, for the electric part after the inverters 16.54%. These values are slightly lower than the datasheet, which can be explained by the not ideal orientation and Balance of System. If you combine both the efficiencies, the system achieves a total efficiency of 69.67%.

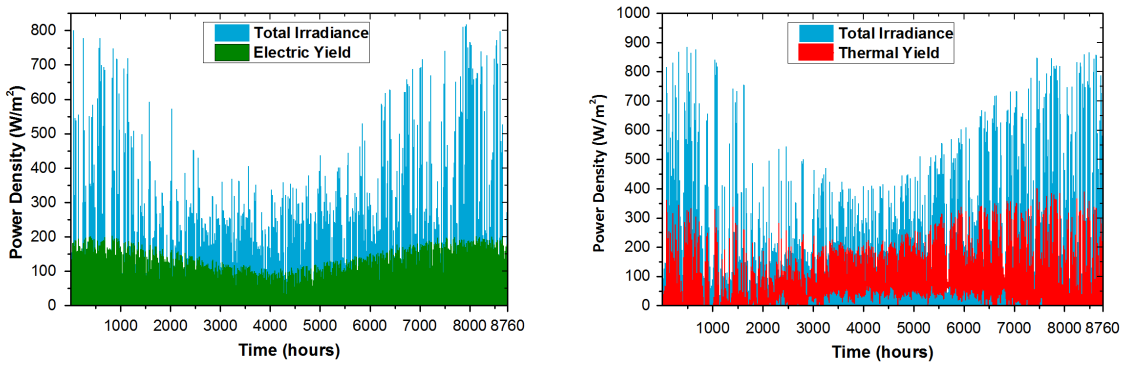

Figure 4.19: a) The AC electric yield (in green) and b) thermal yield (in red) plotted with the energy density on the back as function of time for the system on the ICC

The last output the water temperature is difficult to calculate. The temperature rise at panel level is between 2 and 3°C in the summer to 4 to 5°C in the winter. For the total system it is hard to tell, because it depends on the amount of tank capacity and the demand from the building.

The different components of the hybrid system

This section will go deeper into the different components of the system and which choices are made. The hybrid solar panel, the inverter, tank and pump will be elaborated.

The hybrid solar panel; The hybrid solar panel which is used in this model is made by Fototherm. This is a company from Italy. The hybrid solar panel is chosen because it has a high output power, high thermal and electric efficiency, it has a complete datasheet and it is commercially available. A small overview of the specification of the hybrid solar panel is given in Table 4.9 below. The complete datasheet can be found in Appendix C. The solar cells in this hybrid solar panel are monocrystalline silicon cells. The advantages are the maturity and it has a good efficiency, the downside is the price.

Table 4.9: Most important specifications of the hybrid solar panel as reported in the datasheet (see Appendix C)

Technique	60 Monocrystalline silicon cells
Dimensions	1660x990x51 mm
Rated power	285 Wp
Open circuit voltage	39.2 V
Short circuit current	9.7 3A
Electrical efficiency	17.3%
Nominal thermal power	921 W
Volume flow rate	1.5-2.5 l/min
flow losses	536-887 mm H_2O
Thermal efficiency	58.3%
lifetime	25 years

Inverter; The DC electricity produced by the solar panels has to be converted to AC to be able to feed back to the indoor grid or the national grid, this can be done with an inverter. Presently there are three different technologies:

1. Centralized inverters or string inverter
2. Micro inverters
3. Power optimizers

Centralized inverters are traditionally the most common choice, but in the last years the market is changing to the Module-level Power Electronics(MLPE). The centralized inverter converts a string of solar panels and the micro inverter or power optimizers is module level based.

The main advantage of the string inverter is the cost and you need less converters. The advantages of MLPE are that they [67,68]: i)Are more efficient (higher energy yield), ii) have lower weight and smaller size, iii) can monitor each individual panel, iv) are plug and play, v) have a higher lifetime, vi) need no active cooling and vii) bring greater design freedom. The micro inverter or power optimizers work better when the orientation is not perfect or in case of shadow. For the system on the ICC is this perfect because the orientation is not ideal and Hong Kong has days with a lot of clouds. There is not a lot of space for an inverter and maintenance should be as low as possible. Temperatures are warm in Hong Kong which can result in problems for a centralized inverter which has to convert high powers.

The difference between a micro inverter and a power optimizer is the micro inverter converts the DC electricity immediately at the solar panel to a AC voltage and current and a power optimizer only assures that every panel keeps the maximum power and is not affected by the other panels [69, 70]. The power optimizer still needs an inverter to convert the power from DC to AC. The advantage of the power optimizer above the micro-inverter is they are cheaper

and easier to implement in any voltage range because the centralized inverter is still included. The power optimizer has also a slightly better efficiency.

However micro-inverters are safer [69], because of the conversion to AC there are no high DC currents in the system which decreases the fire risk and decreases the power losses in the cables. Another big advantage is that there is no centralized inverter which is a weak spot. If the centralized inverter is broken the whole string is not producing anymore.

For the hybrid solar system micro-inverters are chosen because of the higher safety and because no extra centralized inverter is required. The micro-inverter is built for the European market but is feasible for Hong Kong as well, because Hong Kong's electric grid is a heritage from the British Empire. The micro-inverter which is chosen is from the company APS and it can convert the current and voltages and control two solar panels in the same time. This can save in cost because half the amount of inverters is required and still keeps the advantages of a micro-inverter. Table 4.10 includes some specifications and the complete specification can be found in the data sheet in the Appendix D

Table 4.10: Some of the specifications of the micro-inverter as reported in the datasheet (see Appendix D)

Input(DC)	
PV power	180-310 Wp
MPPT voltage range	22-45 V
working voltage range	12-55 V
maximum current	10.5 A x2
Output(AC)	
maximum power	500 W
maximum current	2.17 A
voltage	200-270 V, 60 Hz
efficiency	95.5%
lifetime	25 years

Tank and pump; The tank used in the system is based on the tank used in residential housing, named the *"twin-tank"*. [8] In Appendix B a schematic layout of the tank is given. The tank is chosen for this approach because of the lack of data about the water system in the ICC. In case of the ICC there will be not just one tank but more tanks on different maintenance floor through the building. In this way the water does not have to travel to far to a tank and from the tank to the destination. The system will make use of the tanks which are already installed and when needed the tanks can get more capacity.

The pump choice is based on a suggestion made by the producer of the solar panels. The brand and type of the pump are Wilo yonos PARA. The pump maximum static pressure is 6 bar and the maximum volume flow is $3.3/, m^3/h$ this is equivalent for delivering the needed flow of water to 27 panels. The pressure drop per panel is small compared with the pressure

Table 4.11: Some of the specifications of the pump and the tank as reported in the datasheets (see Appendix B and E)

Twin-tank	
Dimensions	
capacity	550000 L
Wilo water Pump	
flowrate	$3.3m^3/h$ *or* $3300L/h$
maximum pressure	5 bar
power usage	37 W
lifetime	10 years

the pump can produce. The power used by the pump is 37 W, this can be delivered by the hybrid solar panels in the system. In Appendix E more information can be found in the data sheet.

Summary

The total system is the last modeling step in the process of acquiring thermal yield, electrical yield and the water temperature. The water temperature is calculated at the hybrid solar panel, because to many assumptions have to be made to acquire a good estimation of the water coming at the consumer. The system exists of Fototherm hybrid solar panels which are made in Italy. The technique used in the panels is Monocrystalline silicon. The panels have a rated power of 285 Wp and a nominal thermal output of 921 W. The electrical efficiency is 17.3% and the thermal efficiency 58.3% under standard test conditions. The system makes use of APS micro-inverters, mainly because of safety reason, high operation temperatures and a higher yield in case of partly shading on the panels. The pump is from Wilo and delivers a flow rate of 3.3 m^3/h. The tank used in the system is a twin tank which is used in residential housing, it has a capacity of 55,000 liter. An overview of the amount of main parts in the system is given in Table 4.12

Table 4.12: An overview of the amount of main components in the system

Component	amount
Hybrid solar panel	19808
micro-inverter	9904
pump	734

There is slight difference between AC and DC yield, this is due to the small losses in the micro-inverter and the cabling. The thermal yield is calculated on solar panel level and multiplied by the amount of panels, not including the losses in tank and piping. If the efficiency of the panels is compared with an efficiency of no cooling, so normal panels, the average difference is 1% with maxima of 3%, this is mainly due to more stable open circuit voltage on the hybrid solar panel. The AC yield fits closer to the consumption pattern in winter than in summer, one of the reasons is the solar path in the summer is from South-East to North-West and in

winter from South-East to South-West. The total annual thermal output of the system on the ICC is calculated to be 12.5 GWh and the annual AC electrical output is 3.39 GWh. The efficiencies of the system are for thermal 53.13% and for electric part 16.54%

4.5 Economic analysis

This section will elaborate further on the costs of the system. Next to the financial aspect it will also elaborate on the energy payback time and the greenhouse gas payback time.

In Table 4.13 an overview of the cost is presented. The prices are based on a literature survey and contact with different suppliers. The prices presented are an average of the values found in the literature, because the literature presented different calculations. The costs exists of an initial price of the whole system and an annually cost of repair maintenance and operations. The cost analysis is divided into five parts: The hybrid solar panels, the electrical part, the thermal part, the labor and the yearly costs for repair, maintenance and operations.

1. Hybrid solar panels; The price for the solar panels is from information sent by the manufacturer of the solar panel, Fototherm [71]. The normal price of the Fototherm solar panel is 870 euro, but because of the scaling up of the system the manufacturer sells the panels for 350 euro, see email contact with the supplier in Appendix F The estimation for the structural costs is based on an average module price of different studies done on solar systems and then adjusted to fit this specific case. The studies are partly done by the National Renewable Energy Laboratory (NREL) of the United States [72, 73], one feasibility study carried as a fulfillment of a degree in Master of Science in Architecture [74] and one research article from two universities of Hong Kong. [75]

2. The electrical part consist of the micro-inverter costs, the wiring, connectors, extra electronics costs and the protection devices costs. These costs are an average out of different studies [72–74, 76]. Protection devices are safety cutoff switches, lighting arrestors and AC breakers. The amount of inverters is half that of the amount of solar panels due to the inverter's capability of handling two solar panel at the same time.

3. The thermal part of the cost analysis includes the pumps, piping, control equipment and extra costs. The price of the pump comes from a shop and does not include yet the advantages of scaling up of the system. In the cost analysis the cost for the tanks is not taken into account because there are already tanks in the building, which can be used. The piping and control equipment are estimation based on literature [76, 77]. One of the sources is a design guide for solar hot water systems, developed by a group of government, institutional and private sector parties. The cost for the tanks is left out, because one of the assumptions made is the current tank capacity is sufficient for the system.

4. The labor part includes costs for installation, testing, engineering and designing of the total system on the facade of the ICC. The labor cost are based on an average of three values from different sources [73, 75, 76]. The prices are partly based on the United States and partly on the one in Hong Kong. It is an estimation and calculated per module and then scaled up by the amount of modules. In real case there will be decrease in total cost by scaling up.

5. Repair, Maintenance and Operations is the final part of the cost analysis or shorter the M&O costs. These costs are annually based. It is important to carry out maintenance to keep the efficiency high and the panels clean, which assures higher yields. Two new sources are used next to the ones which are already used. One is a cost analysis inside of an solar thermal system analysis and the other one is a energy analysis both carried out by the NREL [78,79]. Examples of maintenance are:

- Check the piping and wiring
- Cleaning the solar panels
- Check on the pumps and inverters
- Flush the entire system once every 10 years

The M&O cost is according to the different sources around 1% of the initial cost annually. The system is designed for 20-25 years. The lifetime of the hybrid solar panels and inverters is the same as for the system, but the pumps need to be replaced once in 10 years, so around the same time, when the whole system needs to get flushed.

Table 4.13: An overview of the costs in the system. The prices are calculated in Hong Kong Dollars(Hkd). The third column shows the price for a system with one module of 285 Wp. Note 1 € is equivalent to 8.67 Hkd

System	Description	price Hkd	amount	total price million Hkd
Hybrid solar panel				
	Fototherm FT285AL	3034.03	19,808	60.1
	Structural elements	1389.76	19,808	27.5
Electrical part				
	APS Grid-connected Micro-inverter	1690.39	9,904	16.7
	Wiring, connectors, electronics	762.93	19,808	15.1
	Protection devices	1750.98	9,904	17.3
Thermal part				
	Wilo Yonos Para pump	1446.54	734	1.1
	Piping	1009.70	19,808	20.0
	Controls and other costs	397.46	19,808	7.9
Labor				
	Installation, testing, engineering	4099.23	19,808	81.2
Total investment				247.0

The table is visualized as a pie chart in Figure 4.20, to get an overview of the distribution of cost in percentages. The pumps have the smallest portion in the costs and the biggest costs are not the hybrid solar panels, but the cost of labor in yellow. The labor cost, cost for the inverter and pumps can be lower if there was more information available about the economic of scale. In the cost of the hybrid solar panels a discount is included, because of the sizing

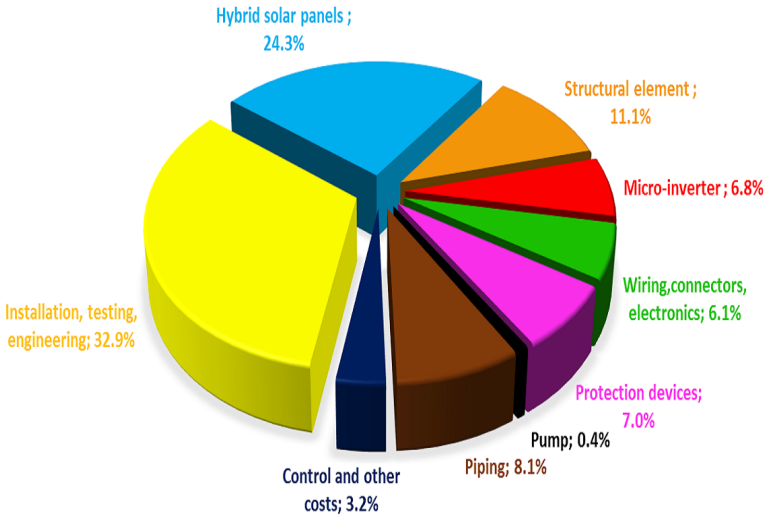

Figure 4.20: Distribution of cost for the large hybrid solar panel system on the facades of the ICC

of the system. The pumps in the system are the lowest cost, but has to be replaced every 10 years, because of the shorter lifetime.

To find out the timespan needed for the system to get cost-effective the electric and thermal energy output are converted to values in money. In Hong Kong the price of electricity is 0.98 Hkd/kWh [80] and the prize for gaseous fuel used for heating water is 0.714 Hkd/kWh. [81] Table 4.14 shows a balance of cashflows in and out of the system. A example of a cashflow in is the savings incurred due to the electricity generated. A cashflow out is the cost for maintenance and operations.

Table 4.14: A balance of costs and profits to calculate the cost payback time of the hybrid solar system. Note 1 € is equivalent to 8.67 Hkd

Total system costs	million Hkd
Initial investment	247.0
Annual maintenance and operations	2.5
Once in ten years pump replacement	1.1
Annual costs	2.5
Useful energy savings	kWh
Thermal energy	$3.39 \cdot 10^6$
Electrical energy	$1.25 \cdot 10^7$
Cost savings	million Hkd
Gaseous fuel	8.9
Electricity	3.3
Annual savings	12.2
Cost payback time (CPBT)	25.4 years

The cost payback time (CPBT) has been calculated at 25.4 years. The cost payback time seems high, but the effect of the economy of scale is for most components not included yet. The reason is the lack of data on a hybrid systems with the size of the one designed for the ICC. Another aspect which is not currently considered is the influence on air conditioning load, due to the hybrid solar panels on the facades converting incoming solar energy. A lower air conditioning load is expected, but this is something for future work. If the hybrid solar system was included in the building design an even lower CPBT is expected, because according to the benchmark [82] carried out in a study done by the University of Applied Sciences and Arts of Southern Switzerland, are BIPV less expensive than glazed curtain wall. It is true a BIPVT is a bit heavier and more complex than a BIPV, but it is promising.

The next parameters which will be evaluated are the energy payback time (EPBT) and the greenhouse payback time (GPBT). The EPBT shows the amount of years it takes for the product to produce the energy it consumed during its lifetime, by for example transport or manufacturing. In a solar system the biggest share is in the production of the solar panels. The GPBT respectively gives the amount of years it takes to save the greenhouse gases(GHG) which were needed by producing and installing of the total system. In Table 4.15 shows an overview of the embodied energies on the left and embodied greenhouse gases on the right for the different components of the system. The Balance of System includes the inverter, piping, wiring, controller, pump and other electronics

Table 4.15: The embodied energy(left) and greenhouse gases(right) for the building integrated hybrid solar system on the ICC, together with the annual savings.

	Embodied energy kWh/m^2	**Embodied GHG** $kgCO_2\text{-eq}/m^2$
Hybrid solar panels	1328.52	427.33
Balance of System	101.69	26.50
Structural	61.49	38.01
	On system level kWh	$kgCO_2\text{-eq}$
Hybrid solar panels	$3.79 \cdot 10^7$	$1.39 \cdot 10^7$
Balance of System	$3.31 \cdot 10^6$	$8.63 \cdot 10^5$
Structural	$2.00 \cdot 10^6$	$1.24 \cdot 10^6$
Total	$4.32 \cdot 10^7$	$1.60 \cdot 10^7$
	Energy Saving kWh	**GHG savings** $kgCO_2\text{-eq}$
Thermal	$1.25 \cdot 10^7$	$2.39 \cdot 10^6$
Electrical	$3.39 \cdot 10^6$	$2.55 \cdot 10^6$
Payback time	(EPBT) 2.76 years	(GPBT) 3.24 years

The values used in the EPBT calculations are acquired by a previous study done on a 9.66 m^2 hybrid solar photovoltaic/thermal system in Hong Kong. [81] The values found were scaled up to fit the system on the ICC. The EPBT is 2.76 years and can be lower like the cost if the

hybrid solar panels were installed during the construction of the ICC. The consuming power of the pump is taken into account by calculating the EPBT, the pump is active for an average of 6069 hours per year according to the thermal model in TrnSys. Which is equivalent to 224.6 kWh per year per pump. The consumption of the pumps together accounts for 5% of the total electrical energy output.

The values used in the GPBT calculation are acquired from a thesis about a life cycle assessment of a novel BIPVT system. [83] The system used in the thesis has an area of 25 m^2. To acquire the values for the system on the ICC a scaling factor has been applied. The values are expressed in kg CO_2 equivalent, the savings are also translated to this unit. The thermal savings are acquired to look to the amount of town gas you save by using the solar panels to heat up water and see how much GHG emission the local town gas has. The GHG emission of town gas in Hong Kong is 2.553 kg CO_2 per 48 MJ of energy. [84]. For the electricity savings the energy mix and with it the GHG emission are investigated for the location of Hong Kong. The electricity fuel mix of the local power company CLP exists of 28% nuclear, 15% gas and 57% coal plus others and the GHG emission factor is 0.79 kg CO_2 per kWh electricity. [84].

There is one last parameter which can be used for comparison purposes and this is the life cycle emission factor expressed in gCO_2-eq per kWh. This factor is the total embodied GHG divided by the total energy it produces during its lifetime. The proposed BIPVT system on the ICC has a life cycle emission factor of 50.5 gCO_2-eq per kWh, which is comparable with literature on (building integrated) solar systems, which were in the range from 13-280 gCO_2-eq/kWh. [85].

Summary

The last analysis concerns economic metrics, such as the cost payback time, the energy payback time and the greenhouse gas payback time. The total investment costs of the system is calculated at 247 million Hong Kong Dollars which is equivalent to 28.5 million euro. The cost payback time is calculated to be 25.4 years. In this estimation of the cost economy of scale was only considered for the cost of the hybrid panels. Another aspect which is not included is the savings in air conditionings units, which will definitely shorten the cost payback time. The total embodied energy and embodied GHG are $4.32 \cdot 10^7$ kWh and $1.60 \cdot 10^7$ $kgCO_2$-eq. The energy payback time is 2.76 years and the greenhouse gas payback time 3.24 years, which is comparable with literature.

Chapter 5

Conclusion & Recommendations

5.1 Conclusion

The objective of this thesis was to investigate the opportunities for hybrid building integrated photovoltaic/thermal system in the city of Hong Kong. A hybrid solar panel is a solar panel combining photovoltaic cells with a thermal collector on the back and in this way obtaining an electrical yield and a thermal yield. The scope is narrowed down to one case in Hong Kong, a commercial skyscraper: The International Commerce Centre. To achieve this objective a framework of different software tools is used combining the individual strengths.

Hong Kong is a city located in the South East of China and has 1835.6 Sun hours a year and a mean global solar radiation of 1302 kWh/m^2. Every hour during the day the area of Hong Kong receives 500 GW of solar power. As expected the altitude of the Sun becomes high during the summer according to the Sun anelemma of Hong Kong. During the winter the Sun altitude reaches around 40°, in summer it almost reaches 85°. The energy consumption of Hong Kong is 88.5 TWh, from which 34.9 TWh is electricity. The commercial sector is with 66% the biggest consumer of electricity. One of the biggest loads are the air-conditioning units in Hong Kong with 30%. One of the by-products of this thesis project is the decreasing of air-conditioning units.

During this project different models have been built to calculate the performance of a hybrid solar system on the ICC. The framework consists of exists of three sub-models: (i) the irradiance model (built in Matlab) (ii) the thermal model (built in TrnSys) and the integrator model (iii) (built in Matlab). In the modeling of the total system different software tools are used, like SketchUp, Meteonorm, Matlab and TrnSys, in this way the strength of each tool is combined. The final outputs of the model are the thermal yield, electrical yield and the water temperature. The last section includes the formulae used to calculate the parameters for the life cycle assessment. While the theoretical framework presented in this chapter is available in literature as independent sub-models, the innovation of this thesis is to combine all of them using specialized software for accurate calculation

The shadow coefficient which is needed to calculate the amount of radiation on a given surface is calculated in SketchUp. The average shadow coefficient of the whole building is around 50%. The most shadows are found on the North-East facade. This is due to the buildings around the ICC. The best performance is measured on the southern facades during the winter months, this can be explained by the tilt of the hybrid solar panels, which is 90° and the solar altitude which is high in the summer. A decrease in altitude on the building gives an increase in shadow, which is due to the surrounding buildings. The shadows are much more uniform on the North-East facade and covering the whole width of the building.

The South facades have almost double the sunhours compared to the North facades. The most sunhours are on the South facade during the January month and for the North facing facade during April and July. The irradiance is higher in the winter period than in the summer period, which is due to the solar position in summer in combination with the tilt of the hybrid solar panels. The sky view factor is included in the calculations which consequences in a decrease in output on the lower parts of the building. The effect of the sky view factor on the East facade is higher than on the West facades.

The thermal model is simulated and different parameters varied. The focus on modeling is a high electrical output even if this leads to a lower thermal yield. When decreasing the demand and the size of the tank the water temperature coming out of the solar panels rises, which is expected because the water temperature in the tank rises which results in a higher solar panel inlet temperature. The water temperature characteristics follows closely to the thermal power density characteristics. In the model the influence of height on the wind speed, panel temperature and ambient temperature is included. The flow rate is varied in the system and the best flow rate for the system is chosen to be 120 l/h. The average thermal efficiency is 53.12%, with the highest efficiencies on the North facades.

The total system is the last modeling step in the process of acquiring thermal yield, electrical yield and the water temperature. The water temperature is calculated at the hybrid solar panel, because to many assumptions have to be made to acquire a good estimation of the water coming at the consumer. The system exists of Fototherm hybrid solar panels which are made in Italy. The technique used in the panels is Monocrystalline silicon. The panels have a rated power of 285 Wp and a nominal thermal output of 921 W. The electrical efficiency is 17.3% and the thermal efficiency 58.3% under standard test conditions. The system makes use of APS micro-inverters, mainly because of safety reason, high operation temperatures and a higher yield in case of partly shading on the panels. The pump is from Wilo and delivers a flow rate of 3.3 m^3/h. The tank used in the system is a twin tank which is used in residential housing, it has a capacity of 55,000 liter. The system exists of: 19,808 hybrid solar panels, 9,904 micro-inverters and 734 water pumps and controllers.

There is slight difference between AC and DC yield, this is due to the small losses in the micro-inverter and the cabling. The thermal yield is calculated on solar panel level and multiplied by the amount of panels, not including the losses in tank and piping. If the efficiency of the panels is compared with an efficiency of no cooling, so normal panels, the average difference is 1% with maxima of 3%, this is mainly due to more stable open circuit voltage on the hybrid solar panel. The AC yield fits closer to the consumption pattern in winter than in summer,

one of the reasons is the solar path in the summer is from South East to North West and in winter from South East to South West. The total annual thermal output of the system on the ICC is calculated to be 12.5 GWh and the annual AC electrical output is 3.39 GWh. The efficiencies of the system are for thermal 53.13% and for electric part 16.54%.

The last analysis concerns economic metrics, such as the cost payback time, the energy payback time and the greenhouse gas payback time. The total investment costs of the system is calculated at 247 million Hong Kong Dollars which is equivalent to 28.5 million euro. The cost payback time is calculated to be 25.4 years. In this estimation of the cost economy of scale was only considered for the cost of the hybrid panels. The total embodied energy and embodied GHG are $4.32 \cdot 10^7$ kWh and $1.60 \cdot 10^7$ $kgCO_2$-eq. The energy payback time is 2.76 years and the greenhouse gas payback time 3.24 years, which is comparable with literature.

5.2 Recommendations

A number of recommendations can be given to improve upon the work done. In this thesis there is a focus on a commercial skyscraper, the next step should be residential housing and what kind of difficulties are likely. For example many high-rise building close together, more shadow influences. Who will be responsible of the solar panels? Who benefits and who will pay for the panels?

Another interesting topic is the influence of the climate of Hong Kong on the hybrid solar panels. What is the influence of urban heat islands and smog on the performance of the system? Hong Kong, as many world cities, is troubled with smog. How often do the solar panels need to be cleaned to assure a good performance? What is the influence of albedo from other surrounding buildings? The facades are also facing other buildings, this is not ground albedo but often glass which reflects well.

The hydraulic losses in the system when scaling up are not taken into account, for this more information is needed on the system level and data from the building. This are losses which can not be neglected for the final design of a real system for the International Commerce Centre. There is also still work on the tank size and the total amount off tanks in the system as well. More research on the demand, because during this project a significant decrease was found in the thermal yield in case the demand decreased. The thermal yield calculated is the thermal yield at the hybrid solar panel. This still needs to be converted to an actual thermal yield which can be measured in water rise at consumer level. How much will the temperature rise at the tap for the consumer or at the boiler level?

The last recommendation which will definitely benefit this thesis is to make a prototype and perform measurements on the ICC itself and verify the simulations and calculation with real measurement data. When making a prototype the influence of the building integrated hybrid solar panels on the climate inside of the building can also be measured, there are already studies which investigate this effect, but this was not in scope in the thesis.

Appendix A

The thermal model build in TrnSys

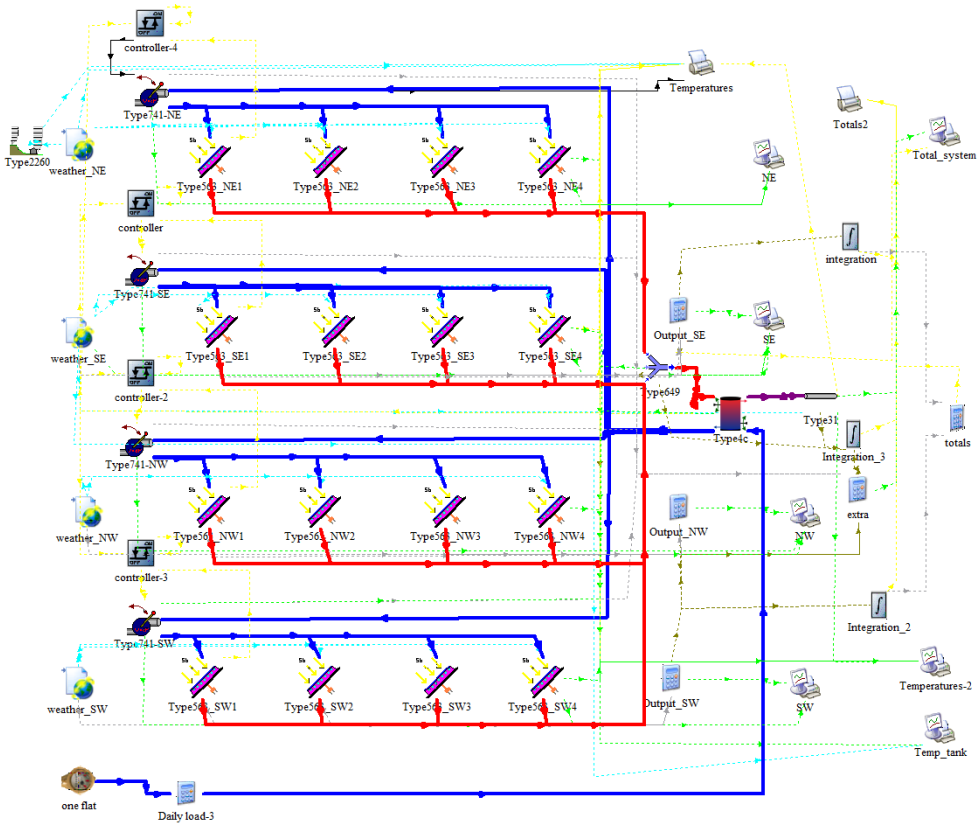

Figure A.1: The model build in TrnSys

Appendix B

Twin-tank

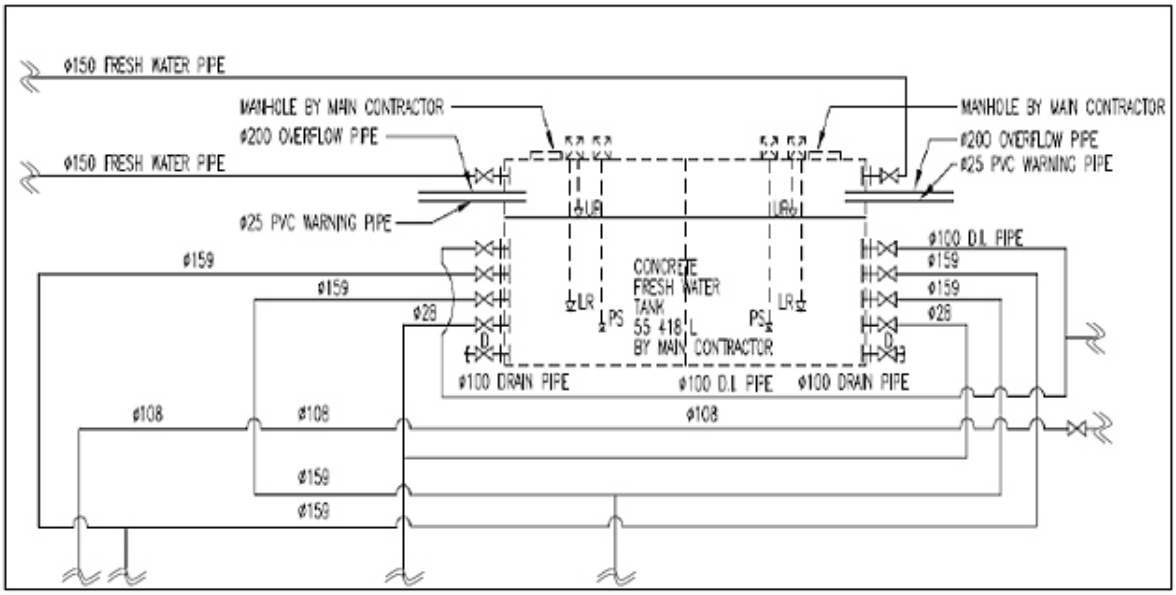

Figure B.1: A schematic picture of the tank provided by the government [8]

Appendix C

Fototherm hybrid solar/thermal panel

FOTOTHERM®

Series AL
275/280/285

APPLICATIONS

Facilities with an electricity requirement and increased need for warm water as their base load, such as

- Residential roof-tops
- Commercial, industrial and agricultural rooftops
- Solar power stations
- Other on-grid applications

Additional applications are for customers, who do not compromise on aesthetics and look for complete renewable energy sources of electricity and heat for their home; in combination with heat storage and pump it is a perfect solution. A partial or complete integration of the heating system is possible for:

- Swimming pools
- Underfloor heating
- Other agricultural, industrial or residential systems

ANWENDUNGEN

Einrichtungen mit einem erhöhten Bedarf an Warmwasser und einem hohen Stromverbrauch als Grundlast

- *private Dächer*
- *kommerzielle, industrielle und landwirtschaftliche Dächer*
- *Solarkraftwerke*
- *andere netzangebundene Anwendungen*

Außerdem attraktiv für Kunden, die in Fragen der Ästhetik keine Kompromisse eingehen wollen und auf der Suche nach einem integrierten erneuerbaren Energiesystem für ihr Zuhause sind; in Verbindung mit Wärmepumpe und Wärmespeicher die ideale Lösung. Eine partielle oder vollständige Integration des Heizsystems ist möglich für

- *Swimming Pools*
- *Fußbodenheizung*
- *andere landwirtschaftliche, industrielle und private Systeme*

SPECIFICATIONS

FOTOTHERM® proudly introduces the PVT Hybrid module in an elegant black design. A perfect symbiosis of electrical and thermal performance that saves you space on the roof and installation time.
You can expect both an increased PV gain and better performance of the thermal system.
The module is certified by IEC / EN 61215 (2nd ed.), IEC / EN 61730 certification, Solar Keymark.

Positive power classification +5 Wp.

10 years product warranty

25 years module power output warranty ≥ 80%

SPEZIFIKATIONEN

FOTOTHERM© präsentiert das PVT-Hybrid-Modul in elegantem schwarzen Design.
Eine perfekte Symbiose aus elektrischer und thermischer Leistung, die sowohl den benötigten Platzbedarf auf dem Dach, als auch die Installationszeit reduziert. Sowohl der Ertrag des PV-Systems als auch die Leistung des Thermie-Systems werden gesteigert.
Die Module sind nach IEC / EN 61215 (2nd ed.), IEC / EN 61730 certification und Solar Keymark zertifiziert.

Positive Leistungsklassifizierung 0Wp/+5 Wp

10 Jahre Produktgarantie

25 Jahre Modul-Leistungsgarantie (Leistung ≥ 80%)

CERTIFICATIONS - *ZERTIFIZIERUNGEN*

IEC / EN 61215:2005
IEC / EN 61730:2004

Solar Keymark

ISO 9806:2013

Series AL

ELECTRICAL DATA - *ELEKTRISCHE DATEN*		FT275AL	FT280AL	FT285AL
Rated power - *Nennleistung*	(Pmpp)	275 Wp	280 Wp	285 Wp
Open circuit voltage - *Leerlaufspannung*	(Voc)	39,1 V	39,2 V	39,2 V
Rated voltage - *Nennspannung*	(Vmpp)	31,1 V	31,2 V	31,3 V
Short circuit current - *Kurzschlussstrom*	(Isc)	9,62 A	9,67 A	9,73 A
Rated current - *Nennstrom*	(Impp)	8,83 A	8,97 A	9,10 A
Electrical efficiency - *Wirkungsgrad*	(η)	16,7 %	17,0 %	17,3 %
Maximum system voltage (Iec) - *Max. Systemspannung*	(V)		1000V DC	
Reverse current load (Ir) - *Rückstrombelastbarkeit*	(A)		20	
Temperature coefficient (Pmpp) -*Temperaturkoeffizient (Pmpp)*	(γ)		-0,43%/°C	
Temperature coefficient (Voc) - *Temperaturkoeffizient (Voc)*	(β)		-0,30%/°C	
Temperature coefficient (Isc) - *Temperaturkoeffizient (Isc)*	(α)		0,05%/°C	

Under STC conditions: irradiance = 1000W/m2, cell temperature = 25°C
Elektrische Werte bei Standard-Testbedingungen (STC): 1000 W/m2; 25°C; AM 1,5

THERMAL DATA - *THERMAL DATEN*	
Aperture area - *Aperturfläche*	1,58 m^2
Thermal efficiency η_0 * - *Wirkungsgrad η_0 **	58,3 %
Nominal thermal power ** - *Thermischen Nennleistung ** *	921 W
Volume flow rate - *Empfohlener Durchsatz*	1,5 - 2,5 l/min
Flow losses - *Druckverlust*	536 - 887 mmH_2O
Fluid volume - *Kollektorinhalt*	0,96 l
Coefficient $\alpha 1$ - *Wärmedurchgangskoeffizient $\alpha 1$ **	6,08
Coefficient $\alpha 2$ - *Wärmedurchgangskoeffizient $\alpha 2$ **	0,00
Effective thermal capacity - *Effektive Wärmekapazität*	18,2 kJ K^{-1}
IAM K0 at 50° C - *Winkelkorrekturfaktor K0 (50°)*	96,0 %

* Based on aperture area - *In Bezug Aperturfläche*
** PV OFF conditions referred to (Tm-Ta)=0 - *Testbedingungen PVOFF in Bezug (Tm-Ta)=0*

SPECIFICATIONS - *TECHNISCHE DATEN*	
Cells - *Zellen*	60 Monocrystalline silicon 156 mm - *Monokristallines Si , Zellgröße 156 x 156*
Electrical connectors - *Stecker*	MC4
Hydraulic connector - *Hydraulikanschluss Messing*	1/2" female - *weiblich*
Maximum mechanical load - *Max. Modulbelastung Druck*	5400 P_a
Dimensions - *Länge x Breite x Höhe*	1660x990x51 mm
Weight - *Gewicht*	32 Kg

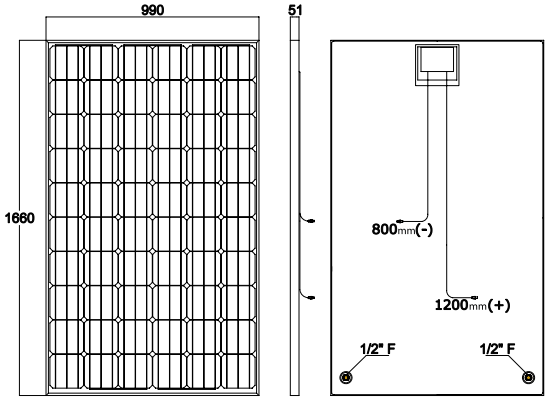

Appendix D

APS micro-inverter

APS M1P-EU

Grid-connected Microinverter

Version: 2.1

(For Europe)

ALTENERGY POWER SYSTEM INC.

YC250-EU Technical Specifications

Type	YC250A/I-EU
Input Data (DC)	
Recommended PV Module Power (STC)Range	180-310W
MPPT Voltage Range	22-45VDC
MPPT Voltage Range @ Full Power	26-45VDC
Operation Voltage Range	16-52VDC
Maximum Input Voltage	55VDC
Startup Voltage	22V
Maximum Input Current	10.5A
Maximum DC Short Circuit Current	15A
Output Data (AC)	
Maximum Continuous Power	250W
Nominal Output Current	1.08A
Nominal Output Voltage	230VAC
Default Output Voltage Range	184-253VAC[1]
Extended Output Voltage Range	149-278VAC
Rated Grid Frequency	50Hz
Default Output Frequency Range	48-51Hz[1]
Extended Output Frequency Range	45.1-54.9Hz
Power Factor	>0.99
Total Harmonic Distortion	<3%
Maximum Current per Branch	25A
Maximum Units per Branch	14 for 20A Breaker[2]
Efficiency	
Max. Inverter Efficiency	95.5% (With HF Transformer)
Night Power Consumption	120mW
Mechanical Data	
Operating Ambient Temperature	-40 °C to +65°C
Operating Internal Temperature	-40 °C to +85°C
Storage Temperature Range	-40 °C to +85°C
Dimensions (W x H x D)	160mm X 150mm X 29mm
Weight	1.5kg
AC BUS	12AWG
Waterproof Level	IP65
Cooling	Natural Convection
Wet Locations Classification	For Wet Locations
Pollution Degree Classification	PD3
Relative Humidity Ratings	0-95%
Maximum Altitude Rating	All data at this technical Specifications has been tested under <2000m
Overvoltage Category	OVC II for PV input circuit, OVC III for mains circuit
Features & Compliance	
Communication	Power Line

Design lifetime	25 yrs
Monitoring	Life monitoring via EMA software
Grid Connection Compliance	EN50438
Safety and EMC Compliance	EN 62109-1; EN 62109-2;EN61000-6-1; EN61000-6-2; EN61000-6-3; EN61000-6-4;

[1]Programmable through ECU to meet customer need. [2]Depending on the local regulations.

The specifications are subject to change without notice.

YC500-EU Technical Specifications

Type	YC500A/I-EU(for 2 independent MPPT)
Input Data (DC)	
Recommended PV Module Power (STC)Range	180-310W
MPPT Voltage Range	22-45VDC
MPPT Voltage Range @ Full Power	26-45VDC
Operation Voltage Range	16-52VDC
Maximum Input Voltage	55VDC
Startup Voltage	22V
Maximum Input Current	10.5AX2
Maximum DC Short Circuit Current	15A
Output Data (AC)	
Maximum Continuous Power	500W
Nominal Output Current	2.17A
Nominal Output Voltage	230VAC
Default Output Voltage Range	184-253VAC[1]
Extended Output Voltage Range	149-278VAC
Rated Grid Frequency	50Hz
Default Output Frequency Range	48-51Hz[1]
Extended Output Frequency Range	45.1-54.9Hz
Power Factor	>0.99
Total Harmonic Distortion	<3%
Maximum Current per Branch	25A
Maximum Units per Branch	7 for 20A Breaker[2]
Efficiency	
Max. Inverter Efficiency	95.5% (With HF Transformer)
Night Power Consumption	120mW
Mechanical Data	
Operating Ambient Temperature	-40 °C to +65°C
Operating Internal Temperature	-40 °C to +85°C
Storage Temperature Range	-40 °C to +85°C
Dimensions (W x H x D)	221mm X167mm X 29mm
Weight	2.5kg
AC BUS	12AWG
Waterproof Level	IP65
Cooling	Natural Convection
Wet Locations Classification	For Wet Locations

Pollution Degree Classification	PD3
Relative Humidity Ratings	0-95%
Maximum Altitude Rating	All data at this technical Specifications has been tested under <2000m
Overvoltage Category	OVC II for PV input circuit, OVC III for mains circuit
Features & Compliance	
Communication	Power Line
Design lifetime	25 yrs
Monitoring	Life monitoring via EMA software
Grid Connection Compliance	EN50438
Safety and EMC Compliance	EN 62109-1; EN 62109-2;EN61000-6-1; EN61000-6-2; EN61000-6-3; EN61000-6-4;
[1]Programmable through ECU to meet customer need. [2]Depending on the local regulations.	

The specifications are subject to change without notice.

Contact Information

ALTENERGY POWER SYSTEM Inc.
1 Yatai Road, Jiaxing, PR China 314050
Phone: +86-21-68889199
Fax: +86-21-33928752
www.APSmicroinverter.com

Statement: All products are subject to technical improvements without notice.

Appendix E

Wilo pump

WILO

Pumpen Intelligenz.

Catalogue

Yonos PARA

The new standard in High Efficiency

ErP READY 2015

APPLIES TO EUROPEAN DIRECTIVE FOR ENERGY RELATED PRODUCTS

Glandless Pumps and Accessories

Version 12.01

WILO
Pumpen Intelligenz.

Heating and cooling

Hydraulic operational areas

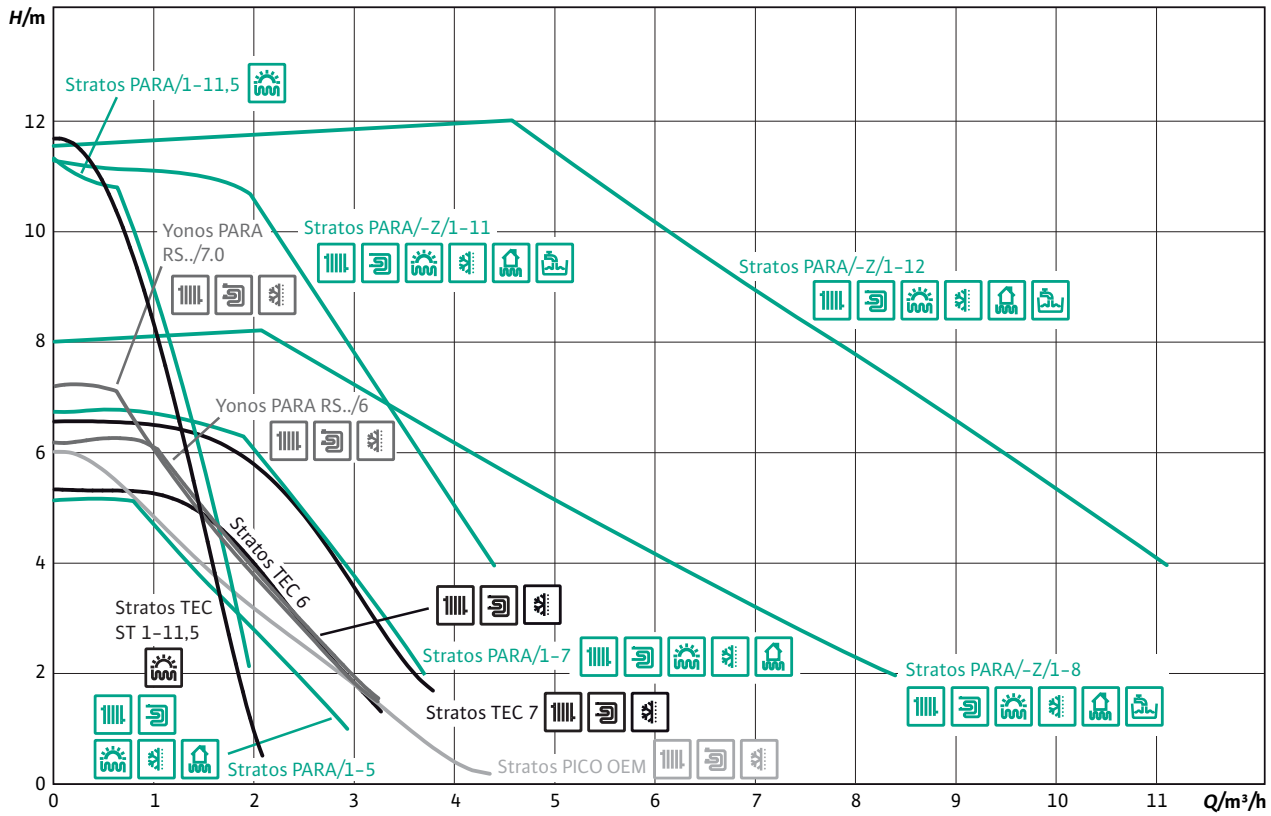

Tolerances of each curve according to EN 1151-1:2006

Wilo-Yonos PARA

The Wilo-Yonos PARA is the latest high-efficiency pump series which is specially designed in order to fulfill the special demands of the OEM industry. The Wilo-Yonos PARA sets the standard for energy-saving solutions required for integrated hydraulic systems. Equipped with a self controlled Red button or externally PWM control, the Wilo-Yonos PARA is the perfect choice for a one-to-one replacement of most existing electronic pumps. This series is available in various cast iron and composite (available 09/2012) pump housings and is thus highly versatile. At the leading edge of technology, the Wilo-Yonos PARA provides best-in-class performances: it has a three times higher starting torque than most comparable heating pumps and fulfils highest mechanical, electrical and hydraulical requirements.

Special features/product benefits

- "Best in class" High Efficiency pump of the market due to ECM technology
- Up to 80% electricity savings compared to previous uncontrolled range of heating pumps
- Self controlled pump (Red button) or externally controlled (PWM signal)
- Unique LED user interface gives information about the pump functioning
- High starting torque for reliable start-up
- Hot water heating systems of all kinds, in the temperature range of 0 °C to +95 °C
- Designed for easy integration due to compact design
- Inrush current peak less than 3A
- Self protecting modes of electronic motor
- Preventing flow noises
- Stand-by consumption less than 1 W
- Functions adapted specially to the demands of the OEM market
- Standard delivery with power cable and signal cable
- Cataphoretically coated (KTL) cast iron pump housing to prevent corrosion when condensation occurs, or OEM composite (available 09/2012) pump housing

Heating application

In nearly all circulation systems, correctly sized controlled glandless pumps ensure adequate heat supply at all times at significantly reduced energy costs, while at the same time preventing noise generation.

Electronic performance control

Self controlled model with Red button (Type RKA/RKC)
Available control modes
Control mode Δp-c:
In the Δp-c control mode, the electronic module keeps the differential pressure generated by the pump constant at the set differential pressure setpoint HS over the permissible volume flow range.

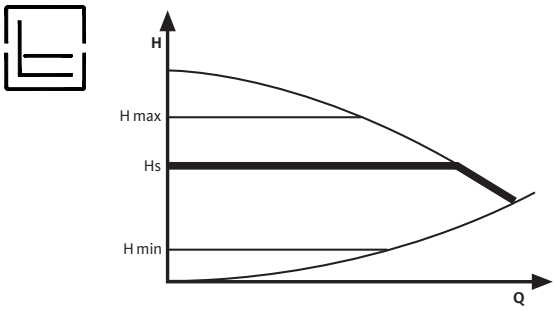

Control mode Δp-v:
In the Δp-v control mode, the electronic module changes the differential pressure setpoint to be maintained by the pump in linear fashion between Hs and ½ Hs. The differential pressure setpoint value H varies with the volume flow Q.

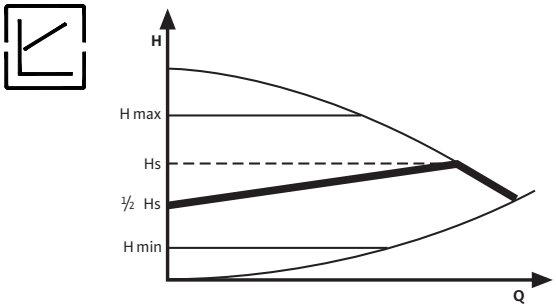

Venting routine
The integrated venting routine supports a bleeding of the overall heating system. After a manual setting, the routine runs for 10 minutes alternating at low and high speed of the pump. At the end of the process, the pump switches automatically to a pre-set speed. After that, the desired control mode can be set at the red button.

Constant speed I, II, III
In this operating mode the pump is not self regulating its speed. The pump is operating constantly with a fixed speed in pre-setted position.

Wilo-Yonos PARA

Manual control panel
Control button
The control mode and the differential pressure setpoint at Δp-c for constant differential pressure, Δp-v for variable differential pressure and pre-setting the constant speed can be set easily and safely, directly at the pump. Depending on customer wishes, a pre-setting of the control mode/setpoint can be done at the factory.

RKA type

RKA

- Local setting of the constant differential pressure setpoint at Δp-c on the right side
- Local setting of the variable differential pressure setpoint at Δp-v on the left side
- Medium position for activating the venting function

RKC type

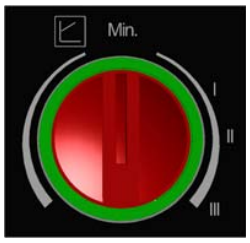

RKC

- Local setting of the variable differential pressure setpoint at Δp-v on the left side
- A fixed constant speed is set on the right side. In this operating mode the pump is not self regulating its speed.
- Medium position for minimum speed

External control via a PWM signal
The actual/setpoint level assessment required for control is referred to a remote controller. The remote controller sends a PWM signal as an actuating variable to the Wilo-Stratos PARA.
The PWM signal generator gives a periodic order of pulses to the pump (the duty cycle), according to DIN IEC 60469-1. The actuating variable is determined by the ratio between pulse duration and the pulse period. The duty cycle is defined as a ratio without dimension, with a value of 0 ... 1 % or 0 ... 100 %. This is explained in the following with ideal pulses which form a rectangular wave.

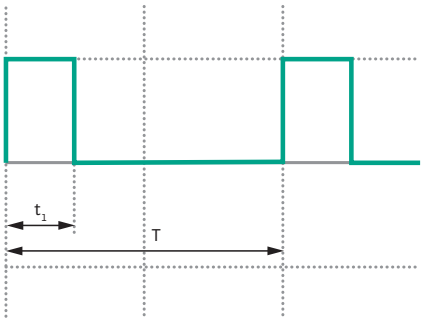

$t_1 / T = 0{,}25 = 25\,\%$

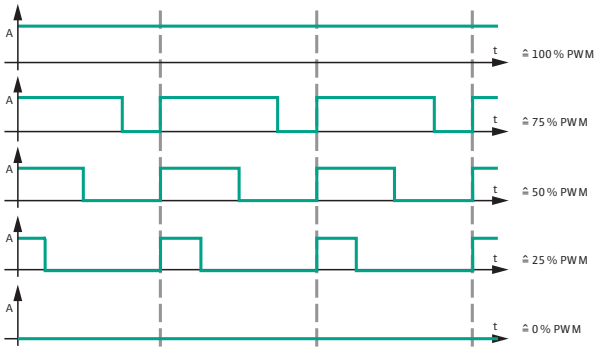

PWM signal logic 1 (heating):

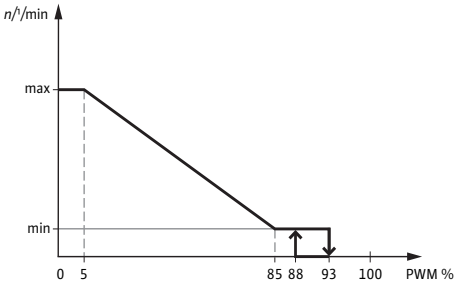

PWM input signal [%]

< 5	Pump runs at maximum speed
5-85	Pump speed decreases linearly from maximum to minimum
85-93	Pump runs at minimum speed (operation)
85-88	Pump runs at minimum speed (start-up)
93-100	Pump stops (Standby)

Signal frequency: 100 Hz-5000 Hz (1000 Hz nominal)
Signal amplitude: 5V-15V (min. power 5mA)
Signal polarity: single

Wilo-Yonos PARA

Electrical connection

To ensure a safe and easy electrical connection, the Wilo-Yonos PARA pumps are equipped with a mains cable or, depending on the available functions, with a mains and control cable as standard.

Mains connection
For mains power supply 1~230 V/50 Hz
Standard: 3-core cable

black/brown:	L1, 1~230V/50Hz
blue:	Neutral N
yellow/green:	Earth conductor

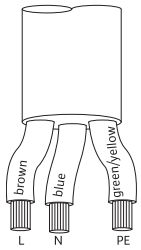

Optional: OEM plug

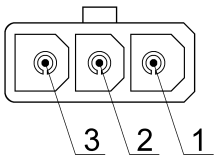

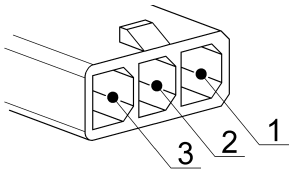

1) L1, 1~230 V/50 Hz
2) Neutral N
3) Earth conductor

The mating plug to the OEM-plug can be ordered with one of the following suppliers. (Wilo does not assume any liability for the products supplied by these manufacturers):
LTE (www.lte.it)
FACON (www.facon.it)

Optional: Wilo Connector
No tools are required to connect the mains cable to the Wilo-Connector:

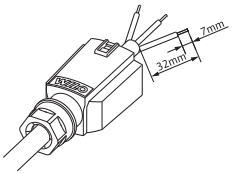

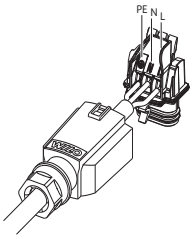

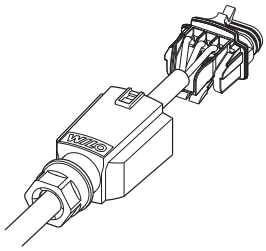

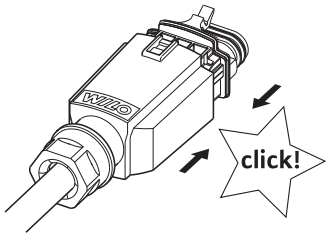

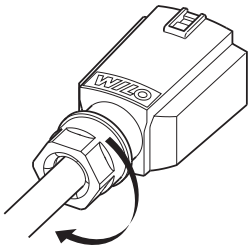

Control cables
2-core cable
For connecting the analogue interface PWM

PWM + (brown)
PWM – (blue)

Wilo-Yonos PARA

Available cable versions

Mains connection	
Standard	3-core cable 1 m with brassed end splices
Optional	– 0.5 m cable with end splices – 1.5 m cable with end splices – 2 m cable with end splices – according to customer specification
2-core control cable	
Standard	1 m with brassed end splices
Optional	– 0.5 m with end splices – 1.5 m with end splices – 2 m with end splices – according to customer specification

Permissible temperature range

The Wilo-Yonos PARA range is equipped with a self protecting mode: In the event of too high temperature, outside the permissible temperature range, the electronics reduces automatically the power consumption until normal operating conditions return.

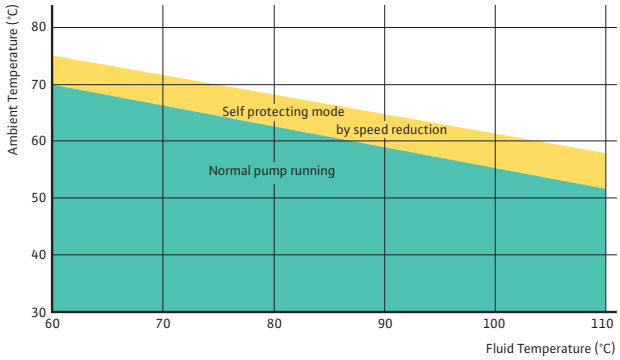

Example: at a fluid temperature of 90 °C and at an ambient temperature of 59 °C, the delivery head can decrease by 0.5 m depending on the pressure losses of the system.

Wilo-Yonos PARA

Designation, name plate of the Wilo-Stratos PARA/-Z series

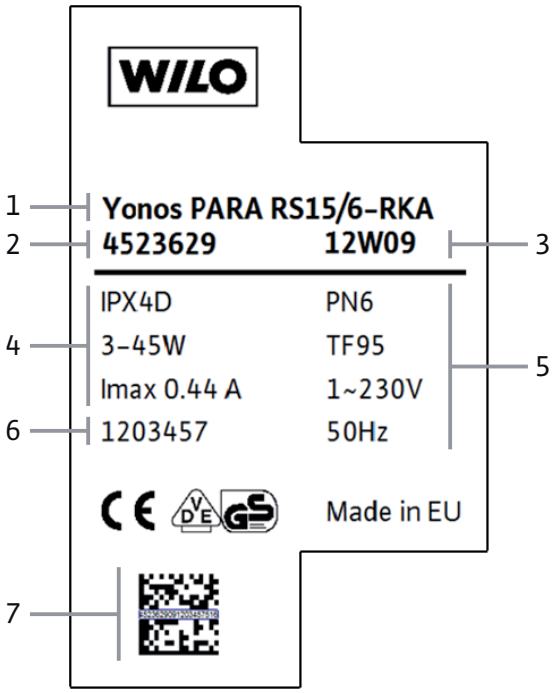

1 Pump type
2 Article number
3 Production date (year/week)
4 Protection class IP/Power consumption/Electricity
5 Operating pressure/max. Fluidtemperature/Voltage/Frequency
6 Wilo Label number
7 Code and serial number

Permitted installation positions

Wilo-Yonos PARA

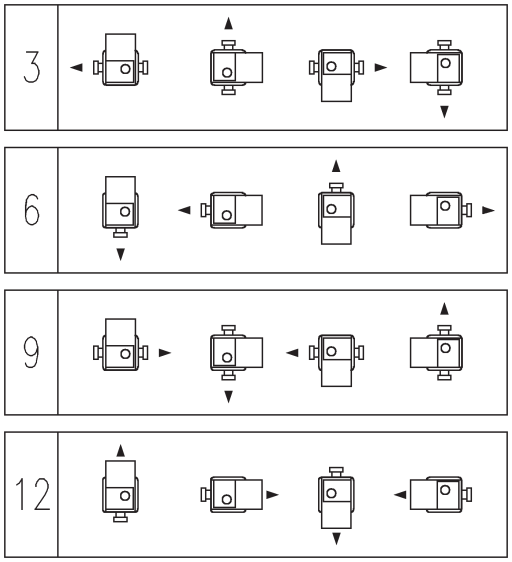

3, 6, 9 and 12 o'clock are the electronic module positions for the indicated direction of flow at the pump housing.

Series overview

Series: Wilo-Yonos PARA

> Application
Hot-water heating systems of all kinds, cooling applications

> Special features/product advantages
- Red Knob technology or PWM controlled
- Unique LED user interface
- Self-protecting modes
- Designed for optimised integration
- Water temperature range: 0°C to 95°C
- Ambient temperature range: 0°C to 70°C
- Self controlled pump (Red Knob) or externally controlled (PWM signal)

> Additional information **Page**

Series overview

Hydraulic operational areas

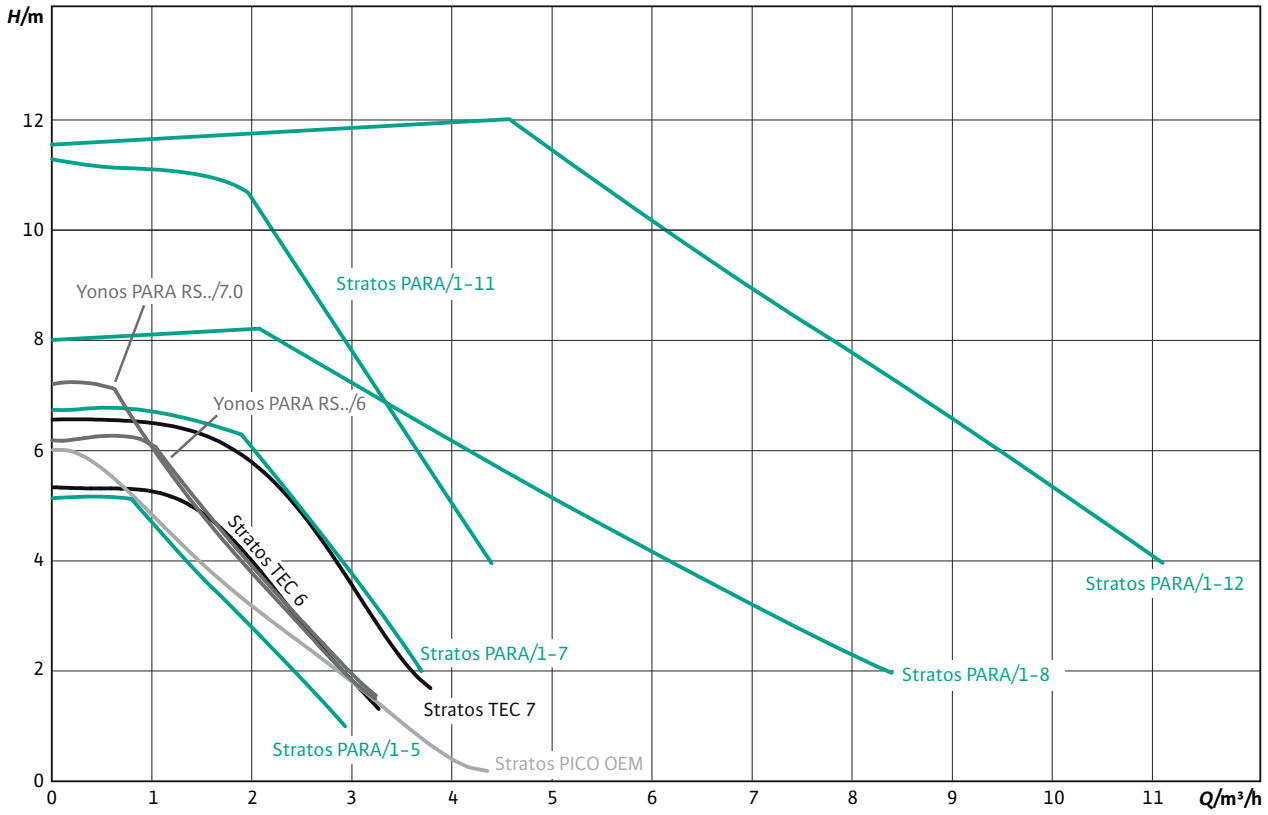

Tolerances of each curve according to EN 1151-1:2006

Equipment/function

	Wilo-Yonos PARA...	
	RKA / RKC	**PWM**
Operating modes		
Manual control mode (n=constant)	• (RKC)	• via PWM
Δp-c for constant differential pressure	• ($H_{min.}$= 1 m, $H_{max.}$= 6 m)	–
Δp-v for variable differential pressure	• ($H_{min.}$= 1 m, $H_{max.}$= 6 m)	–
Manual functions		
Operating mode setting	•	–
Differential-pressure setpoint setting	•	•
Automatic functions		
Infinitely variable power adjustment depending on the operating mode	•	•
Deblocking function	•	•
Soft start	•	•
Full motor protection with integrated trip electronics	–	–
Venting routine	• (RKA)	–
External control functions		
Control input "Analogue In 0 ... 10 V“ with cable break function (remote speed adjustment)	–	–
Control input "Analogue In 0 ... 10 V“ without cable break function (remote setpoint adjustment)	–	–
Control input PWM	–	•
Signal and display functions		
Collective fault signal (potential-free NC contact)	–	–
Individual run signal (potential-free NO contact)	–	–
Equipment/scope of delivery		
Red button	•	–
Version without red button (=external control)	–	•
Wrench attachment point on pump body	•	•
Including power cable	•	•
Including power plug	–	–
Including control cable	–	•
Including seals for threaded connection	on request	on request
Including installation and operating instructions	on request	on request
Including thermal insulation	on request	on request
Incl. ClimaForm for cooling	–	–
Individual packaging	on request	on request
Collective packaging	•	•

• = available, – = not available
* see table “Possible combinations of functions and equipment”

Series description Wilo-Yonos PARA Red Knob 15/6, 20/6, 25/6, 30/6

ErP READY 2015 APPLIES TO EUROPEAN DIRECTIVE FOR ENERGY RELATED PRODUCTS

Design
Glandless circulation pump with cast iron pump housing and threaded connection. EC-motor with automatic power adjustment and self-protecting modes . Operation by Red Knob technology and delivered with power cable.

Application
Hot-water heating systems of all kinds, cooling applications

Type key

Example:	**Wilo-Yonos PARA RS 15/6 RKA FS 130 12 I**
Yonos	Electronically controlled high-efficiency pump
PARA	pump range adapted to requirements of the OEM market
RS	Heating inline cast iron pump housing
15/	Nominal diameter: **15** threading 1” **20** threading 1 ¼ “ **25** threading 1 ½” **30** threading 2”
6	Max delivery height in [m] at Q = 0 m^3/h
RKA	The pump is controlled by Red Knob technology: ΔP-v /ΔP-c RKC = ΔP-v, constant speed I, II, III
FS	Overmoulded cable with brassed end splices. Optional: connector
130	Pump housing length: 130 mm or 180 mm
12	Box orientation
I	Individual packaging
(not specified)	Collective packaging (standard)

Technical data

Approved fluids (other fluids on request)	
Heating water (in accordance with VDI 2035)	•
Water-glycol mixtures (max. 1:1; above 20% admixture, the pumping data must be checked)	•
Power	
Max. delivery head	6.2 m
Max. volume flow	3.3 m^3/h
Permitted field of application	
Temperature range for applications in HVAC systems at max. ambient temperature	of 57°C = 0° C to 95° C of 59°C = 0° C to 90° C of 67°C = 0° C to 70° C
Maximum static pressure	6 bar
Electrical connection	
Mains connection	1~230 V, 50/60 Hz
Motor/electronics	
Electromagnetic compatibility	EN 61800-3
Emitted interference	EN 61000-6-3/EN 61000-6-4
Interference resistance	EN 61000-6-2/EN 61000-6-1
Speed control	Frequency converter
Protection class	IPX 4D
Insulation class	F
Minimum suction head at suction port for avoiding cavitation at water pumping temperature	
Minimum suction head at 50 / 95 / 110 °C	0.5 / 4.5 / 11 m

• = available, – = not available

Pump curves Wilo-Yonos PARA Red Knob 15/6, 20/6, 25/6, 30/6

Wilo-Yonos PARA 15/6, 20/6, 25/6, 30/6

Δp-v (variable)

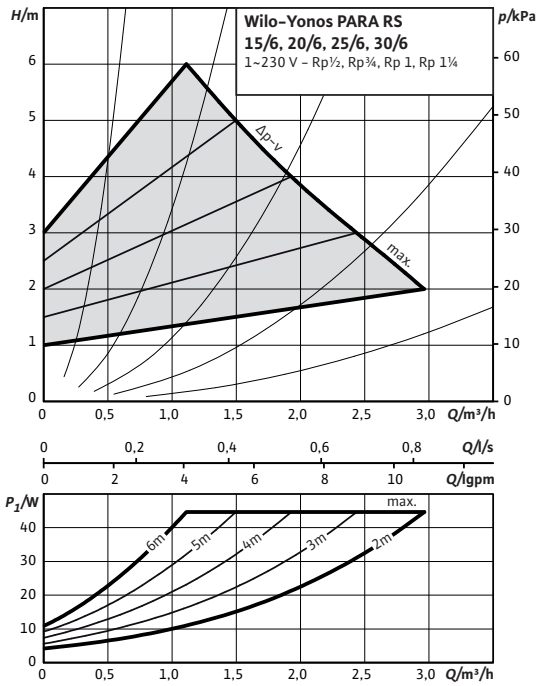

Tolerances of each curve according to EN 1151-1:2006

Wilo-Yonos PARA 15/6, 20/6, 25/6, 30/6

Δp-c (constant)

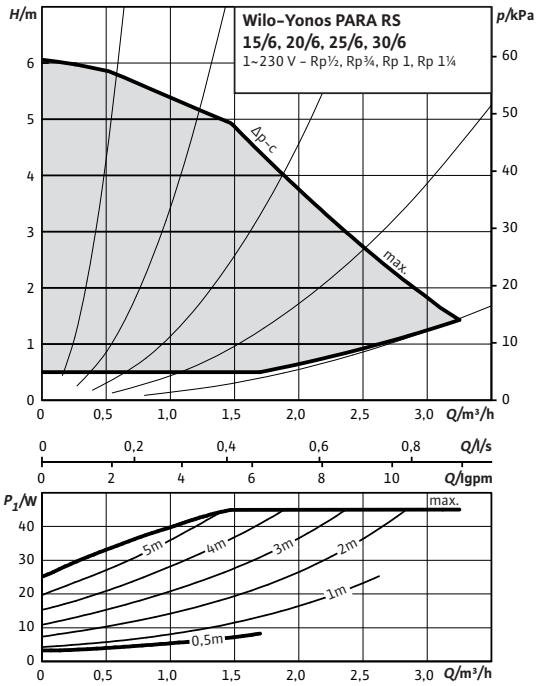

Tolerances of each curve according to EN 1151-1:2006

Wilo-Yonos PARA 15/6, 20/6, 25/6, 30/6

Constant speed I, II, III

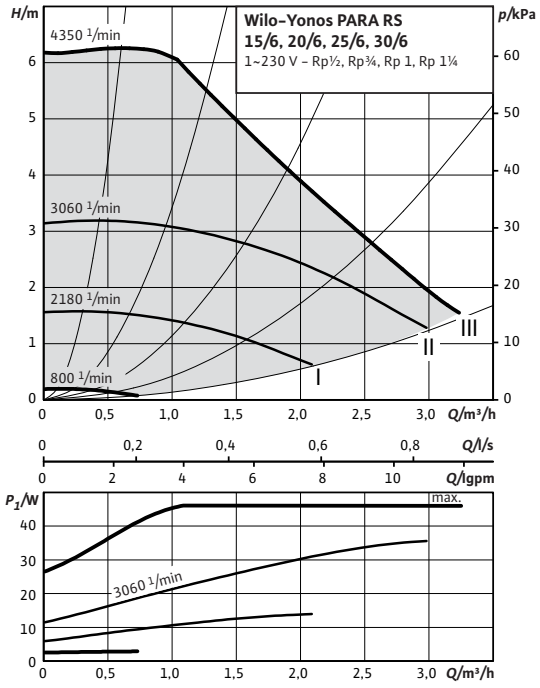

Tolerances of each curve according to EN 1151-1:2006

Dimensions, motor data Wilo-Yonos PARA Red Knob 15/6, 20/6, 25/6, 30/6

Motor data

Wilo-Yonos PARA...	Nominal motor power	Speed	Power consumption 1~230 V	Current at 1~230V	Motor protection
	P_2	n	P_1	I	–
	W	rpm	W	A	–
RS .../6 RKA/RKC	37	800 - 4250	3-45	0.03 - 0.44	integrated

Materials

Wilo-Yonos PARA...	Pump housing	Impeller	Pump shaft	Bearing
RS .../6 RKA/RKC	Cast iron with cataphoresis treatment	PP composite with GF 40%	Stainless steel	Carbon, metal impregnated

Dimension drawing

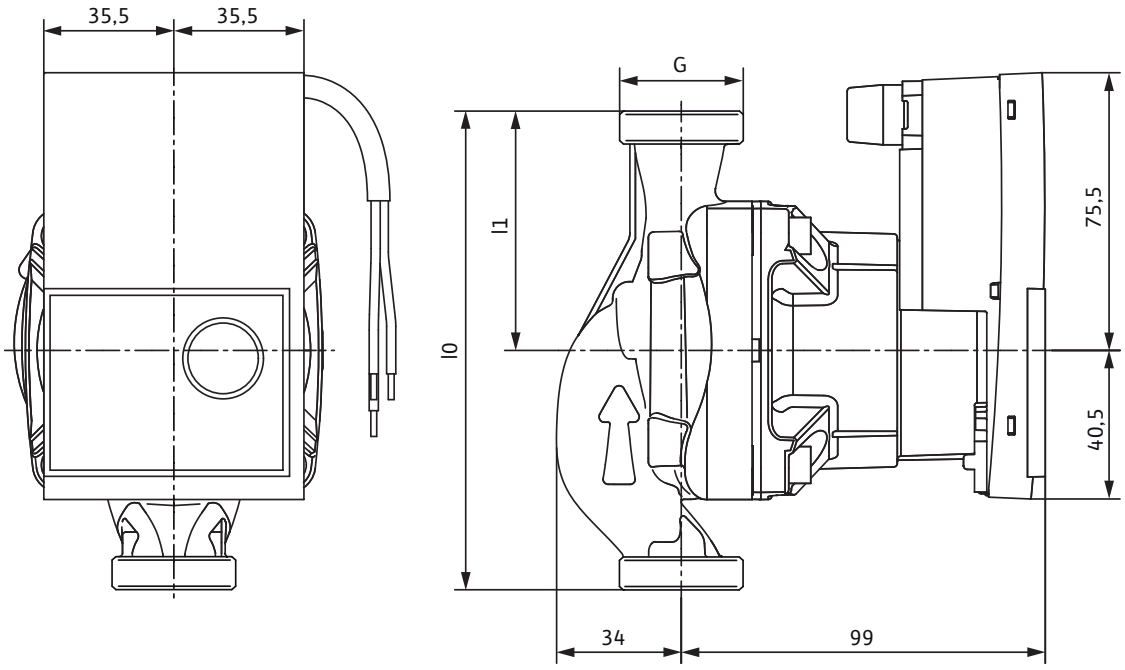

Dimensions, weights

Wilo-Yonos PARA...	Threaded pipe union	Thread	Overall length	Dimensions	Weight approx.
	–		l_0	l_1	m
	–		mm		kg
RS 15/6	Rp ½	G 1	130	65	1.6
RS 20/6	Rp ¾	G 1¼	130	65	1.6
RS 25/6	Rp 1	G 1½	130	65	1.7
RS 25/6	Rp 1	G 1½	180	90	2
RS 30/6	Rp 1¼	G 2	180	90	2,1

Series description Wilo-Yonos PARA PWM 15/7.0, 20/7.0, 25/7.0, 30/7.0

ErP READY 2015 – APPLIES TO EUROPEAN DIRECTIVE FOR ENERGY RELATED PRODUCTS

Design
Glandless circulation pump with cast iron pump housing and threaded connection. EC-motor with automatic power adjustment. Standard delivery with OEM-plug and PWM-cable. Remote Control via external PWM signal. LED user interface.

Application
Hot-water heating systems of all kinds, cooling applications

Type key

Example:	**Wilo-Yonos PARA RS 15/7.0 PWM FS 130 12 I**
Yonos	Electronically controlled high-efficiency pump
PARA	pump range adapted to requirements of the OEM market
RS	Heating inline cast iron pump housing
15/	Nominal diameter: **15** threading 1” **20** threading 1 ¼ “ **25** threading 1 ½” **30** threading 2”
7.0	Nominal delivery head range [m]
PWM	The pump is controlled by an external system via PWM signal
FS	Overmoulded cable with brassed end splices Optional: connector
130	Pump housing length: 130 mm or 180 mm
12	Box orientation
I	Individual packaging
(not specified)	Collective packaging (standard)

Technical data

Approved fluids (other fluids on request)	
Heating water (in accordance with VDI 2035)	•
Water-glycol mixtures (max. 1:1; above 20% admixture, the pumping data must be checked)	•
Power	
Max. delivery head	7.2 m
Max. volume flow	3.3 m^3/h
Permitted field of application	
Temperature range for applications in HVAC systems at max. ambient temperature	of 57°C = 0° C to 95° C of 59°C = 0° C to 90° C of 67°C = 0° C to 70° C
Maximum static pressure	6 bar
Electrical connection	
Mains connection	1~230 V, 50/60 Hz
Motor/electronics	
Electromagnetic compatibility	EN 61800-3
Emitted interference	EN 61000-6-3/EN 61000-6-4
Interference resistance	EN 61000-6-2/EN 61000-6-1
Speed control	Frequency converter
Protection class	IPX 4D
Insulation class	F
Minimum suction head at suction port for avoiding cavitation at water pumping temperature	
Minimum suction head at 50 / 95 / 110 °C	0.5 / 4.5 / 11 m

• = available, – = not available

Pump curves Wilo-Yonos PARA PWM 15/7.0, 20/7.0, 25/7.0, 30/7.0

Wilo-Yonos PARA 15/7.0, 20/7, 25/7.0, 30/7.0

External control via PWM

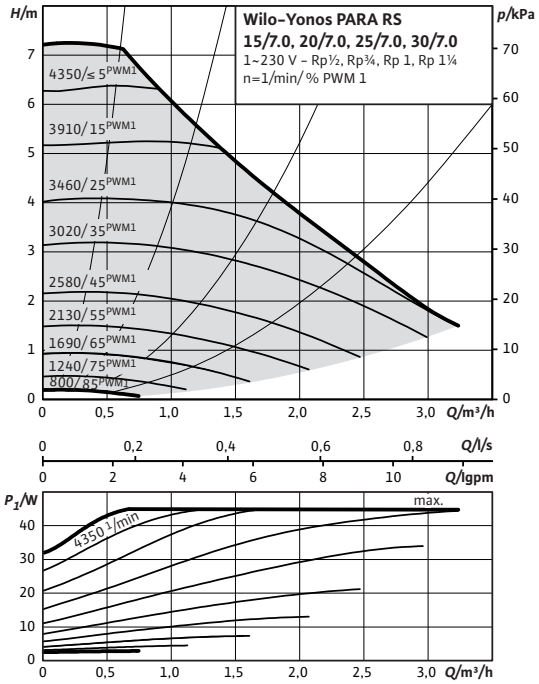

Tolerances of each curve according to EN 1151-1:2006

Dimensions, motor data Wilo-Yonos PARA PWM 15/7.0, 20/7.0, 25/7.0, 30/7.0

Motor data

Wilo-Yonos PARA...	Nominal motor power	Speed	Power consumption 1~230 V	Current at 1~230V	Motor protection
	P_2	n	P_1	I	–
	W	rpm	W	A	–
RS .../7.0 PWM	37	800 - 4250	3-45	0.03 - 0.44	integrated

Materials

Wilo-Yonos PARA...	Pump housing	Impeller	Pump shaft	Bearing
RS .../7.0 PWM	Cast iron with cataphoresis treatment	PP composite with GF 40%	Stainless steel	Carbon, metal impregnated

Dimension drawing

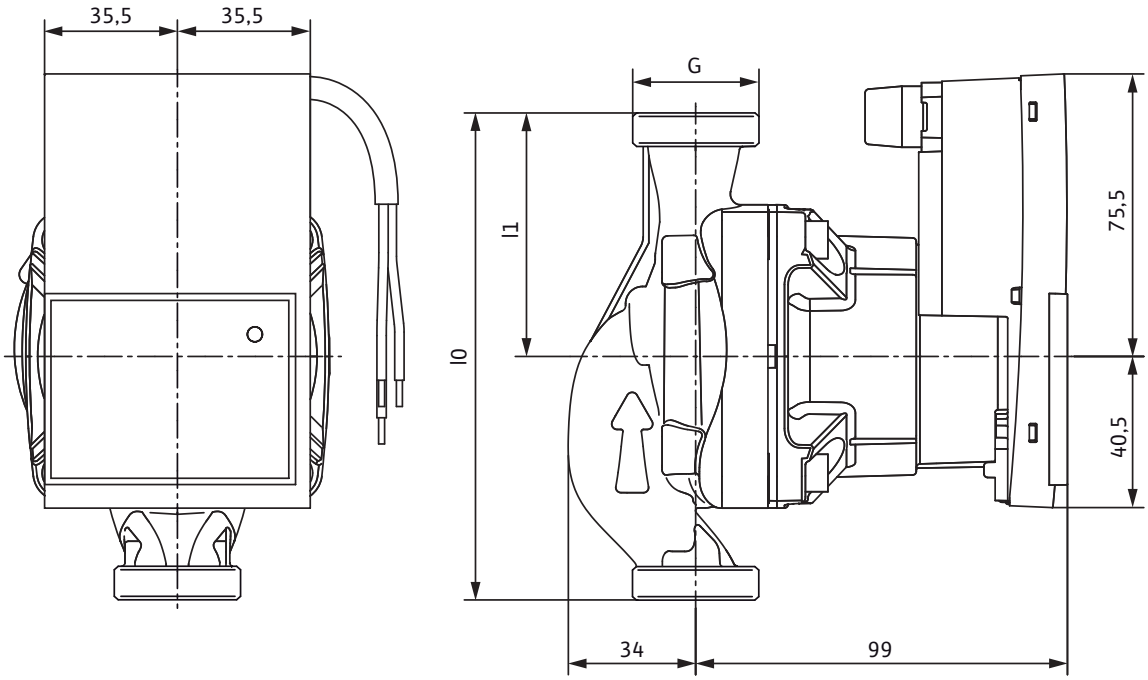

Dimensions, weights

Wilo-Yonos PARA...	Threaded pipe union	Thread	Overall length	Dimensions	Weight approx.
	–		l_0	l_1	m
	–		mm		kg
RS 15/7.0	Rp ½	G 1	130	65	1.6
RS 20/7.0	Rp ¾	G 1¼	130	65	1.6
RS 25/7.0	Rp 1	G 1½	130	65	1.7
RS 25/7.0	Rp 1	G 1½	180	90	2
RS 30/7.0	Rp 1¼	G 2	180	90	2,1

WILO
Pumpen Intelligenz.

Wilo Intec
50 av. Casella
F–18700 Aubigny sur Nère
T +33 2 48 81 62 62
F +33 2 48 58 20 29
information@wilointec.com
www.wilointec.com

Vincent FLEURIER
Sales & Marketing Director
T: +33 2 48 81 62 74
vincent.fleurier@wilointec.com

Robert CARRE
Key Account Manager France & Spain
T: +33 2 48 81 62 72
robert.carre@wilointec.com

Gilles MOULIN
Sales Coordinator Subsidiaries
T: +33 2 48 81 62 25
gilles.moulin@wilointec.com

Hakan ARPINAR
Key Account Manager Turkey
T : +90 530 035 8439
hakan.arpinar@wilo.com.tr

Dario FRAZZA
Key Account Manager Italy
T: +39 335 762 6181
dario.frazza@wilointec.com

Kevin PADMORE
Sales Manager UK
T: +44 776 801 8879
kevin.padmore@wilointec.com

Pierre BEQUET
Key Account Manager
T : +33 2 48 81 62 85
pierre.bequet@wilointec.com

Thomas MERSCHEIM
Key Account Manager Germany
T: +49 172 352 3933
thomas.merscheim@wilo.com

Ronald RIJKHOFF
Key Account Manager Netherlands
T: +31 653 126 749
ronald.rijkhoff@wilo.nl

Version 12.01/March 2012 Wilo Intec/EN

Appendix F

Email contact solartherm

Dear Benjamin

thank you for your email

for a volume like your below email (19808pcs), we can sell the module type **FT285AL** at net price of **350€/pcs**

kind regards

Ing. Luca Maresia
tel: +39(0) 432 931595
fax: +39(0) 432 931599
cel: +39 392 9020495
email: luca.maresia@fototherm.com
pec: fotovoltaico@pec.fototherm.com

FOTOTHERM S.P.A.

Via degli Olmi, 1
33050 Gonars (UD)
www.fototherm.com

Il 25/07/2016 12:58, benjamin stobbe ha scritto:

Dear Luca,

Sorry for the late response.

I was wondering if you could help me one more time. I'm actually busy with my master thesis this is why I was asking the information. But if I scale up the system is there than a kind of discount. I'm talking about using the solar panels on facades of a skyscraper and a system of 19808 solar panels. Sorry for the questions.

Thanks a lot in advance.

Best regards,

Benjamin Stobbe

Bibliography

[1] The Organisation for Economic Co-operation and Development (OECD), "Oecd," 2016. http://www.oecd.org/about/membersandpartners/.

[2] Energy Information Administration, "International energy statistics," 2014. https://www.eia.gov/cfapps/ipdbproject/IEDIndex3.cfm?tid=3&pid=3&aid=1.

[3] International Energy Agency, "Energy and climate change 2015." http://www.iea.org/publications/freepublications/publication/weo-2015-special-report-energy-climate-change.html.

[4] Wikimedia Commons, "Band gap comparison," 2015. https://upload.wikimedia.org/wikipedia/commons/thumb/0/0b/Band_gap_comparison.svg/2000px-Band_gap_comparison.svg.png.

[5] K. Jaeger, O. Isabella, A. H. Smets, R. A. van Swaaij, and M. Zeman, *Solar Energy Fundamentals, Technology and Systems*. Delft University of Technology, 2014.

[6] PowerVolt, "Picture of a hybrid solar panel," 2016. http://www.minimisegroup.com/hybrid-solar-pvt-panels.html.

[7] J. Ji, J. Han, T. tai Chow, H. Yi, J. Lu, W. He, and W. Sun, "Effect of fluid flow and packing factor on energy performance of a wall-mounted hybrid photovoltaic/water-heating collector system," *Energy and Building*, vol. 38, pp. 1380–1387, 2006.

[8] Water Supplies Department, "Twin-tank system," 2016. http://www.wsd.gov.hk/en/plumbing_and_engineering/tts/index.html.

[9] Hong Kong Observatory, "The weather of 2015," 2015. http://www.weather.gov.hk/wxinfo/pastwx/ywx2015.htm.

[10] United Nations, Department of Economic and Social Affairs, Population Division, "World population prospects: The 2015 revision," 2015. New York, United Nations.

[11] Central Intelligent Agency, "The world factbook," 2016. http://www.hko.gov.hk/cis/climahk_e.htm.

[12] renewables the magaine international, "German power exports still more valuable than imports," 2014. http://www.renewablesinternational.net/german-power-exports-still-more-valuable-than-imports/150/537/79015/.

[13] renewables the magaine international, "German wind and solar power overwhelming neighboring grids," 2015. http://www.renewableenergyworld.com/news/2015/07/german-wind-and-solar-power-overwhelming-neighbor-country-s-grids.html/.

[14] pvresources, "Large-scale pv power plants - top50," 2016. http://www.pvresources.com/en/pvpowerplants/top50pv.php.

[15] J. Benemann, O. Chehab, and E. Schaar-Gabriel, "Building-integrated pv modules," *Solar Energy Materials and Solar Cells 67*, vol. 67, pp. 345–354, 2001.

[16] J. Prakash, "Transient analysis of a photovoltaic/thermal solar collector for co-generation of electricity and hot air/water.," *Energy Conversion and Management*, vol. 35, pp. 967–972, 1994.

[17] B. Roblesocampo, E. Ruizvasquez, H. Cansecosanchez, R. C. Cornejo-Meza, and G. T.-M. et al., "Photovoltaic/thermal solar hybrid system with bifacial pv module and transparent plane collector.," *Solar Energy Materials and Solar Cells*, vol. 91, pp. 1966–1971, 2006.

[18] E. W.C.LO, "Overview of building integrated photovoltaic (bipv) systems in hong kong," 2010.

[19] T. T. Chow, W. He, and J. Li, "Hybrid photovoltaic-thermosyphon water heating system for residential application," *Solar Energy*, vol. 80, pp. 298–306, 2006.

[20] T. T. Chow, "Performance analysis of photovoltaic0thermal collector by explicit dynamic model," *Solar Energy*, vol. 75, pp. 143–152, 2003.

[21] H. A. Zondag, D. W. de Vries, and W. van Helden et all, "The thermal and electrical yield of a pv-thermal collector," *Solar Energy*, vol. 72, pp. 113–128, 2000.

[22] S. Dubey and G. Tiwari, "Thermal modeling of a combined system of photovoltaic thermal (pv/t) solar water heater," *Solar Energy*, vol. 82, pp. 602–618, 2008.

[23] J. Ji, T.-T. Chow, and W. He, "Dynamic performance of hybrid photovoltaic/thermal collecter wall in hong kong," *Building and Environment*, vol. 38, pp. 1327–1334, 2003.

[24] T. Chow, J. Hand, and P. Strachan, "Building-integrated photovoltaic and thermal applications in a subtropical hotel building," *Applied thermal Engineering*, vol. 23, pp. 2035–2049, 2003.

[25] T. Chow, W. He, and J. Ji, "An experimental study of facade-integrated photovoltaic/water-heating system," *Applied thermal Engineering*, vol. 27, pp. 37–45, 2007.

[26] T. Chow, W. He, and J. Ji, "Simulation study of building integrated solar liquid pv-t collectors," *International Journal of Photoenergy*, vol. 2012, pp. 1–8, 2012.

[27] T. T. Chow, W. He, J. Li, and A. L. S. Chan, "Performance evaluation of photovoltaicâĂŞthermosyphon system for subtropical climate application," *Solar Energy*, vol. 41, pp. 123–130, 2007.

[28] J. Li, J. P. Lu, T. T. Chow, W. He, and G. Pei, "A sensitivity study of a hybrid photovoltaic/thermal water-heating system with natural circulation," *Applied Energy*, vol. 84, pp. 222–237, 2007.

[29] T. Anderson, M. Duke, G. Morrison, and J. Carson, "Performance of a building integrated photovoltaic/thermal(bipvt) solar collector," *Solar Energy*, vol. 83, pp. 445–455, 2000.

[30] Y. Assoa, C. Menezo, G. F. G, R. Yezou, and J. Brau, "Study of a new concept of photovoltaic-thermal hybrid collector," *Solar Energy*, vol. 81, pp. 1132–1143, 2007.

[31] Census and Statistics Department, "Population," 2015 note = `http://www.censtatd.gov.hk/hkstat/sub/so20.jsp`.

[32] Survey and Mapping Office, Lands Department, *Hong Kong geographic data*, 2 2015.

[33] Planning Department, "Land utilization in hong kong 2013," 2014. `http://www.pland.gov.hk/pland_en/info_serv/statistic/landu.html`.

[34] Hong Kong Observatory, "Climatological information services, climate of hong kong," 2015. `http://www.hko.gov.hk/cis/climahk_e.htm`.

[35] Delft University of Technology, *A Student introduction to solar energy*, 6 2015.

[36] national geographic, "Encyclopedic entry equinox." `http://education.nationalgeographic.com/encyclopedia/equinox/`.

[37] Census and Statistics Department, "Hong kong energy statistics," 2015 note = `http://www.statistics.gov.hk/pub/B11000022015AN15B0100.pdf`.

[38] Mathworks, "Matlab r2015a," 2015. `http://nl.mathworks.com/`.

[39] C. Rigollier, O. Bauer, and L. Wald, "On the clear sky model of the esra, european solar radiation atlas, with respect to the heliosat method," *Solar Energy*, vol. 68, pp. 33–48, 2000.

[40] Meteotest, "Meteonorm 7 v. 7.1.4.29605," 2015. `http://meteonorm.com/`.

[41] A. Smets, O. Isabella, K. Jäger, and R. van Swaaij en Miro Zeman, *Solar Energy*. UIT Cambridge, England, 2016.

[42] D. H. Li and J. C. Lam, "A study of atmospheric turbidity for hong kong," *Renewable energy*, vol. 25, pp. 1–13, 2002.

[43] F. Kasten and A. T. Young, "Revised optical air mass tables and approximation formula," *Applied Optics*, vol. 28, pp. 4735–4738, 1989.

[44] R. Perez, P. Ineichen, R. Seals, J. Michalsky, and R. Stewart, "Modeling daylight availability and irradiance components from direct and global irradiance," *Solar Energy*, vol. 44, pp. 271–289, 1990.

[45] A. C. T.T. Chow and Z. L. K.F. Fong, "Hong kong solar radiation on building facades evaluated by numerical models," *Applied thermal engineering*, vol. 25, pp. 1908–1921, 2005.

[46] D. H. Li and J. C. Lam, "Evaluation of slope irradiance and illuminance models against measured hong kong data," *Building and environment*, vol. 35, pp. 501–509, 2000.

[47] A. M. Nooriana, I. Moradi, and G. A. Kamali, "Evaluation of 12 models to estimate hourly diffuse irradiation on inclined surfaces," *Renewable energy*, vol. 33, pp. 1406–1412, 2008.

[48] Sandia National Laboratories, "PV_LIB toolbox for matlab," 2015. https://pvpmc.sandia.gov/modeling-steps/1-weather-design-inputs/plane-of-array-poa-irradiance/calculating-poa-irradiance/poa-sky-diffuse/perez-sky-diffuse-model/.

[49] Links System Software, "Lss chronolux, version 1.2.2," 2013. https://extensions.sketchup.com/en/content/lss-chronolux.

[50] The University of Wisconsin, "Trnsys 17," 2015. http://www.trnsys.com/.

[51] H. Li and H. Yang, "Study on performance of solar assisted air source heat pump systems for hot water production in hong kong," *Applied Energy*, vol. 87, p. 2818âĂŞ2825, 2010.

[52] M. Cavcar, "The international standard atmosphere," 2016. http://home.anadolu.edu.tr/~mcavcar/common/ISAweb.pdf.

[53] E. A. de la Breteque, "Thermal aspects of c-si photovoltaic module energy rating," *Solar Energy*, vol. 83, pp. 1425–1433, 2009.

[54] J. A. Duffie, Beckman, and W. A., "Flat-plate collectors," in *Solar Engineering of Thermal Processes*, pp. 236–321, John Wiley & Sons, Inc., 2013.

[55] J. T. et al, *TESSLibs 17: Component Libraries for the TRNSYS Simulation Environment*. Thermal Energy System Specialists, LCC, 2014.

[56] standard.

[57] G. Tiwari and R. Mishra, *Advanced Renewable Energy Source*. RSC Publishing, Cambridge, UK, 2012.

[58] Solid Green Consulting and A. Hall, "Sunhours, version 2.0.7," 2015. http://www.sunhoursplugin.com/.

[59] A. Yezioro and T. Gutman, "Shading tools plugin v1.0." http://ayezioro.technion.ac.il/Downloads/ShadingII/index.php.

[60] Time and Date AS 1995-2015, "Hong kong, hong kong sunrise, sunset and daylength," 2015 note = http://www.timeanddate.com/sun/hong-kong/hong-kong?month=12&year=2015.

[61] R. Giridharan, S. Lau, and S. Ganesan, "Nocturnal heat island effect in urban residential developments of hong kong," *Energy and Buildings*, vol. 37, pp. 964–971, September, 2005.

[62] S. C. M. Hui, "Electrical services systems - electrity supply, load estimation and power distribution." Lecture from the University of Hong Kong, 2015.

[63] R. Giridharan, S. Lau, and S. Ganesan, "Case study: Hong kong international commerce centre," *CTBUH Journal*, vol. IV, pp. 1–17, 2010.

[64] Glass Education Center, "Spandrel glass," 2016. http://educationcenter.ppg.com/glasstopics/spandrel_glass.aspx.

[65] EMPORIS, "International commerce centre," 2016. http://www.emporis.com/buildings/101555/international-commerce-centre-hong-kong-china.

[66] P. Leung and H. Yeung, "Icc hong kong: Exemplary performance," *CTBUH Research Paper*, vol. -, pp. 1–13, 2015.

[67] A. Amirahmadi, L. Chen, U. Somani, H. Hu, N. Kutkut, and I. Batarseh, "High efficiency dual-mode current modulation method for low-power dc/ac inverters," *IEEE transactions on power electronics*, vol. 29, pp. 2638–2642, 2014.

[68] M. A. Maehlum, "Micro-inverters vs. central inverters," 2014. http://energyinformative.org/are-solar-micro-inverters-better-than-central-inverters/.

[69] energysage, "String inverters vs. microinverters vs. power optimizers," 2016. https://www.energysage.com/solar/101/string-inverters-microinverters-power-optimizers.

[70] I. Clover, "Microinverters vs. optimizers," *pv magazine*, October, 2014. http://www.pv-magazine.com/archive/articles/beitrag/microinverters-vs-optimizers-_100016637/618/#axzz47fsDE7jP.

[71] Fototherm, "Fototherm," 2016. http://www.fototherm.com/en/.

[72] A. Goodrich, T. James, and M. Woodhouse, "Nrel: Residential, commercial, and utility-scale photovoltaic (pv) system prices in the united, states: Current drivers and cost-reduction opportunities," tech. rep., National Renewable Energy Laboratory (NREL), 2012.

[73] T. James, A. Goodrich, M. Woodhouse, R. Margolis, and S. Ong, "Building-integrated photovoltaics (bipv) in the residential sector: An analysis of installed rooftop system prices," tech. rep., National Renewable Energy Laboratory (NREL), 2011.

[74] S. Kayal, "Application of pv panels in a large multi-story buildings: Feasibility study," Master's thesis, California Polytechnic State University, 2009.

[75] T.T.Chow, A. Chan, K. Fong, Z. Lin, W. He, and J. Li, "Annual performance of building-integrated photovoltaic/water-heating system for warm climate application,"

[76] U. Eicker, *Solar Technologies for Buildings*. John Wiley & Sons, 2006.

[77] US Army Corps of Engineers, *Central Solar Hot Water Systems Design Guides*. -, 2011.

[78] T. Merrigan, "Solar thermal systems analysis." Presentation Solar buildings, 2005.

[79] National Renewable Energy Laboratory, "Distributed generation energy technology operations and maintenance costs," 2016. `http://www.nrel.gov/analysis/tech_cost_om_dg.html`.

[80] China Light and Power (Hong Kong), "Non-residential tariff," 2016. https://www.clp.com.hk/en/customer-service/tariff/business-and-other-customers/non-residential-tariff.

[81] T.T.Chow and J. Li, "Environmental life-cycle analysis of hybrid solar photovoltaic/thermal systems for use in hong kong,"

[82] F. Frontini, P. Bonomo, and A. Chatzipanagi, "Bipv product overview for solar facades and roofs," tech. rep., Swiss BIPV Competence Centre, SUPSI, 2015.

[83] Y. Sun, "Life cylce assessment of a novel building-integrated photovoltaic-thermal (bipvt) system," Master's thesis, Combia University, 2014.

[84] Carbon Care Asia Ltd., "The legislative council complex greenhouse gas accounting report." Accounting report, 2014-2015.

[85] J. Alvebratt and M. Blidmark, "Life cycle assessment of a building-integrated solar technology," Master's thesis, Chalmers University of Technology, 2014.